ไพโรไลซิสเชิงเร่งปฏิกิริยาของน้ำมันเมล็ดเรพเป็นเชื้อเพลิงเหลวในเครื่องปฏิกรณ์แบบต่อเนื่อง

นางสาววลัยรัตน์ อุตตมะปรากรม

วิทยานิพนธ์นี้เป็นส่วนหนึ่งของการศึกษาตามหลักสูตรปริญญาวิทยาศาสตรดุษฎีบัณฑิต
สาขาวิชาปิโตรเคมี
คณะวิทยาศาสตร์ จุฬาลงกรณ์มหาวิทยาลัย
ปีการศึกษา 2558

CATALYTIC PYROLYSIS OF RAPESEED OIL TO LIQUID FUELS IN CONTINUOUS REACTOR

Miss Walairat Uttamprakrom

A Dissertation Submitted in Partial Fulfillment of the Requirements
for the Degree of Doctor of Philosophy Program in Petrochemistry
Faculty of Science
Chulalongkorn University
Academic Year 2015

Thesis Title	CATALYTIC PYROLYSIS OF RAPESEED OIL TO LIQUID FUELS IN CONTINUOUS REACTOR
By	Miss Walairat Uttamprakrom
Field of Study	Petrochemistry
Thesis Advisor	Professor Tharapong Vitidsant, Ph.D.
Thesis Co-Advisor	Associate Professor Prasert Reubroycharoen, Ph.D.

Accepted by the Faculty of Science, Chulalongkorn University in Partial Fulfillment of the Requirements for the Doctoral Degree

.....Dean of the Faculty of Science
(Associate Professor Dr. Polkit Sangvanich)

THESIS COMMITTEE

.....Chairman
(Professor Dr. Pattarapan Prasassarakich)
.....Thesis Advisor
(Professor Tharapong Vitidsant, Ph.D.)
.....Thesis Co-Advisor
(Associate Professor Prasert Reubroycharoen, Ph.D.)
.....Examiner
(Associate Professor Dr. Voravee Hoven)
.....Examiner
(Associate Professor Dr. Nuanphun Chantarasiri)
.....External Examiner
(Assistant Professor Dr. Witchakorn Charusiri)

วลัยรัตน์ อุตตมะปรากรม : ไพโรไลซิสเชิงเร่งปฏิกิริยาของน้ำมันเมล็ดเรพเป็นเชื้อเพลิงเหลวในเครื่องปฏิกรณ์แบบต่อเนื่อง (CATALYTIC PYROLYSIS OF RAPESEED OIL TO LIQUID FUELS IN CONTINUOUS REACTOR) อ.ที่ปรึกษาวิทยานิพนธ์หลัก: ศ. ดร. ธราพงษ์ วิทิตศานต์, อ.ที่ปรึกษาวิทยานิพนธ์ร่วม: ผศ. ดร. ประเสริฐ เรียบร้อยเจริญ, 163 หน้า.

การแตกตัวเชิงเร่งปฏิกิริยาของน้ำมันเมล็ดเรพเป็นเชื้อเพลิงเหลวในเครื่องปฏิกรณ์แบบต่อเนื่อง ดำเนินการทดลองใน 2 ส่วน ส่วนแรกเป็นการดำเนินการทดลองในระบบแบบกะด้วยเครื่อง micro-reactor ขนาด 70 ลูกบาศก์เซนติเมตร เพื่อหาภาวะเหมาะสมของแต่ละตัวเร่งปฏิกิริยาที่ให้ร้อยละของผลิตภัณฑ์ของของเหลวและแนฟทาสูงที่สุด จากตัวเร่งปฏิกิริยาทั้ง 5 ชนิด คือ CaO, MgO, HZSM-5, 1%wt Fe/AC และ 5%wt Fe/AC ภายใต้การออกแบบการทดลองแบบเชิงประกอบสองระดับ โดยขอบเขตของตัวแปรที่ศึกษามีดังนี้ อุณหภูมิในการทำปฏิกิริยา 390 และ 450 องศาเซลเซียส ระยะเวลาในการทำปฏิกิริยา 30 และ 60 นาที ความดันไฮโดรเจนเริ่มต้น 1 และ 5 บาร์ และปริมาณตัวเร่งปฏิกิริยาร้อยละ 0.5และ 1.0 โดยปริมาตรของเครื่องปฏิกรณ์ พบว่า การแตกตัวเชิงเร่งปฏิกิริยาของน้ำมันเมล็ดเรพบนตัวเร่งปฏิกิริยา MgO ให้ร้อยละของแนฟทาสูงอย่างชัดเจน การแตกตัวเชิงเร่งปฏิกิริยาของน้ำมันเมล็ดเรพบนตัวเร่งปฏิกิริยา HZSM-5 ให้ร้อยละของแก๊สโมเลกุลไฮโดรคาร์บอนขนาดเล็ก อาทิเช่น CH_4, CO_2, CO ในปริมาณที่สูงมาก ส่วนการการแตกตัวเชิงเร่งปฏิกิริยาของน้ำมันเมล็ดเรพบนตัวเร่งปฏิกิริยา Fe/AC ให้ร้อยละของดีเซลเป็นหลัก อัตราการเปลี่ยนของ Long residue เป็นผลิตภัณฑ์ ณ ช่วงเวลาต่างๆ ถูกนำมาศึกษาจลนพลศาสตร์ของ HZSM-5, 1%wt Fe/AC และ MgO พบว่าทั้ง 3 ตัวเร่งปฏิกิริยามีอัตราการเกิดปฏิกิริยาเป็นอันดับ 2 โดยให้ค่าพลังงานกระตุ้น 29.497 KJ/mol, 44.616 KJ/mol and 77.314 KJ/mol ตามลำดับ จากนั้นจึงทำการศึกษาการผลิตเชื้อเพลิงเหลวในระบบต่อเนื่องขนาด 3 ลิตร โดยใช้ MgO ขอบเขตของตัวแปรที่ศึกษามีดังนี้ อุณหภูมิในการทำปฏิกิริยา 390 และ 450 องศาเซลเซียส อัตราการป้อนสาร 3 และ 9 มิลลิลิตร/นาที และอัตราการไหลของไนโตรเจน 50 และ 150 มิลลิลิตร/นาที ปริมาณตัวเร่งปฏิกิริยาร้อยละ 30 และ 60 โดยปริมาตรของเครื่องปฏิกรณ์ พบว่า ที่อุณหภูมิในการทำปฏิกิริยา 450 องศาเซลเซียส อัตราการป้อนสาร 5 มิลลิลิตรต่อนาที อัตราการไหลของไนโตรเจน 150 มิลลิลิตรต่อนาที และปริมาณตัวเร่งปฏิกิริยาร้อยละ 50 โดยปริมาตรของปฏิกรณ์ ให้ร้อยละผลิตภัณฑ์ของของเหลวและแนฟทาสูงที่สุด 75.44 และ 36.62 ตามลำดับ เชื้อเพลิงเหลวที่ได้มีค่าความร้อน 44.93 เมกะจูลต่อกิโลกรัม ค่าความเป็นกรด 1.49 มิลลิกรัมโพแทสเซียมไฮดรอกไซด์ต่อกรัม ค่าความหนืด 0.99 เซนตริกสโตก ร้อยละขององค์ประกอบคาร์บอน 85.69 โดยน้ำหนัก และมีหมู่ฟังก์ชันหลักจำพวกอะลิฟาติกไฮโดรคาร์บอน (C-H Stretching) 2850-3000 cm^{-1} เช่นเดียวกับน้ำมันแก๊สโซลีน 95

สาขาวิชา ปิโตรเคมี ลายมือชื่อนิสิต .....

ปีการศึกษา 2558 ลายมือชื่อ อ.ที่ปรึกษาหลัก .....

ลายมือชื่อ อ.ที่ปรึกษาร่วม .....

5373824523 : MAJOR PETROCHEMISTRY
KEYWORDS: CATALYTIC PYROLYSIS, BATCH REACTOR, CONTINUOUS REACTOR,MAGNESIUM OXIDE, CALCIUM OXIDE, HZSM-5, IRON ON ACTIVATED CARBON,KINETIC

WALAIRAT UTTAMPRAKROM: CATALYTIC PYROLYSIS OF RAPESEED OIL TO LIQUID FUELS IN CONTINUOUS REACTOR. ADVISOR: PROF. THARAPONG VITIDSANT, Ph.D., CO-ADVISOR: ASSOC. PROF. PRASERT REUBROYCHAROEN, Ph.D., 163 pp.

Catalytic cracking of rapeseed oil to liquid fuel in continuous reactor was divided into 2 parts. The experiments in the first part were done in batch system using 70 mL micro-reactor in order to find the optimal condition of each catalyst which gives highest %yield of liquid product and naphtha. There were 5 catalysts used in this study which included CaO, MgO, HZSM-5, 1%wt Fe/AC and 5%wt Fe/AC. The experiments were done using 2^k factorial experimental design. The ranges of variables were as followed: reaction temperature at 390 and 450 °C, reaction time at 30 and 60 minutes, initial hydrogen pressure at 1 and 5 bar and catalyst content at 0.5 and 1.0%wt. The results shown that the catalytic cracking of rapeseed oil over MgO gave the significantly on naphtha, the reaction over HZSM-5 gave the highest yield of small hydrocarbon gas as well as CH_4, CO_2, CO whereas, the reaction over Fe/AC gave the most yield of diesel. The kinetic study were investigated due to the conversion of long residue with the reaction time over various catalyst. The results illustrated the second order equation with the Ea of 29.497 KJ/mol, 44.616 KJ/mol and 77.314 KJ/mol due to the study of HZSM-5, 1%wt Fe/AC and MgO respectively. The experiments in the second part were to produce liquid fuel in 3 L continuous reactor by using MgO since it gave best %yield of liquid product and naphtha from five catalysts. The ranges of variables were as followed: reaction temperature at 390 and 450 °C, feeding rate at 3 and 9 mL/min, N_2 gas flow rate at 50 and 150 mL/min and catalyst content at 30 and 60% V/V. It was found that at reaction temperature of 450 °C, feeding rate 5 mL/min, N_2 gas flow rate 150 mL/min and catalyst content 50%V/V gave highest % yield of liquid product and naphtha of 75.44 and 36.62, respectively. The obtained liquid product had heating value of 44.94 MJ/kg, acid value of 1.49 mg KOH/g, viscosity of 0.99 cst, C content of 85.69%wt and the primary functional group were aliphatic hydrocarbons (C-H stretching) 2850-3000 cm^{-1} as same as gasoline 95.

Field of Study: Petrochemistry
Academic Year: 2015

Student's Signature .....
Advisor's Signature .....
Co-Advisor's Signature .....

ACKNOWLEDGEMENTS

I would like to acknowledge the enormous help given to me in creating this dissertation. For their assistance, their patience, and their guidance, I wish to express deepest gratitude to Prof. Tharapong Vitidsant, my advisor and Asst. Prof. Prasert Reubroycharoen Ph.D., my co-advisor for his advice, concern and encouragement throughout the course of this research.

I would like to thank Prof. Pattarapan Prasassarakich Ph.D.,Chairman; Assoc. Prof. Voravee Hoven Ph.D. Assoc. Prof. Nuanphun Chantarasiri Ph.D. and Asst. Prof. Witchakorn Charusiri Ph.D. members of the dissertation committee for precious time, their valuable suggestions and comments.

I would especially like to extend my gratitude and appreciation to my colleague at Energy Research Institute Chulalongkorn University and everyone though their names are not mentioned here. Please remember that without all of you, the preparation of this dissertation could not have been possible.

Also special thanks to my parents,Vachira and Wilawan Uttamaprakrom, for their love, tenderness, care, and support throughout my study for the doctoral degree. Without them, I can not imagine myself having had an opportunity to pursue my doctoral education.

CONTENTS

Page

Page

Page

Page

FIGURE CONTENTS

Page

Page

Page

Page

TABLE CONTENTS

Page

CHAPTER I

INTRODUCTION

The dramatically growth of world population eventually led to increase an energy demand while the fast depletion of fossil fuel sources and overconsumption with an uncertain energy supply, the resources of this kind of fossil fuels are limited and would be run out upon incessant use. Both of the deficiency of resources and increase of energy price will become considerably more severe leads to intensive research and development on renewable energy furthermore, the depletion of fossil energy resources have led to the attentiveness of an alternative energy development as a substitute fuels for conventional petroleum product[1].

Nowaday, vegetable oil crop is widely considered to have potential one of the promising energy sources which have become more gorgeous recently which have been recognized as a promising feedstock for producing liquid fuels in future that can alleviate the energy consumption[1] were many technologies available to convert vegetable oil into biodiesel and direct used as a feed stock into agricultural engine. However, the one of disadvantage of direct used of vegetable oil as liquid fuels are low-quality fuels that cannot be used in conventional gasoline and diesel fuel engines because they are immiscible with petroleum-derived fuels, primarily on account of their high oxygen content [2]. Other challenges for the utilization of pyrolysis oils are that it is acidic, has high water content. In order to improve the property of vegetable oil to an effectiveness biofuels, chemical processes are required to increase its volatility, thermal stability and reduce viscosity [2].

Catalytic cracking are convenient methods for upgrading of the bio-oil. It can be an interesting approach for product selectivity, such as removal of oxygenated groups, increasing calorific value, lowering the viscosity and improving stability. Furthermore, thermal cracking is the only one that can continuously and directly produce a liquid fuels at atmospheric pressure which occurs by heat transfer from a heat source to the vegetable oil in a reactor in the absence of oxygen under temperature rapidly heated at high temperature condition which are promising potential a thermal

fragmentation of long chain hydrocarbon molecule. Thermal cracking is used high-temperature to break down long chain hydrocarbon molecule into smaller hydrocarbon molecules such as alkanes, alkenes, alkadiene and carboxylic acid by heating at high-temperature, the decomposition process is decomposed by heated to form a vapor that can be quenched to produce a bio-fuels as well as naphtha, diesel-like oil, and other value chemicals used either a fuels for directed combustion or can replace conventional fuels for transportation liquid[1]. If there is a good control of cracking it will yieldthe required product. If excessive heat will cause the hydrocarbon molecules as that is too small in gas state which is undesirable and unusable. Furthermore, in catalytic cracking, vegetable oil are deoxygenated in the presence of some shape selective catalysts such as zeolites, whereas in hydrodeoxygenation, hydrogen reacts with oxygenated compounds at high pressures. Deoxygenation with zeolite catalysts can be done in atmospheric pressure, and it does not require the supply for H_2. Cracking reactions involve the rupture of C–C bonds associated with dehydration, decarboxylation, and decarbonylation to produce gasoline and diesel range compounds alleviates the need of H_2 gas which provides a major advantage over the hydrodeoxygenation process [3].

Rapeseed (Brassica napus) is the native name for the group of oilseed plants in the Brassicaceae family. It can be put apart two types - industrial rapeseed or canola. Optically, the seeds of the two types are indistinguishable. The characteristic distinction between the two types is their specific chemical or fatty acid components. Basically, “industrial rapeseed” points to any rapeseed with a high composition of erucic acid in the oil. Canola points to the edible oil plant that is indicated by low erucic acid [4]. Rapeseed is the third largest oil plants in the world after soybean oil and palm oil due to high productivity and high rate of oil production per area. Bio-fuels production from Rapeseed oil, thus not affecting the demand and supply, because it is not suitable for consumption. In many countries, rapeseed oil has been strongly illustrated as potential oils for biodiesel production due to high amount of unsaturated oleic fatty acids and low amount of saturated fatty acids which have affirmative impact on the combustion properties, resistance to oxidation at high temperatures and resistance to the flow at low temperatures[5].

Conversion of rapeseed oil to bio-fuel by catalytic pyrolysis reaction involved heat and catalyst, the transformation of product to the proper structure to be used as needed. The obtained liquid fuel depends on the active catalysts. The preference of catalytic pyrolysis are higher octane, a lesser amount of heavy oil & unsaturated gas and products, comprising a larger percentage of paraffinic and aromatic hydrocarbon, lower coke yield and governor the quality of hydrocarbon product. Thus, the advantage of biofuels production from catalytic cracking of vegetable oil which ability to achieve of energy production replace of petroleum fuels for sustainable energy sources and environmental friendly. Furthermore, biofuels has ability to achieve of energy and high utilization of natural resources in responding to concerned decrease pollution tothe environment resulting from waste disposal[1].

A variety of catalysts were studied on catalytic pyrolysis process to improve the physical and chemical properties of bio-fuel to nearby petroleum fuel. Many metal oxides have been studied for the catalytic pyrolysis of oils; these include alkali earth metal oxides, transition metal oxides, mixed metal oxides and supported metal oxides. Junming, X. et al.[6] studied cracking of Tung oil and Jatropha oil by heating together with CaO catalyst in continuous reactor which were given the conversion of liquid product at 81%wt and 76 %wt from Tung oil and Jatropha oil, respectively. As the results agreement with Junming, X. et al. [7] derived the diesel fuel from soybean oil, Tong oil, Sojak oil, Curcas oil and Palm oil by pyrolysis using base catalyst such as Na_2CO_3, K_2CO_3 and CaO which have chemical composition similar to petroleum based fuel: low acid value and good solubility in diesel oil at low temperature [8]. In addition, Wang, D. et al.[9] studied pyrolysis of corncob with MgO. The results show that the molality of acids decreases 75.88%wt, while the molality of hydrocarbons and CH_4 increases 19.83%wt and 51.05%wt. Among the zeolite catalysts, ZSM-5 zeolites have been investigated widely in different reaction such as cracking, isomerization, of hydrocarbons owing to their activity, shape selectivity and high surface [10]. Bielansky, P. et al. [11] used pure rapeseed oil as feedstock for FCC plants by using an acidic spray dried REUSY-catalyst which is partially coated with ZSM-5-zeolites crytal led to a total fuel yield on total feed of approximately 65m%, the gasoline achieved is oxygen free and contains a high octane gasoline fraction. Moreover, the studies of the effects of ZSM-5 composition mesoporosity on the yield and distribution of aromatics

[12] were reported that the concentration of acid sites inside the zeolite is critical for maximizing aromatic yield. Mesopores within the zeolite slightly increased of coke formation and decreased the formation of the monocyclic aromatics. The selective removal of external acid sites from the ZSM-5 catalysts only slightly increased the catalyst activity but also decreased the selectivity to the desired aromatic products [12-15]. Activated carbon supported iron catalysts: Iron was acid catalysts and widely modified on various catalyst used to improve the chemical properties of the catalyst as well as iron additive on catalytic performance of HZSM-5 which were improved an acidity of HZSM-5 which correlated with catalytic cracking activity as substrate due to its porous structure and adsorption property [16-22].

In study, naphtha fraction which was intensive production from the catalytic pyrolysis of rapeseed oil were investigated in micro-reactor, for this purpose a pyrolysis system was utilized, the discussion are based on the effects of final reaction of temperature, feeding of hydrogen gas due to hydrogen atmospheric, time of reaction according to retention time and effectiveness of heat transfer from heating source into the thermal conversion reaction and %wt of various types of catalyst on the product yields. The 2^k factorial design was performed to investigate the variables which affected on liquid product as well as aromatic content and product distribution. In order to predict the optimum condition in a process to obtain the highest yield of desired product, a statistical approach has been used by several researchers. There are classical as well as statistical methodologies available for optimizations. Statistical methodologies involve the use of mathematical methods for designing and analyzing results [23]. The chemical techniques and physical properties were used to determine on the liquid product which can be used replace a petroleum fuels for the production of sustainable renewable energy. Furthermore, kinetic parameter such as Activation Energy, reaction order and pre-exponential factor were obtained.

Objectives

1. To investigate variables that effected the catalytic pyrolysis of rapeseed oil on the product distribution in batch process as well as the optimum condition with highest percentage of liquid product and naphtha yield.
2. To study the reaction order of catalytic pyrolysis of rapeseed oil in batch reactor and calculated the activation energy (Ea) and pre-exponential factor (k_0) from Arrhenius equation.
3. To determine the catalyst that gave the best percentage of liquid product and naphtha yield in continuous process for producing liquid product.

Research methodology

1. Characterizing primary properties of rapeseed oil including physical properties, decomposition temperature range, chemical composition, fatty acid composition, the boiling point range and the ultimate analysis.
2. Characterizing primary properties of catalyst including composition of five catalysts CaO, MgO, HZSM-5, 1wt%Fe/AC and 5wt%Fe/AC) by EDX and determine surface area of catalyst by BET.
3. Investigating the effectiveness of five catalysts by percentage and product distribution of liquid product in order to find a suitable catalyst in batch process by studying the effects of variables.
4. Investigating the effect of variables on catalytic pyrolysis of rapeseed oil in order to find the optimum condition for desired product by determing these variables:
   1) Effect of temperature on catalytic pyrolysis of rapeseed oil at 390 and 450°C.
   2) Effect of catalyst content on catalytic pyrolysis of rapeseed oil at 0.5 and 1.0%wt.
   3) Effect of initial hydrogen gas pressure on catalytic pyrolysis of rapeseed oil at 1 and 5 bar.
   4) Effect of reaction time on catalytic pyrolysis of rapeseed oil at 30 and 60 min.

5. Using 2^k factorial experimental design to find the variables affect on catalytic pyrolysis of rapeseed oil and use Design expert program to find the optimum condition.

6. Investigating the kinetics, reaction order of catalytic pyrolysis of rapeseed oil in micro-reactor as well as activation energy (Ea) and the pre-exponential factor (k_0) from Arrhenius relationship.

7. Using the selected catalyst from batch process that gave the best percentage of liquid product and naphtha yield then studied the selected catalyst in continuous process to produce the highest percentage of liquid product and naphtha yield. The variables in this experiment are:

   1) Effect of reaction temperature on catalytic pyrolysis of rapeseed oil at 390 and 450°C.
   2) Effect of catalyst content on catalytic pyrolysis of rapeseed oil at 30%wt and 60%wt.
   3) Effect of feeding rate on catalytic pyrolysis of rapeseed oil at 3 and 9 ml/min.
   4) Effect of N_2 gas flow rate on catalytic pyrolysis rapeseed oil at 50 and 150 ml/min.

8. Characterizing liquid product.

   1) To determine the composition of liquid product by simulated distillation gas chromatograph (DGC)
   2) To determine the heating value of liquid product according to ASTM 3286.
   3) To determine the acidity of liquid product.
   4) To determine the ultimate analysis of liquid product.

9. Comparing liquid product with gasoline standard.

10. Analyzing data, make conclusion, write a thesis and research publications.

Expected Benefits

1. To know the performance of five catalysts from the optimum condition that gave the highest percentage of liquid product and naphtha yield.
2. To know the reaction order in order to find the catalytic pyrolysis mechanism of rapeseed oil.
3. To obtain the liquid product that has similar properties to gasoline 95.

CHAPTER II

THEORY AND REVIEWS

1. Rapeseed [4, 5]

Rapeseed is the common name for the group of oilseed plants in the Brassicaceae family. It can be put apart two types - industrial rapeseed or canola. Optically, the seeds of the two types are indistinguishable. The characteristic distinction between the two types is their specific chemical or fatty acid components. Basically, “industrial rapeseed” points to any rapeseed with a high composition (at least 45 percent) of erucic acid in the oil. Canola points to the edible oil plant that is indicated by low erucic acid (less than 2 percent). In Europe, rapeseed as a share of manufacturing to 80 percent of all other raw materials for biodiesel production. Germany is regarded as both a leader in the use of biodiesel and biodiesel production technology from rapeseed.

***Fig 2.* 1** Characteristics of Rapeseed [24]

2. Vegetable oils [25]

Vegetable oils are oils extracted from various parts of oil crops such as seed and flesh. The main components are triglycerides with high viscosity and C_3H_3 is its chemical structure connecting with fatty acids which have different composition. Fat content is 94-96% of the molecular weight of triglycerides. Resulting in difference in properties of each vegetable oil. Vegetable oils are insoluble and non-volatile at room temperatures. It provides high energy and vitamin E. Most vegetable oils contain large amounts of polyunsaturated fatty acids but there is no cholesterol because plants do not synthesize cholesterol.

2.1 Structure and composition of vegetable oils

The main components of vegetable oils are triglyceride as in Fig. 2.2 which consisted of 1 glycerol molecule and 3 fatty acid molecules. Vegetable oils are insoluble and non-volatile at room temperatures.

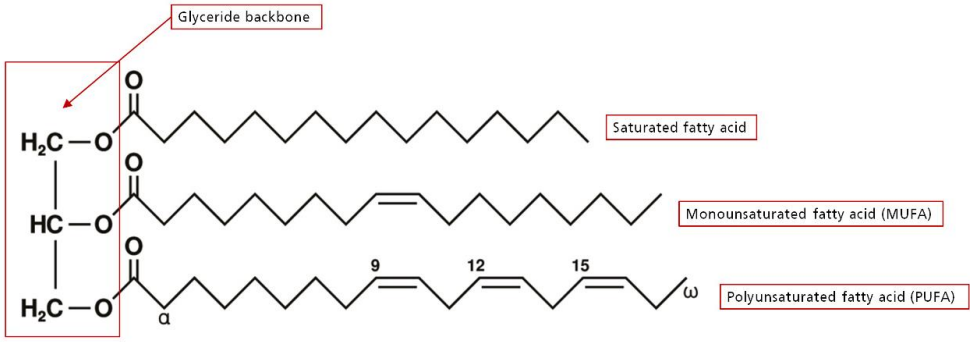

Fig 2. 2 Triglyceride Structure [26]

Fatty acid is an organic acid that contains carbon, hydrogen and oxygen. It usually has an even number of carbon atoms from two atoms and higher. The general chemical formula is R-COOH consisted of two parts, carboxyl with carbon, hydrogen and oxygen and another part is carbon chain with carbon bond as chain. Typically, carbon has four carbon valences the rest valences from binding with carbon will bind with hydrogen. There are various fatty acid, all of them has one carboxyl group. Chemical characteristics of carbon chain resulted in different properties of fatty acid. Fatty acid is divided into two groups:

2.1.1 Saturated fatty acid is fatty acid which the bonds between carbon atoms in molecule are single bond and cannot accept additional hydrogen. The general chemical formula is $C_nH_{2n+1}COOH$. It is stable, does not react with oxygen so there are no lipid oxidation, high melting point compared to unsaturated fatty acid with equal carbon atoms. The most common saturated fatty acid is palmitic acid (C16:0) found in animal fat, coconut oil and palm oil, etc.

2.1.2 Unsaturated fatty acid is a fatty acid which the bonds between the carbon atoms in molecule is double bond at one or more positions. Unsaturated fatty acid commonly found in many vegetable oils such as rapeseed oil, corn oil and olive oil. The most abundant unsaturated fatty acid in vegetable oil is oleic acid (C18:1) and linoleic acid (C18:2)

Table 2.1 – 2.2 show fatty acids found in most vegetable oils and ratio of saturated fatty acid and unsaturated fatty acid in some vegetables oil

Table 2. 1 Fatty acids found in most vegetable oils [27]

Fatty acids	Lipid number	Isomer
Saturated		
Lauric	12:0	-
Myristic	14:0	-
Palmitic	16:0	-
Stearic	18:0	-
Monosaturated		
Oleic	18:1	9c
Pentrocerenic	18:1	6c
Erusic	22:1	13c
Polyunsaturated		
Linoleic	18:2	9c12c
Linoleic(α)	18:3	9c12c15c
Linoleic (γ)	18:3	6c9c12c

Table 2. 2 The ratio of saturated fatty acid and unsaturated fatty acid in some vegetables oil [27]

Vegetable Oil	**Lipid Number**				
	16:0	**18:0**	**18:1**	**18:2**	**18:3**
Cocoa butter	26	34	35	-	-
Corn	13	3	31	52	1
Cotton seed	27	2	18	51	Tr
Lin seed	6	3	38	41	Tr
Olive	10	2	78	7	1
Palm	44	4	39	11	Tr
Safflower	7	3	14	75	-
Rapeseed (High Erusic)	3	1	16	14	10
Rapeseed (Low Erusic)	4	2	56	26	10
Tung Oil	10.2	3.7	7.1	1.8	82.3
Jatropha	14.9	6	41.2	37.4	-
Soybean Oil	11	4	22	53	8
Sesame Oil	9	6	41	43	-
Sunflower Oil	6	5	20	60	Tr

3. Biofuel [27, 28]

Biofuel is liquid synthetic fuel produced from bio-chemical processing such as pyrolysis, fermentation and trans-esterification unlike fossil fuels, biofuel is renewable energy which is restorable and reconstitutable. The crop used in biofuel production can be replanted and biofuel are not accumulated carbon dioxide in the atmosphere. Biofuel can be divided by the molecular composition as follows:

1.1 Oxygenated biofuel such as ethanol, butanol and biodiesel.

1.2 Hydrocarbon biofuel such as pyrolysis oil, green gasoline, green jet and green diesel.

Biofuels divided by source such as:

- Primary biofuels: Biofuels derived from nature and no thermo-chemical treatment such as firewood and bark.

- Secondary biofuels: Gaseous biofuels (such as synthetic gas, methane and hydrogen gas), liquid (such as pyrolysis oil, ethanol and biodiesel) and solid from transformation of primary biofuels. Most of these biofuels are used in transportation and industrial processes at high temperatures.

The development era of secondary biofuels synthesis method can be classified by raw materials as follows:

- 1st Generation: Biofuel production from edible raw materials by the physical-chemical conversion and biochemical conversion. Raw materials are cassava, sugarcane, corn, and edible vegetable oil such as palm oil and soybean oil. The limitations of 1st generation production are: it may cause a shortage of human and animal food sources and a shortage of arable land if there is no proper allocation of raw materials for biofuels production and for consumption or cultivated land are inappropriately allocated.

- 2nd Generation: Biofuel production through thermo-chemical and bio-chemical from plants that are not used for consumption or various wastes from agriculture, industries and communities such as rice husk, straw, wood chips, used vegetable oil, used plastics and sludge from wastewater treatment system.

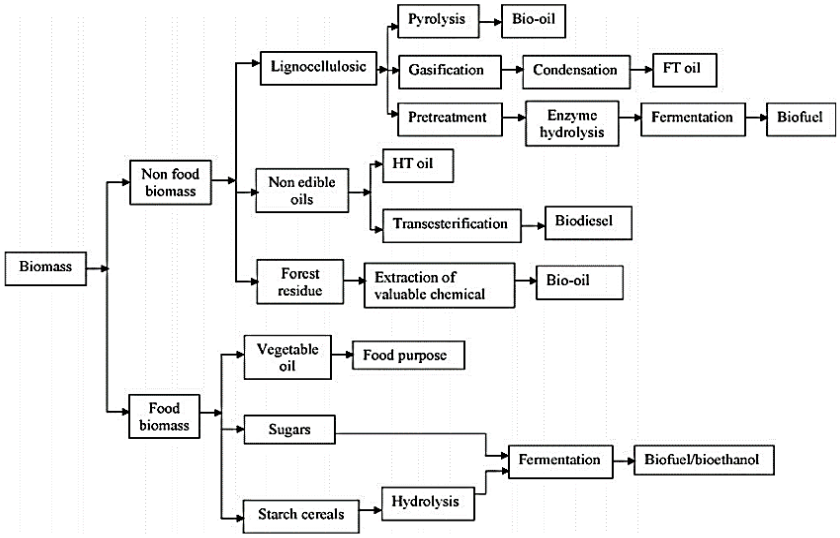

Fig 2. 3 The 1st Generation biofuel production from food biomass & The 2nd Generation biofuel production from non food biomass [28]

- 3rd Generation: Biofuel production from freshwater algae and seaweed. There are many advantages for cheaper raw materials and does not require to share the cultivated area with other plants for consumption because they can be cultured in freshwater or seawater.

- 4th Generation: Biofuel production by using genetic engineering technology such as genetic manipulation of algae in order to accumulate high amount of CO_2. However, the limitations of this technology are high price and not be done commercially.

4. Cracking mechanism of vegetable oils.

Vegetable oils contain triglycerides through the carboxyl group that are glycerol is the core. All double bonds are cis-configuration position. The physical and chemical features of vegetable oil depends on the type and ratio of essential fatty acids [29-31]. Another alternative that can change vegetable oils into clean fuel with properties close to refined petroleum, is to transform vegetable oil by heat (pyrolysis). There are two models of triglycerides below.

4.1. Thermal and catalytic cracking of vegetables oil [32, 33]

In case of there is water mixed in vegetable oil, hydrolysis occurs and gives glycerol and carboxylic acid, the free fatty acid as shown in Fig. 2.4. If there is no water in vegetable oil, the reaction give free fatty acid, ketone and acrolein compound which will further crack and react as in (2.1) – (2.16) hydrocarbon, paraffin and olefin such as hydrocarbon gas, gasoline, kerosene, light gas oil and CO_2.

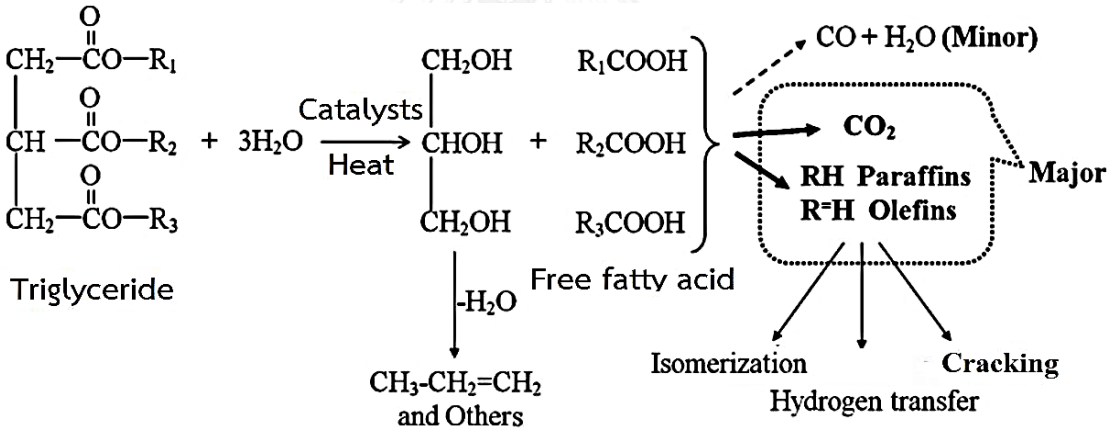

Fig 2. 4 Catalytic thermal cracking of vegetable [34]

Cracking of vegetable oil without water [35]

1) Decompostion of triglyceride

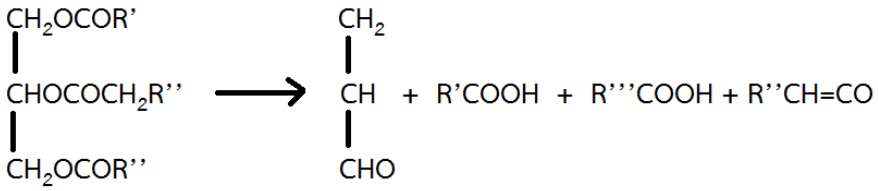

(2.1)

2) Decomposition of free fatty acids

$$RCOOH \longrightarrow CO_2 + RH \quad (2.2)$$

$$2\ RCOOH \longrightarrow CO_2 + H_2O + RCOR \quad (2.3)$$

3) Decomposition of ketene and acrolein

$$2R''CH{=}CO \longrightarrow 2CO + RHC{=}CHR \quad (2.4)$$

$$CH_2{=}CHCHO \longrightarrow CO + C_2H_4 \quad (2.5)$$

$$RCOCH_2R \longrightarrow R\text{-}R + CH_2CO \quad (2.6)$$

$$2RCOCH_2R \longrightarrow 2R_2 + CO + C_2H_4 \quad (2.7)$$

4) Decomposition into elements

$$C_nH_{2n+2} \longrightarrow nC + (n+1)H_2 \quad (2.8)$$

5) Dehydrogenation of paraffins

$$C_nH_{2n+2} \longrightarrow C_nH_{2n} + H_2 \quad (2.9)$$

6) Splitting Decomposition of paraffins

$$C_nH_{2n+2} \longrightarrow C_{n-m}H_{2n-2m+2} + C_mH_{2m} \quad (2.10)$$

7) Alkylation of paraffins, reverse of number 6

8) Isomerization of paraffins

$$N\text{-}C_nH_{2n+2} \longrightarrow iso\text{-}C_nH_{2n+2} \quad (2.11)$$

9) Aromatic cyclization of paraffins

$$C_{(2n+6)}H_{(2n+14)} \longrightarrow C_nH_{2n+1} + 4H_2 \quad (2.12)$$

10) Polymerization of paraffins

$$2C_nH_{2n} \longrightarrow C_{2n}H_{4n} \quad (2.13)$$

$$C_nH_{2n} + C_mH_{2m} \longrightarrow C_{(n+m)}H_{2(n+m)} \quad (2.14)$$

11) Depolymerization of olefins, reverse of number 10

12) Decomposition of olefins to diolefins

13) Decomposition of olefins to acetylenic hydrocarbons

14) Aromatization of cyclization of olefins

15) Hydrogenation of olefins

$$C_nH_{2n} + H_2 \longrightarrow C_nH_{2n+2} \quad (2.15)$$

16) Isomerization of olefins

$$N\text{-}C_nH_{2n} \longrightarrow \text{iso-}\ C_nH_{2n} \quad (2.16)$$

4.2. The hydrogen cracking [36, 37]

Cracking along with using hydrogen is combination of catalytic cracking and hydrogen addition. The products are high branched molecule including parafiins and naphthene. This reaction starts with carbonium ion formation at acidic surface of catalyst as in equation (2.17).

$$R_1\text{-}\ CH_2\text{-}CH_2\text{-}R_2 \xrightarrow{\text{Catalyst}} R_1\text{-}\ CH_2\text{-}{}^{+}CH\text{-}R_2 + H^{+} \quad (2.17)$$

Carbonium ion may rearrange and eliminate proton from olefins of crack at β-position to give olefins and new carbonium ion as products. After that hydrogenation and dehydrogenation. Olefins in hydrogenation become paraffin compound as in equation (2.18) – (2.20) [36, 37].

$$R_1\text{-}\ CH_2\text{-}{}^{+}CH\text{-}R_2 \xrightarrow{-H^{+}} R_1\text{-}\ CH{=}CH\text{-}R_2 \quad (2.18)$$

$$R_1\text{-}\ CH_2\text{-}{}^{+}CH_2\text{-}R_2 \xrightarrow{\text{B-Scission}} R_2\text{-}\ CH{=}CH_2 + R_1{}^{+} \quad (2.19)$$

$$R_2\text{-}\ CH{=}CH_2 + H_2 \xrightarrow{\text{Catalyst}} R_2\text{-}\ CH_2\text{-}CH_3 \quad (2.20)$$

Hydrogenation result in saturated product and hydrogenation at acid site of catalyst also eliminate coke on catalyst surface. Cracking along with hydrogenation is exothermic reaction resulting in high temperature in reactor. It needs to properly control temperature because if the temperature is too high, coke will form and catalyst loss it activity or causes damage to reactor as well as desire product is not formed[37].

4.3. The catalytic cracking of vegetables oil with metal oxide [6, 7, 33, 34]

When heating, triglyceride which is the composition of vegetable oil decomposes and gives free fatty acid and glycerol. The obtained free fatty acid further decompose via decorboxylation give CO_2, paraffin and olefins as products as shown in Fig. 2.5. These products further react especially olefins due to reactive unsaturated bond.

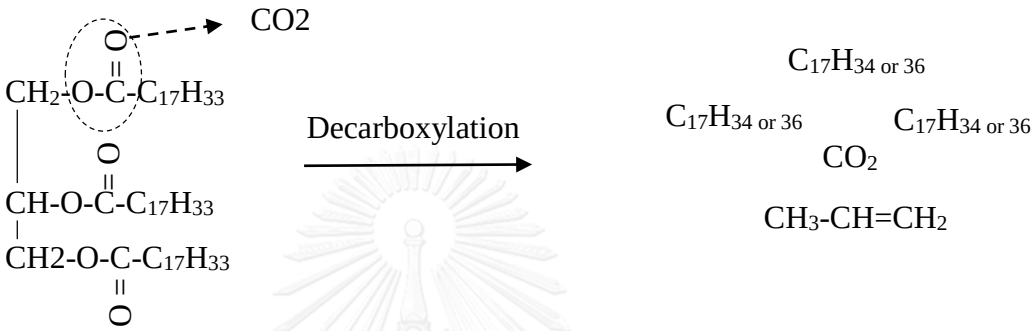

Fig 2. 5 Decarboxylation

Important cracking reaction of vegetable oil:

1. Hydrolysis of triglyceride: the products are glycerol and free fatty acid as in equation (2.21).

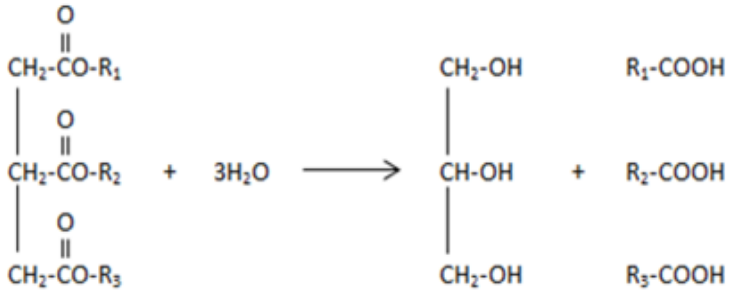

(2.21)

2. Hydration of glycerol: the products are hydrogen gas and water as in equation (2.22).

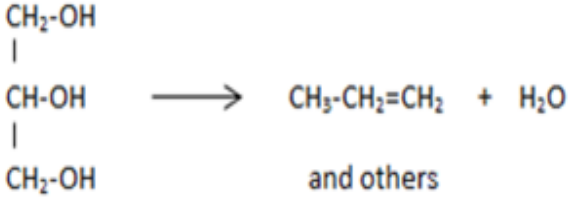

(2.22)

3. Decomposition of free fatty acid: the products are carbon dioxide gas and hydrocarbon compound as in equation (2.23).

$$RCOOH \rightarrow CO_2 + R\text{-}H \quad (2.23)$$

4. Decarboxylation: removing of –COOH group (decarboxylation) from fatty acid. The products are hydrocarbon compound and carbon dioxide gas as in equation (2.24).

$$R\text{-}COOH \rightarrow R\text{-}H + CO_2 \quad (2.24)$$

Metal oxide catalysts such as MgO and CaO with base properties improve decarboxylation and react with free fatty acid to give $MgCO_3$/$CaCO_3$ and hydrocarbon compound as in equation (2.25).

$$MgO + R\text{-}COOH \rightarrow MgCO_3 + R\text{-}H \quad (2.25)$$

$MgCO_3$ can decompose into MgO allow the continuous catalysis as in equation (2.26).

$$MgCO_3 \rightarrow MgO + CO_2 \quad (2.26)$$

If use CaO instead of MgO in equation (2.48), the reaction give $CaCO_3$ that is more stable than $MgCO_3$ which requires high reaction temperature (above 973 K) to decompose into CaO.

5. Decarbonylation of ketone give hydrocarbon compound and carbon monoxide as products as in equation (2.27).

$$R\text{-}CHO \rightarrow R\text{-}H + CO \quad (2.27)$$

Hydrocarbon compound from reaction according to (2.23), (2.24) and (2.25) is paraffin and olefin which can further react as follow:

6. Cracking of large hydrocarbon molecule into smaller hydrocarbon molecule as in equation (2.28).

$$CH_3\text{-}(CH_2)_4\text{-}CH_2\text{-}CH_2\text{-}C^{\bullet}H_2 \rightarrow CH_3\text{-}(CH_2)_4\text{-}C^{\bullet}H_2 + CH_2{=}CH\text{-}CH_3 \quad (2.28)$$

7. Large hydrocarbon molecule transfer hydrogen to free radicals as a small hydrocarbon molecule and large hydrocarbon molecule becomes a new free radicals which can further react as in equation (2.29).

$$CH_3\text{-}CH_2\text{-}C^{\bullet}H_2 + CH_3\text{-}(CH_2)_4\text{-}CH_3 \rightarrow CH_3\text{-}CH_2\text{-}CH_3 + CH_3\text{-}(CH_2)_4\text{-}C^{\bullet}H_2 \quad (2.29)$$

8. Isomerization transforms the structure of hydrocarbon molecule from straight chain into branch chain structure as in equation (2.50).

$$CH_3\text{-}CH_2\text{-}CH_2\text{-}CH_3 \rightarrow \begin{matrix} CH_3\text{-}CH\text{-}CH_3 \\ \quad\quad | \\ \quad\quad CH_3 \end{matrix} \qquad (2.50)$$

5. Catalyst [32, 35, 36, 38, 39]

The catalyst is a substance that increase reaction rate or resulting in faster reaction when added to reaction mixture and selective to desired products in any chemical reaction. Catalyst may be or may be not involved in reaction. However, when the reaction is terminated the catalyst must not be used in the reaction, or have to be at the same amount. That is, catalyst is a substance that increases reaction rate without causing any changes to thermodynamic of system. Moreover, adding catalyst make system reach equilibrium faster because it lowers activation energy of the reaction resulting in more molecules with higher energy or equal to activation energy so chemical reaction is faster.

Catalyst properties

1. Do not disturb the equilibrium of the reaction.
2. Lower activation energy of reaction.
3. Must be substance (not energy).

5.1. Heterogeneous catalyst

A catalyst in different phase with substrate mostly in solid which used to accelerate reaction of gaseous or liquid substrate. Chemical reaction takes place at the surface of catalyst with sorption-desorption of substrate on catalyst surface as a part of reaction. The advantages of heterogeneous catalysis are such as less toxic of heterogeneous catalyst, can be used in high temperature or high pressure reaction, easy to separate catalyst from remaining substrate and product, can be reused and longer lifetime.

Example of a heterogeneous catalyst

- Metal such as iron for synthesis reaction, ammonia and platinum for oxidation of ammonia.
- Supported metal such as nickel on silica for hydrogenation of unsaturated hydrocarbon.
- Metal oxides such as vanadium for partial oxidation of hydrocarbon and formation of sulfuric.
- Zeolite, aluminosilicate complex with specific structure such as ZSM-5 for hydrocarbon cracking.

5.2.1 Heterogeneous reaction mechanism

Reaction catalyzed by heterogeneous catalyst occur on the surface of catalyst always have more than one process with sorption-desorption of substrate on catalyst surface as a part of reaction.

Most of heterogeneous reactions use three phases reactor including of solid as substrate, catalyst, liquid and gas products. The reaction is divided into 7 stages as follows:

1. External diffusion is the diffusion of reactants A from fluid stream through the outer surface of the catalyst to the boundary layer surrounding the catalyst as shown in Fig. 2.6. There is no chemical change in this process.

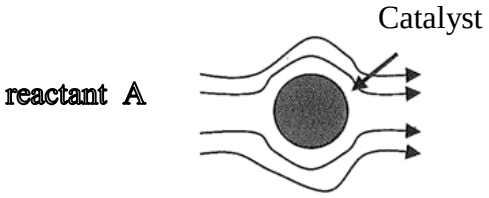

Fig 2. 6 Diffusion of reactants from fluid stream through the outer surface of the catalyst [39]

2. Internal pore diffusion is the diffusion of reactants A outer surface of the catalyst into catalyst pore as in Fig. 2.7. Since catalyst pore have variable size and shape, there is collision in this stage both between reactant A and wall of porous.

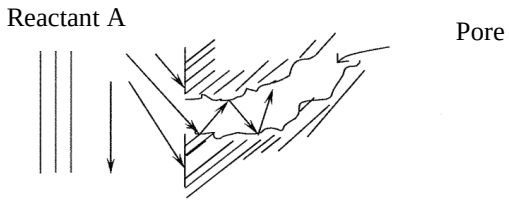

Fig 2. 7 Diffusion of reactants into the internal catalyst pore [39]

3. Adsorption is the adsorption of reactant A on outer surface of catalyst and here are chemical changes in this stage. Catalysis always occur with chemical sorption by chemical bonding between reactant A molecules which called adsorbate and outer surface of solid catalyst which called adsorbent. In Fig. 2.8 this adsorption resulting in the binding of the substrate as a single layer on catalyst surface.

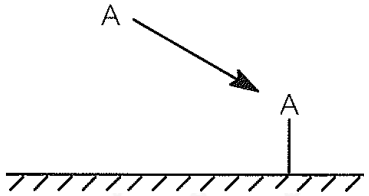

Fig 2. 8 Chemical adsorption of reactant A on catalyst surface [39]

4. Surface reaction, in this stage the reaction occurs at the surface of the catalyst. The reaction of A into B at active site as shown in Fig. 2.9.

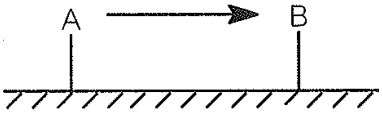

Fig 2. 9 Reaction on catalyst surface from A to B [39]

5. Desorption, in this stage B molecule desorb or detach from catalyst surface after the reaction are terminated as the final step of chemical reaction.

6. Diffusion of product from catalyst porous to the outer surface of catalyst. If the reaction in 4th stage is incomplete, reactant A also diffuse.

7. Diffusion of product B from outer surface of catalyst to the boundary later surrounding catalyst and fluid stream. If the reaction in 4th stage is incomplete, reactant A also diffuse.

5.2 Physical properties of catalyst

The physical properties of catalyst are surface area, pore volume, pore size and pore size distribution.

Surface area of catalyst is very important since surface area is proportional to the catalytic ability. There are active sites resulting from the combination of atoms and molecules on metal surface. Surface area of catalyst can be determined by BET technique which base on inert gas adsorption such as liquid nitrogen gas on catalyst surface. However, this method is quite difficult. Therefore, the best way to increase the surface area of the material is to create many small pores.

Size and number of pores can indicate the amount of surface area within the catalyst. The catalyst with high internal surface area has very dense small pores which result in high dispersion of active site. Pore size in the reaction must be appropriate to precursors and products. It can take the most advantage of active site since pore size is critical to catalytic ability. Pore sizes can be divided into 3 types as:

1. Macropores: Pore size is larger than 50 nm or average pore radius is larger than 25 nm.
2. Mesopores: Pore size is between 2 – 50 nm or average pore radius is between 1 – 25 nm.
3. Micropores or atomic pores: Pore size is smaller than 2 nm or average pore radius is less than 1 nm.

5.3 Adsorption and desorption

Adsorption and desorption are important steps of heterogeneous catalysis. An important characteristic of the catalyst is having suitable surface for adsorption of the reactants. Adsorption is chemical bonding between adsorbent and adsorbate on the active site so that these molecules react further. Desorption is the breaking of chemical bond between adsorbent and adsorbate which recover an active site. Adsorption can be divided into two types: physical adsorption and chemical adsorption.

- Physical adsorption: physical adsorption is caused by weak intermolecular interaction, van der Waals force. Therefore, the heat of adsorption is low (lower than 25 kJ/mol). It is exothermal process. There is no activation energy and no bond cleavage in this process. So the reaction can rapidly occur when molecules reach the adsorbent surface. The reverse reaction of this process can easily occur making it possible to recover the adsorbent or catalyst.

- Chemical adsorption or chemisorption: The simple chemical adsorption is monolayer adsorption. Adsorbent reacts with adsorbate and destroy the original interaction between atoms or groups then atoms are arranged into new compound with stronger chemical bonds. The activation energy is involved. Heat of adsorption is about 60 – 85 kJ/mol. It is irreversible process so it is difficult to remove the adsorbate from the surface of adsorpbent or catalyst.

Table 2. 3 Shows the comparison of differences between physical adsorption and chemical adsorption.

Parameters	Physical adsorption	Chemical adsorption
heat of adsorption	<25 kJ/mol	60-85 kJ/mol
adsorption temperature	around boiling point of adsorbate	generally above boiling point of adsorpbate
intermolecular interaction	Van de Walls force	chemical bond
reversibility	reversible	irreversible
rate, activation energy	very fast, no activation energy	sometimes slow, need activation
adsorption pattern	multilayer, nonspecific	monolayer, specific
pressure effect	strong	weak

6. Metal oxides Catalyst [40]

Metal oxide catalysts : MgO and CaO are the heterogeneous base catalyst. The structure of metal oxides is made up of positive metal ions (cations) which possess Lewis acidity, i.e. they behave as electron acceptors, and negative oxygen ions (anions) which behave as proton acceptors and are thus Bronsted bases (Fig. 2.10)

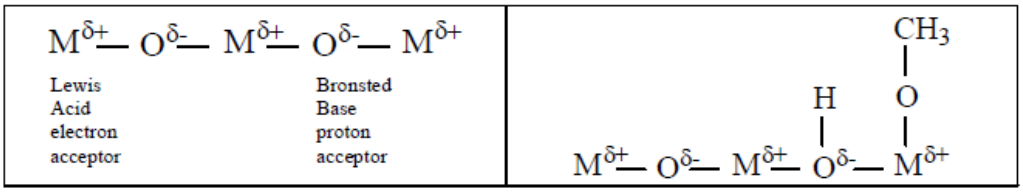

Fig 2. 10 Surface structure of metal oxides [41]

6.1 CaO Catalyst [42]

Calcium oxide (CaO) is the metal oxide catalyst most frequently applied for biodiesel synthesis, probably due to its cheap price, minor toxicity and high availability [43]. It can be synthesized from cheap sources like limestone and calcium hydroxide. Calcium oxide possesses relatively high basic strength.

It can catalyze trans-esterification and cracking reaction. In addition, CaO could be more beneficial in upgrading pyrolysis oils to obtain better liquid yields [9]. Base heterogeneous catalyst in solid state and high melting point. Commonly used as a catalyst because of it low price and high catalysis efficiency. It can catalyze trans-esterification and cracking reaction. It is not corrosive, less soluble in water and easy to separate from reactants and products. Crystal structure of CaO catalyst is showed in Fig. 2.11.

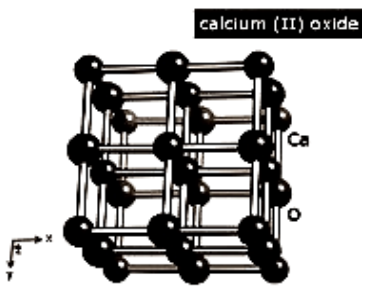

Fig 2. 11 Crystal structure of CaO [44]

6.2 MgO Catalyst [45, 46]

Magnesium oxide (MgO) which is produced by direct heating of magnesium carbonate or magnesium hydroxide has the weakest basic strength. The facet of MgO exposed has an important influence regarding activity and selectivity. Moreover, MgO is high catalysis efficiency cracking of triglyceride in vegetable oil under mild reaction. Base metal oxide with high catalysis efficiency such as trans-esterification of benzaldehyde, decomposition of diacetone alcohol, hydration of acrylonitrile and cracking of triglyceride in vegetable oil etc. Crystal structure of MgO catalyst is showed in Fig. 2.12.

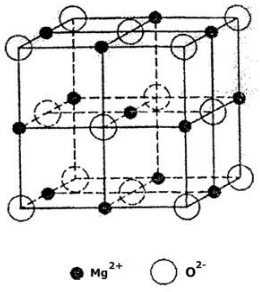

Fig 2. 12 Crystal structure of MgO [47]

7. Zeolite [32, 36, 48]

Zeolite is aluminosilicate complex. Subunit consisting of one silicon or aluminium atom and four oxygen atoms (SiO AlO-4 or 4) boned as tetrahedron. Silicon atom (or aluminium) is at center surrounding with oxygen atom at all four corners. This tetrahedral structure connect with each other by sharing oxygen atom (Fig. 2.13 & Fig. 2.14) resulting in larger crystal structure and there is a space between the molecules. Therefore, zeolites are porous hard connected orderly with each other into three-dimensional structure. Pore size of zeolite is in range of 2 – 10 Å

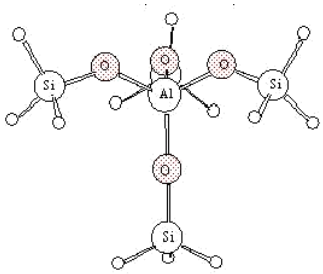

Fig 2. 13 Unit structure of zeolite

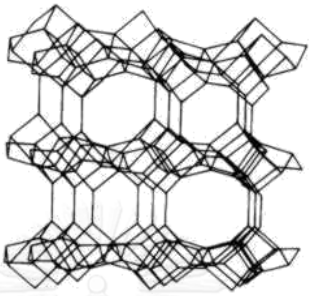

Fig 2. 14 Crystal structure of zeolite

7.1 Important properties of zeolite [39]

Two properties of zeolite that important to catalysis are selectivity and acidity. Selectivity is a result of zeolite structure determined by oxygen atom surrounding the opening. Therefore, the reactants must be smaller than zeolite pores to diffuse and react in pores. For acidity of zeolite, it can be divided into three parts as follow:

1. Acid site such as Bronsted acid has acid site as Si-OH-Al which is important site for catalysis as shown in Fig. 2.15 and Lewis acid, at high temperature in Bronsted acid site can transform into Lewis acid site. It is the conditioning of zeolite due to water are loss from structure as shown in Fig. 2.16.

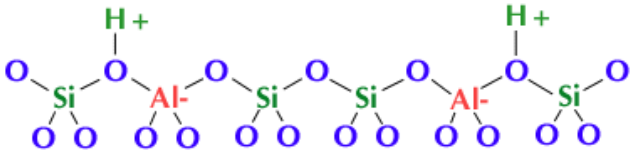

Fig 2. 15 Structure of Bronsted acid site [49]

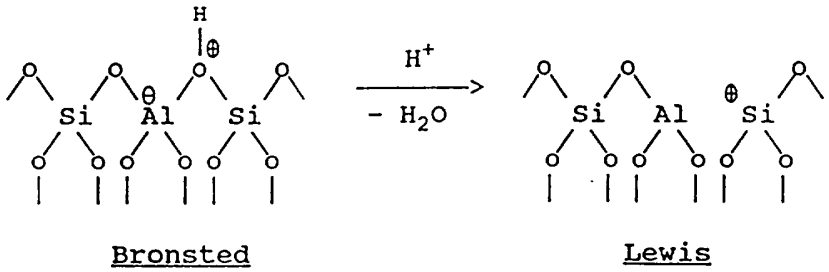

Fig 2. 16 Tranformation of Bronsted acid site into Lewis acid site [39]

2. Amount of acid site is determined by Si/Al ratio. If there is low content of aluminium, zeolite will have more acid site which increase the hydrophobic properties of the zeolite. There are more substrate adsorbed on zeolite surface which may clog at the pores of the catalyst.

3. Acid site strength is also determined by Si/Al ratio. If there is low content of aluminium, zeolite will have more acid site. However, low Si/Al ratio do not affect the strength of the acid site.

7.2 Shape selectivity

The pore and shape in zeolite may effect the selectivity of a reaction in three ways

a) Reactant selectivity

The selectivity occurs when the puncture size of the zeolite is such that it permits only certain smaller molecules and precludes larger molecules.

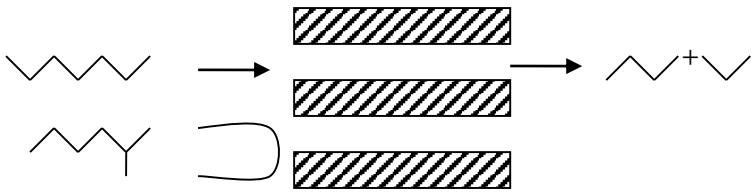

Fig 2. 17 Reactant selectivity [50]

b) Product selectivity

This reaction occurs when large product molecules cannot disperse out, and if formed, they are changed to smaller molecules or to carbonaceous dregs within the pore. These finally may cause pore clog.

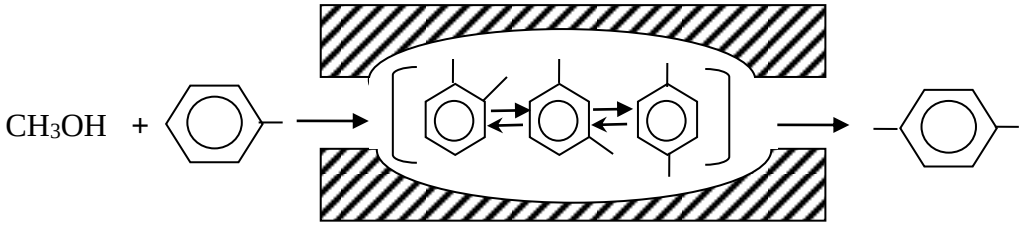

Fig 2. 18 Product selectivity [50]

c) Transient state selectivity

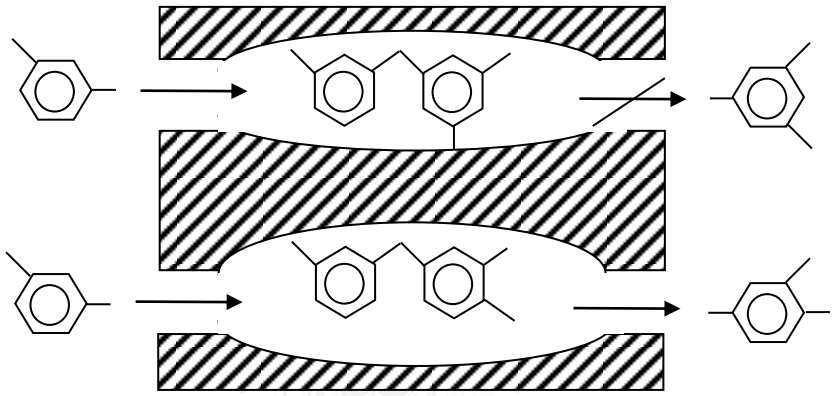

Fig 2. 19 Transient state selectivity [50]

8. Fe/AC

Since activated carbon has high internal surface area, it can adsorb several species. Using some chemical or impregnate metal on surface of activated carbon allow faster adsorption of activated carbon or faster reaction with adsorbent due to changes in the adsorption mechanism by chemical reaction. In this case adsorbate is immobilized by chemical bond. Four important reasons for impregnating chemical or metal on activated carbon surface are:

1. To make activated carbon have constant adsorption efficiency.
2. To improve efficiency in catalysis by synergistic between activated carbon and impregnate.
3. To increase the stability of the active site structure in reaction.
4. To optimize adsorption and catalysis efficiency.

Process after impregnation is calcination and reduction to the metal to get rid of unwanted impurities such as unstable substance, volatile substance. The temperature must be high enough to give initial condition of incipient sintering but not excessive sintering. This may decrease surface area of the activated carbon and active site in the reaction. Metal oxide impregnate on activated carbon is reduced to metal in continuous flow reactor by using hydrogen gas at 300 – 400 °C.

Advantages
- Give liquid product with high naphtha content.
- Decompose large hydrocarbon molecules into small molecules.
- Reaction time is not too long and obtained liquid product with high naphtha content

Disadvantage
- Product is in liquid state with low aromatic content.
- This catalyst is applied to polymeric precursor.
- Coke is easily formed.
- There is long-chain products remaining.

9. Oil quality analysis [36, 51]

An analysis of oil quality in order to determine composition and properties of crude oil by oil refining based on boiling range which divided into small range of 5 – 10 °C. However, oil refining based on boiling range is not popular due to high cost and time consuming. Currently, oil refining is done by dividing into wide boiling point range that suitable for application. The boiling range can be divided into:

1. Initial boiling point (IBP) to 200 °C for gasoline fraction which used in gasoline production.
2. Boiling point between 200 – 250 °C for kerosene fraction which used as lamp oil providing illumination. High quality kerosene oil has no smoke. However, if the freezing point is low it can be used as jet aircraft fuel and depending on other properties of fuel.
3. Boiling point between 250 – 350 °C for light gas oil which used as engine oil.
4. Boiling point between 350 – 370 °C for gas oil fraction which used as diesel engine fuel.

5. Boiling point above 370 °C for high molecular weight residue which can be used in many applications depending on the properties of waste oil such as fuel oil, asphalt or lubricant.

10. Literature reviews

10.1 The research of base catalyst :

Junming, X. et al. [7] studied pyrolysis process of soybean oil using base catalysts at $480-520$ °C and compared acid values of lquid product from catalytic pyrolysis with different catalysts (Al_2O_3, MCM-41, CaO, $CaCO_3$, Na_2CO_3 and K_2CO_3). The GC-MS and FTIR results showed that the products were olefin hydrocarbon, paraffin and carboxylic acid. However, it was found that the content of carboxylic acid was decreased when using base catalysts and lowered acid value compared to acid catalysts. Increasing the amount of catalyst from 1.5%wt to 3.0%wt of soybean oil resulted in lowered percentage of liquid yield as same as acid value was also decreased. The obtained liquid product had cold flow properties and high heating value. This study showed that the pyrolysis soybean oil can be used to produce liquid fuel with properties and chemical composition similar to petroleum fuel.

Junming, X. et al. [8] studied the pyrolysis process of soybean oil by using base catalysts including of Na_2CO_3 and K_2CO_3 at $350-400$ °C. From GC-MS and FTIR results it was found that the products were olefin, paraffin, carboxylic acid and aldehyde. The comparison of liquid fuel from acid catalytic cracking (Al_2O_3, MCM-41) showed that products from cracking processes using Na_2CO_3 and K_2CO_3 had lower acid values and cold flow properties and good solubility in diesel. Therefore, products from pyrolysis of soybean oil have properties and chemical composition similar to petroleum oil.

Srisuwong, T. [52] studied catalytic thermal cracking of Tung oil with CaO and MgO in batch reactor. The results showed that CaO : Tung oil ratio of 2.5% at 440 °C for 38 minutes and hydrogen pressure of 1 bar gauge gave liquid product 37.55 wt% which consisted of naphtha 19.16 wt%, kerosene 11.58% and light gas oil 5.71 wt%. In case of MgO : Tung oil ratio of 2.5 wt% at 402 °C for 30 minutes and hydrogen

pressure of 1 bar gave liquid product 38.83 wt% which consisted of 21.43 wt%, kerosene 8.37 wt% and light gas oil 8.01 wt%. In addition, they also investigated the effect of hydrogen pressure of 1, 3 and 5 bar at constant catalyst ratio, temperature and time. It was found that hydrogen pressure had no effect on liquid yield and composition in liquid product.

Phanupan Prombutr [14] synthesized biofuel from Tung oil, Jatropha oil and rapeseed oil by using FCC, CaO and MgO in batch reactor under hydrogen gas pressure of 1 bar. The results from catalytic cracking of three inedible vegetable oils are not significantly different. The optimum temperature and reaction time of each catalyst is 390 °C and 30 minutes. Liquid content from cracking of Tung oil by using 1 wt% used FCC, 3 wt% CaO and 1 wt% MgO are 78.00, 76.50 and 77.22 wt%. The composition of liquid product from cracking process consisted of naphtha 8.72 - 12.68 wt%, kerosene 9.69 - 12.05 wt%, light gas oil 22.95 - 23.66 wt%, heavy gas oil 4.43 - 4.78 wt%, and long residue 26.52 - 30.72 wt%.

Tani H. et al. [34] studied selective catalytic decaboxylation-cracking of palm oil for liquid fuel with silicon dioxide (SiO_2), magnesium oxide supported on silicon oxide (MgO-SiO_2), carbon (Carbon), magnesium oxide-carbon (MgO-carbon), spent FCC and magnesium oxide (MgO). The results indicated that MgO supported catalyst gave liquid hydrocarbons and CO_2 selectively, from palm oil and other vegetable oil at around 430°C. The hydrocarbon product was composed of paraffins and olefins. Supported MgO promoted the decarboxylation-cracking of triglyceride and free fatty acid. The products showed lower acid value. The product was successfully used for the diesel engine.

Pütün. E. et al. [53] studied the effects of temperature, carrier gas flow rate and MgO in pyrolysis of cotton seed in tubular packed bed reactor under carrier gas flow (N_2) at different temperatures. It was found that without catalyst the highest oil yield was 48.30% at 550 °C, carrier gas flow rate of 200 mL/min. At this optimal condition the pyrolysis of cottonseed at different MgO content (5, 10, 15 and 20 wt% of precursor resulted in decreased oil content but the qualities in term of heating value and hydrocarbon distribution were higher and deoxygenation was lowered from 9.56% to

only 4.90%. Oils from pyrolysis were characterized with column chromatography, FTIR and H-NMR and it was found that there were hydrocarbon compounds such as aliphatic, aromatic and polar hydrocarbons. Aliphatic hydrocarbons were also analyzed with GC-MS. From the results it could be concluded that liquid fuel from catalytic pyrolysis resulted in low molecular weight hydrocarbon compounds in range of diesel when compared to petroleum oil.

Idem, R.O. et al. [54] studied the effect of temperature in range of 400 – 500 °C and flow rate of feedinf on cracking reaction of canola oil to liquid product using calcium oxide and magnesium oxide as catalysts in continuous reactor. For calcium oxide, the optimal condition that gave highest liquid product yield and conversion rate was at the ratio of calcium oxide to canola oil of 2 %wt, 500 °C and flow rate of 12.1 per hour. This condition gave percentage yield of 37.2% liquid product, 4.3% residual oil, 56.2% gas and 2.2% solid by weight and the conversion rate was 95.7%. For MgO, the optimal condition is similar to calcium oxide but the reaction temperature was 400 °C. This optimal condition gave percentage yield of 36.8% liquid roduct, 33.7% residual oil, 19.8% gas and 8.0% solid and the conversion rate of canola oil was 56.3%.

Jungchareonpanit, C. [55] have studied the catalytic pyrolysis of used cooking oil into liquid fuel on MgO and activated carbon in 3-L continuous reactor at temperature of 380-430 °C, feeding rate of used cooking oil of 60-180 mL/h, carrier gas feeding rate of 100-300 mL/min, MgO and activated carbon content of 30-60% of reactor volume and 2 level factorial experimental design is used to study the effect of factor affecting %yield of oil product to obtain the optimum content and compositions. Content and compositions of products are analyzed by Simulated Distillation Gas Chromatography (DGC) under the optimum condition obtained from Design Expert. It is found that the optimum condition for catalytic cracking of used cooking oil into liquid fuel on MgO and activated carbon which are 430 °C, used cooking oil feeding rate of 66.60 mL/h, carrier gas feeding rate of 100 mL/min and MgO and activated carbon content of 60.00% by weight results in liquid fuel 74.78%, naphtha 20.17% and diesel 43.82% by weight.

10.2 The research of acid catalyst :

Buzetzki, E. et al. [56] studied the catalytic cracking of rapeseed oil at 350 – 440 °C and effects of type (NaY, HY, NH4Y, Na-ZSM5, HZSM-5 , CL) and content of zeolite on product composition and liquid fuel properties such as viscosity and acid values. The analysis results showed that without catalysts the %yield of liquid product was low but gas content was high. The zeolite catalysts that affected the catalytic cracking of rapeseed oil the most were NaY, HY and CL. The %yield of liquid product was 85- 90% within 20-30 minutes. The GC/MS analysis showed that liquid products consisted of olefin, paraffin and carboxylic acid. The different catalysts resulted in similar product composition. However, acid values of liquid product were ranged 100-140 mg KOH/g. ZSM5 resulted in highest acid value. This study solved the problem of high acid value and viscosity by mixing with fuel with appropriate viscosity.

Thanh-An Ngo et al. [57] studied the catalysis pyrolysis of soybean oil by using packed-bed reactor under nitrogen flow at 420 and 450 °C. The catalysts used in the study were HZSM-5 (molar ratio of SiO2/Al2O3 = 28, 40 and 180) and MCM-41 coated with Ga, Al and Cu at 2 wt%. The effects of catalysts on pyrolysis process were studied. It was found that the catalysts affects yield and composition of product. The gas products mainly consisted of methane, ethane and propylene gas. For liquid products it was found that Ga/MCM-14 and M28-1 catalysts resulted in highest oil %yields which were 77.3 and 71.3%, respectively. When HZSM-5 was used, the liquid product mainly consisted of aromatic compounds such as aromatics, toluene and xylene. For MCM-41, liquid product mainly consisted of alkanes, alkenes, alkadienes, aromatics and carboxylic acid.

Lima et al. [58] studied the thermal cracking of three vegetable oils including of soybean, palm and castor oils at 350 – 400 °C. The liquid products were obtained at 4 temperature ranges. The chemical and physical properties of liquid product at lower than 200 °C were similar to petroleum fuel. Zeolite catalyst (HZSM-5) was also used in pyrolysis of soybean oil in order to reduce the viscosity of obtained oil. The GC-MS and FTIR analysis of liquid fuels from 3 vegetable oils showed that they consisted of olefin, paraffin, carboxylic acid and aldehyde. The comparison of product

chromatograms from soybean oil pyrolysis with and without catalysts showed that carboxylic acid peak was obviously decreased. It indicated that catalyst resulted in the decreasing of oxygen and the properties of liquid product were more similar to petroleum fuel.

Sawasraksa, R. [59] studied catalytic thermal cracking of Jathropa oil with H-ZSM5 in batch reactor under hydrogen pressure of 6.8 bar gauge at catalyst ratio of 6.35 wt%, 426 °C and 56 minutes. This reaction resulted in 93.62% conversion. The gas, liquid and solid product are 25, 60.5 and 14.5 wt%, respectively. The composition of liquid products consisted of naphtha, kerosene, light gas oil, heavy gas oil and heavy oil residues are 38.35, 0.31, 16.44, 1.56 and 3.84 wt%, respectively. Thermal cracking at same condition gave higher liquid product to 65 wt% and lower naphtha content to 20.10 wt%.

Chookiert, D. et al. [60] studied catalytic cracking of used vegetable oil by using HZSM-5 in batch reactor. The results show that at HZSM-5 : used vegetable oil ratio of 0.5 wt%, 380 °C for 30 minutes under hydrogen gas pressure of 1 bar gave liquid product 71.48 wt% (consisted of naphtha 42.89 wt%, kerosene 5.60 wt%, gas oil 15.52 wt% and heavy oil residue 7.47 wt%), gas 22.14 wt% and solid 6.38 wt%.

Mongkol, M. [61] studied the catalytic cracking of vegetable oil by using 0.05 – 0.2 g of HZSM-5 as catalyst, 0.5 – 2.0 g of Fe/activated carbon. The cracking process was performed at 400 -430 °C, reaction time 30 – 45 minutes, hydrogen gas pressure 10 – 30 bar in order to find the optimum condition for cracking. For Fe/activated carbon the condition that gave highest naphtha yield was at 430 °C, 0.5 g of Fe/activated carbon, reaction time of 60 minutes and hydrogen gas pressure of 10 bar. The liquid fuel yield of this optimum condition was 79.74% by weight, the compositions of product were 28.14% naphtha, 16.56% kerosene, 21.86% light gas oil, 3.26% heavy gas oil and 9.91% residual oil by weight. For HZSM-5, the condition that gave highest naphtha yield were at 430 °C, 0.5 g of HZSM-5, reaction time of 60 minutes and hydrogen gas pressure of 10 bar. The liquid fuel yield of this optimum condition was 83.60 by weight, the compositions of product were 26.75 % gasoline, 13.79% kerosene, 22.99% light gas oil, 3.76% heavy gas oil and 16.30% residual oil by weight.

Wannawong, C. [61] studied catalytic cracking process of physic nut oil by using FCC in 70 mL batch reactor. It was found that when the ratio of FCC to physic nut oil was 1 wt% at 410 °C, reaction time was 30 minutes and hydrogen gas pressure was 1 bar gauge, the gas, liquid and solid product were 12.75, 85,37 and 1.88 wt%, respectively. The compositions of liquid product were 10.36% naphtha, 6.06% kerosene, 44.82% light and heavy gas oil and 24.13% heavy residual oil by weight. In addition the study of effect of hydrogen gas pressure at 1, 3 and 5 bar gauge showed that hydrogen gas pressure did not affect yield and composition of liquid product when the ratio of catalyst to physic nut oil, temperature and time were constant.

10.3 The research of Fe/AC :

Sekine, Y. et al. [62] studied iron and activated carbon catalysts by comparing between Fe/AC and Fe/SiO and investigated the effect of hydrogen gas on the distribution of products in degradation of polypropylene by using catalyst. The results showed that iron catalyst allowed the consumption of hydrogen gas in degradation of solid while activated carbon aided in degradation of heavy oil into light oil which resulting in highest liquid fuel when using Fe/AC catalyst.

Choochuay, P. [17] studied the effect of Fe/AC at 385 – 425 °C for 30 – 90 minutes under initial hydrogen pressure of 20 – 40 kg/cm^2 on cracking of Polybutene-1 into liquid fuel with Fe/AC catalyst. The results showed that at 410 °C, 60 minutes and initial hydrogen pressure 40 kg/cm^2 resulted in 6.86 %wt gas, 88.57 %wt liquid product and 4.57 %wt solid, respectively.

Insuk, S. [18] studied cracking of acrylonitrile-butadiene-styrene and used lubricant oil with Fe/AC catalyst in batch reactor. The optimum condition in reaction is at weight ratio of acrylonitrile-butadiene-styrene and used lubricant oil ratio of 4:6, catalyst ratio of 2.5 %wt, 450 °C, reaction time 90 minutes, hydrogen pressure 100 psi gave maximum liquid product of 60.52 %wt (consisted of naphtha 38.60 %wt, kerosene 7.64 wt%, light gas oil 13.17 %wt, heavy gas oil 1.48 %wt and heavy oil residuals 4.44 %wt, gas 24.21 %wt and solid 13.50 %wt.

Sumarin, J. [19]studied cracking of used lubricant oil by using 5 %wt Fe/AC in piping reactor at 0.1 – 1.0 %wt of Fe/Ac, temperature 390 – 450 °C, flow rate of feed 0.34 – 3.30 g/min. The results showed that the optimum condition form cracking is 1.0 %wt Fe/AC, temperature 430 – 450 °C, flow rate of feed 2.77 g/min which gave liquid product 57.21 - 57.36 %wt that consisted of naphtha 18.81 – 20.32 %wt, kerosene 3.96 – 4.01 %wt, light gas oil 11.27 – 11.87 %wt, heavy gas oil 2.40 – 2.64 %wt and heavy oil residues 19.22 – 20.28 %wt.

Li, M. et al. [21] studied catalytic cracking of fuel oil with Fe/AC and Ni/AC in batch reactor at 430 °C for 60 minutes under hydrogen atmosphere of 6 Moa. The distribution of products by boiling point are < 180 °C : 9.13 %wt, 180 – 360 °C : 31.37 %wt, 360 – 450 °C : 32.75 %wt and > 450 °C : 26.27 %wt.

Taepakdee, P. [63] studied the cracking process of the mixture of used lubricant oil and plastic, polypropylene (PP) and polystyrene (PS). The cracking process was performed by using Fe/activated carbon as catalyst in 70 mL batch reactor under hydrogen atmosphere and 15 g of total raw materials. The studied contitions were the ratio of used lubricant oil at 50 : PP25 : PS25 (PP : PS = 50 : 50) and 60 : PP28 : PS 12 (PP : PS = 70 : 30), the ratio of Fe/AC at 1, 5 and 10 %wt, the ratio of catalyst at 0.15 – 1.5 (0.1 – 1.5 g of Fe/AC per 15 g of raw material), reaction temperature of 390 – 450 °C, reaction time of 45 – 105 min and hydrogen pressure of 1 - 10 bar. It was found that the optimum condition was at used lubricant oil of 50 : PP25 : PS25, Fe/AC ratio of 5 %wt, catalyst ratio of 0.15 %wt, temperature 430 °C, reaction time of 75 min and hydrogen pressure of 1 bar. This optimum condition gave gas 17.37 %wt, liquid product 75.56 %wt (consited of 46.34 %wt naphtha, 10.02 %wt kerosene, light gas oil 11.98 %wt, heavy gas oil 2.76 %wt and heavy residual oil 4.55 %wt) and solid 6.98 %wt.

Jarusiri, W. [20] studied effect of temperature, flow rate of hydrogen gas and flow rate of feeder mixture of used vegetable oil, used lubricant and propylene on catalytic thermal cracking in continuous reactor. The results showed that at the ratio of used vegetable oil, used lubricant oil and propylene of 0.7 : 0.1 : 0.2 %wt, temperature 550 °C, hydrogen gas flow rate 5 mL/min, feeder flowrate 1.23 g/min on 5 %wt Fe/AC

catalyst resulted in maximum naphtha yield of 50.95 %wt, kerosene 10.38 %wt, light gas oil 21.68 %wt, heavy gas oil 10.92 %wt and long residue 16.99 %wt.

Jansopapitr, K. [21] studied catalytic cracking of bovine wax by using 10 %wt Fe/AC in batch reactor. The studied variables are 0.25 – 1 %wt Fe/AC, temperature 400 – 430 °C, reaction time 30 – 90 minutes and hydrogen gas pressure 1 – 5 bar. The results showed that the optimum condition at 0.75 %wt Fe/AC, 400 °C, reaction time 69.51 minutes and hydrogen pressure of 1 bar gave gas 29.37 %wt, liquid product 68.14 %wt (consisted of naphtha 33.68 %wt, kerosene 9.22 %wt, light gas oil 21 %wt and heavy oil residue 4.30 %wt) and solid 2.45 %wt at 95.29 %wt conversion.

CHAPTER III

MATERIALS AND METHODS

3.1 Batch experimental

This research was conducted to study the factors that influence the catalytic cracking reaction of rapeseed oil to liquid fuel on base, acid and neutral heterogeneous catalysts in batch reactor by determining the optimum conditions of the catalytic cracking in batch reactor in order to obtain the maximum yield of liquid fuel with the appropriate composition and investigate the kinetic parameters for each types of catalyst.

3.1.1 Instruments

1. The batch reactor is stainless micro-reactor of 70 mL. The top of reactor is covered by stainless lid with gas compressor device and safety valve. The experiment can be done under the condition of 500 °C and 10 kPa. There is a thermocouple slot for measuring the temperature inside the reactor during the experiment.

Fig 3. 1 70 mL micro-reactor.

2. Temperature controller is used to control the power supply from transformer to heating coils and stop power supply when the required temperature is obtained. It can control the temperature at ± 10 °C.

3. Injection heating coil with voltage of 230 volts and power of 400 watts.

4. K-type thermocouple for measuring temperature with 1.6 mm diameter.

5. Reactor controller device with motor to drive the spindle which can be adjusted the speed as shown in Fig. 3.2 (a) & (b)

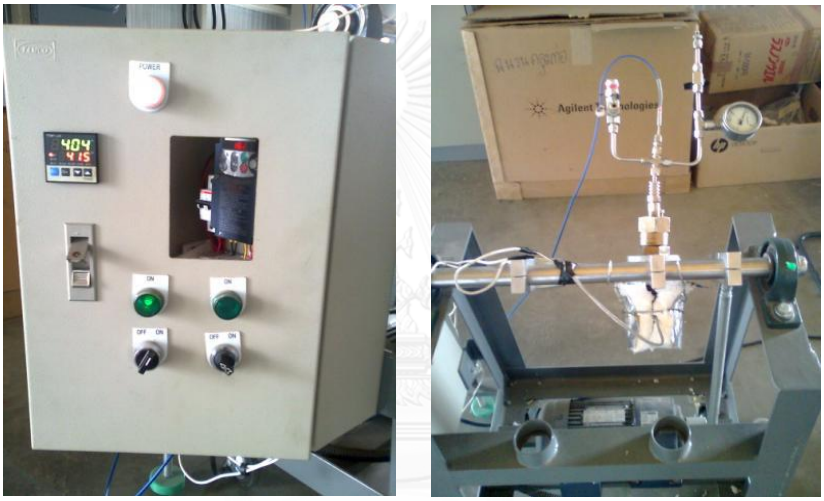

Fig 3. 2 (a) Digital temperature controller (b) Reactor controller

6. Vacuum filter unit consists of glass container connected to suction machine to filter and separate liquid product from solid residue using glass filter.

7. Two decimal places scale

8. Four decimal places scale

9. Stopwatch

10. Oven

11. Glassware (beaker, bottle samples)

12. Gas Chromatography and simulated distillation software from Agilent Technologies model GC7890A for analysis of the composition of liquid fuel products by periodic boiling point according to ASTM D2887 standard as shown in Fig. 3.3.

Fig 3. 3 Gas Chromatography and simulated distillation software

13. Surface area and porosity analyser for analysis of surface area and porosity of catalyst by measuring nitrogen that was adsorbed on sample surface. Then the BET equation is used to calculate the specific surface area. Simulated distillation gas chromatography is shown in Fig. 3.4.

Fig 3. 4 BET Surface area

14. X-Ray Fluorescence Spectrometer (XRF) as shown in Fig. 3.5 was used for analysis of composition of catalyst. XRF technique relied on specific photo emission of substance which has specific wavelength for element. Therefor it can indicate the elements that are present in the sample.

Fig 3. 5 X-Ray Fluorescence Spectrometer

15. Iron on activated carbon reduction unit as shown in Fig. 3.6.

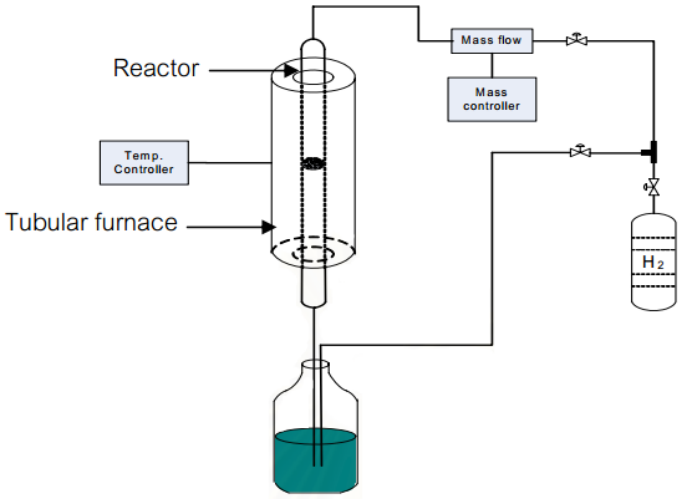

Fig 3. 6 Iron on activated carbon reduction unit.

3.1.2 Reagent and chemical

- Rapeseed oil was received from a market sources in Malaysia and used without further purification.
- 99.99% Hydrogen gas contained in 6 L high pressure tank
- 99.9% Cao and MgO
- HZSM-5 zeolite
- 1% Fe/AC & 5% Fe/AC
- Hydrogen gas (purity 99.5%) used to trace the effected of initial pressure of hydrogen gas which supplied by Environment Co., Ltd. Bangkok, Thailand.

- Toluene (C_7H_8) is a commercial grade (purity 80% minimum) from S.R.Lab Co., Ltd. Bangkok, Thailand. This reagent was used without further purification.

3.1.3 Catalyst Preparation

1. Prepare Iron on activated carbon: 5%wt Fe/AC
2. Sizing the activated carbon with sieve in range of 0.850 – 0685 mm.
3. Weighing 50 g of activated carbon and 15.63 g of $Fe(NO_3)_3 \cdot 9H_2O$.
4. Dissolve $Fe(NO_3)_3 \cdot 9H_2O$ in the optimum volume of distilled water until $Fe(NO_3)_3 \cdot 9H_2O$ completely dissolved.
5. Add $Fe(NO_3)_3 \cdot 9H_2O$ solution on activated carbon gradually, stir and heating at 80 °C until dryness.
6. Put activated carbon and $Fe(NO_3)_3 \cdot 9H_2O$ mixture into oven at 110 °C for drying overnight.
7. Put dried activated carbon in to crucible and calcined at 600 °C for 3 h.
8. Before the impregnation the catalyst is reduced by hydrogen gas at flow rate of 120 mL/min, 400 °C for 1 h.
9. 1%wt Fe/AC was prepared as the method.

3.1.4 Experimental analysis

1. Characterizing primary properties of rapeseed oil including physical properties, decomposition temperature range, chemical composition, fatty acid composition, the boiling point range and the ultimate analysis.-mass spectrometry was used to determine the fatty acid profile of rapeseed oil.
2. Analyzing of the thermal degradation of rapeseed with Thermogravimetric analyzer (TGA).

3. Characterizing primary properties of catalyst including composition of five catalysts CaO, MgO, HZSM-5, 1wt%Fe/AC and 5wt%Fe/AC) by EDX and determine surface area of catalyst by BET.

4. 2-level factorial designs are used to study the influence of various variables affecting on the percentage of liquid product from catalytic pyrolysis of

rapeseed oil on basic, acidic and Fe/AC catalyst by using 2^4 factorial experimental design. The studied variables are reaction temperature, reaction time, initial hydrogen pressure and catalyst content as shown in Table 3.1 and 3.2.

5. Analyze the physical and chemical properties of liquid product from experiment and determine the weight percent of solid, liquid and gas product.

Table 3. 1 The studied variables

Variables	Level	
	Low (-)	High (+)
Temperature (°C) , A	390	450
Mass of catalyst (% wt), B	0.5	1.0
Initial hydrogen pressure (Bar) , C	1	5
Time of reaction (min) , D	30	60

Table 3. 2 Number of trials from 2-level factorial experimental design

Variables			
Temperature (°C), A	**Catalyst Content (% wt), B**	**Initial hydrogen pressure (Bar), C**	**Time of reaction (min), D**
390	0.5	1	30
450	0.5	1	30
390	0.5	5	30
450	0.5	5	30
390	0.5	1	60
450	0.5	1	60
390	0.5	5	60
450	0.5	5	60
390	1.0	1	30
450	1.0	1	30
390	1.0	5	30

Variables

Temperature (°C), A	Volume of catalyst (% wt), B	Initial hydrogen pressure (Bar), C	Time of reaction (min), D
450	1.0	5	30
390	1.0	1	60
450	1.0	1	60
390	1.0	5	60
450	1.0	5	60
420	0.75	3	45

3.1.5. Experimental methodology

1. Weighing 15 g. with two decimal points of rapeseed oil and the reactor together with 15 g of rapeseed oil are also weighted by two decimal points. The catalyst were weighted by four decimal points and put in the reactor. Then, the various parts of the reactor are assembled.

2. Purging air inside the reactor by flushing hydrogen three times then compress hydrogen gas is set up at 1 bar. Since the reactor has a small volume of only 70 mL and hydrogen gas is not the main reactant so there is no need to calculate the amount of hydrogen required by the rapeseed oil.

3. Purging air inside the reactor by slowly passing hydrogen gas then compress hydrogen gas to the given pressure (in case setting up high pressure of hydrogen) by observing the pressure from the regulator connected between the hydrogen tank and reactor. Checking for gas leak at the joints of the reactor if there is no gas leak, slowly closing gas valve in order to prevent gas coming out.

4. Connecting reactor with controller, thermocouple and heating coil. Then putting the insulation around the reactor to prevent heat loss during the experiment. Turning on the temperature controller unit, setting up the reaction temperature and recording the reaction time after reaching the required reaction temperature.

5. After finishing the reaction time, removing insulator and heating coil and quenching the reactor to the room temperature. Then, slowly venting gas outside the reactor (if the gas is vented when the reactor temperature is not close to room

temperature, some of gas that are not condensed will be vented resulted in the experimental error).

6. Opening the lid of reactor, recording the reactor weight after the experiment in order to calculate gas content by using equation (3.1).

Gas content = reactor weight before the experiment
– reactor weight after the experiment (3.1)

7. Separating liquid from solid by using vacuum filtration unit. The reactor is wiped clean with tissue paper that was pre-dried and weighted in order to reduce the error of the calculated results. After solid and tissue paper are wrapped with foil that was pre-dried and weighted. Then drying in the oven at 110 °C for 24 h, weighing and calculating the solid content by using the equation (3.2).

Solid content = weight of filter paper, foil and solid residue after drying
- weight of filter paper, foil before using filtration (3.2)

8. Calculating the amount of liquid product from equation (3.3).

Liquid product content = weight of rapeseed oil
– weight of gas – weight of solid (3.3)

9. Analyzing liquid product by Simulated Distillation Gas Chromatography to determine the distribution of compositions of liquid product in various periodic boiling points and studying physical and chemical properties of the obtained liquid product.

10. Calculating the percentage of liquid product

$$\% \text{ liquid yield} = \frac{\text{weight of liquid product} \times 100}{\text{weight of original oil}}$$

$$\% \text{ overall gasoline yield} = \% \text{ liquid yield} \times \% \text{ gasoline yield}$$

11. Changing the type of catalyst and redoing the procedures from number1-10.

12. Analyzing experimental results and concluding the optimum condition of catalytic pyrolysis of rapeseed oil for each type of catalysts.

3.1.6. Experimental flow diagram

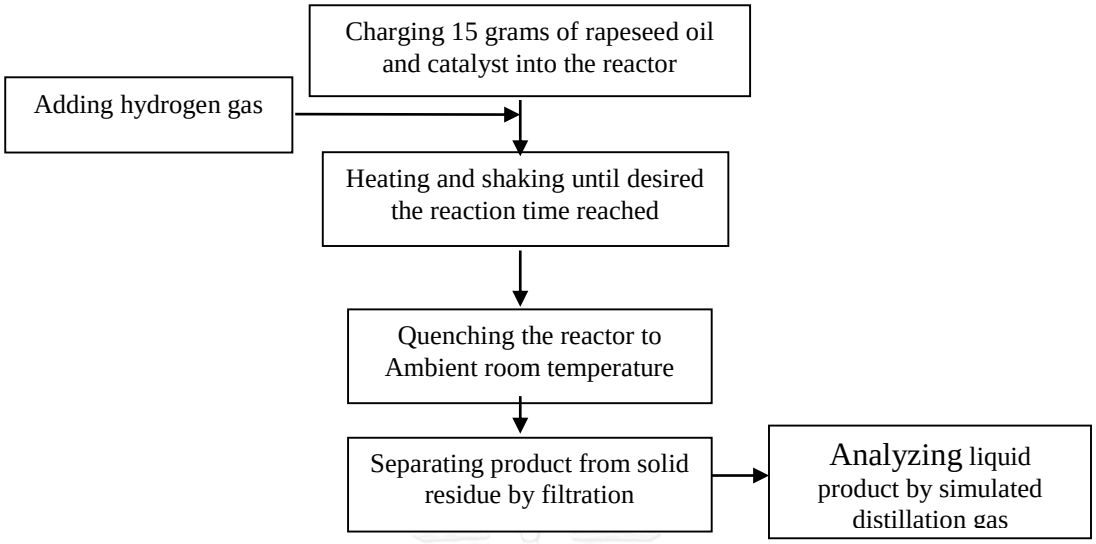

3.2 Continuous experimental

This research aims to study the factors that affect the catalytic cracking reaction of rapeseed oil in continuous reactor to liquid fuel using the efficient catalyst after studying the type of catalysts that gives highest percentage yield of liquid and gasoline from batch reactor.

3.2.1 Instruments

1. 3 L stainless steel continuous-flow reactor is used to carry out the reaction. The reactor is arranged horizontally with existing the shaft of impeller inside reactor. The reactor can withstand heat up to 500 °C. There is a thermocouple slot for measuring the reaction temperature inside the reactor as shown in Fig. 3.7.

Fig 3. 7 3 L-Continuous-flow reactor

2. Digital temperature controller is used to control the power distribution from transformer to heating coils in various parts of the reactor and stop the power distribution when the required temperature is obtained. Temperature control can be divided into:

- Controlling temperature inside the reactor
- Controlling temperature of gaskets on both sides
- Controlling temperature of carrier gas

as well as the screen that display temperature inside the reactor as shown in Fig. 3.8.

Fig 3. 8 Digital temperature controller

3. Putting heating coil, 230 V and 400 W for heating the reactor.

4. K-type thermocouple with 1.6 mm diameter for measuring the temperature of obtained product and reaction temperature of catalysts were set up.

5. Carrier gas, nitrogen gas is used as carrier gas to carry rapidly the obtained product vapour to the condenser. There are gas feed controller at:

- Carrier gas feed controller at gaskets on both sides
- Carrier gas feed controller in reactor

6. Condenser unit consist of: as shown in Fig. 3.9

- (a) Counter-current heat exchanger
- (b) Cooling tower

(a) (b)

Fig 3. 9 Condenser Unit

7. Vacuum filter unit consists of glass container connected to vacuum pump using to filter and separate liquid product from solid residue using filter paper.

8. Two decimal places scale

9. Four decimal places scale

10. Stopwatch

11. Oven

12. Glassware (beaker, bottle samples)

13. Gas Chromatography and simulated distillation for analysis of the composition of liquid fuel products by boiling point as shown in Fig. 3.10.

Fig 3. 10 Simulated distillation gas chromatography

14. Gas Chromatography – Mass spectrometer (GC-MS): Gas Chromatography model GC2010 that use Mass Spectrometer model GCMSQP2010 as a detector from Agilent. The analysis was done on 0.25mm x 30m Capillary column from J&W Scientific model DB-1 with 100% dimethylpolysiloxan, film thickness 0.25 µm as stationary phase and the operation temperature range of this unit is from -60 to 350 °C as shown in Fig. 3.11.

Fig 3. 11 Gas chromatography – mass spectrometer, GC-MS

3.2.2 Reagent and chemical

- Rapeseed oil was received from a market sources in Malaysia and used without further purification.
- 99.99% Nitrogen gas contained in 6 L high pressure tank
- 99.9% MgO

3.2.3 Experiment

2-Level experimental design are used to study the influence of variables affecting on percentage of liquid product from catalytic cracking of rapeseed oil on MgO catalyst by using 2^4 factorial experimental design. The studied variables are reaction temperature, catalyst content, feeding rate and N_2 gas flow rate as shown in Table 3.3.

Table 3. 3 The studied variables in catalytic pyrolysis of rapeseed oil on MgO.

Variables	**Level**	
	Low (-)	**High (+)**
Reaction temperature (°C) , A	390	450
Catalyst content (% V/V), B	30	60
Feeding rate (ml/min) , C	3	9
N_2 gas flow rate (ml/min) , D	50	150

Table 3. 4 Number of trials from 2-level factorial experimental design

Variables			
Reaction temperature (°C), A	**Catalyst content (% wt), B**	**Feeding rate (ml/min), C**	**N_2 gas flow rate (ml/min), D**
390	30	3	50
450	30	3	50
390	30	9	50
450	30	9	50
390	30	3	150
450	30	3	150
390	30	9	150
450	30	9	150
390	60	3	50
450	60	3	50
390	60	9	50
450	60	9	50
390	60	3	150
450	60	3	150
390	60	9	150
450	60	9	150
420	45	6	100

3.2.4. Research methodology

1. Weighing Rapeseed oil is before fed to the reactor using 2 decimal places scale and magnesium oxide catalyst is also weighted to the desired amount using 4 decimal places scale.

2. Connecting the reactor to the controller, heating unit and cover the insulator in order to prevent heat loss during the experimentation. Then connect thermocouple to reactor.

3. Adding magnesium oxide catalyst to continuous reactor and cover with the lid.

4. Turning on the stirrer and feeding carrier gas at the desired rate by setting the controller. Adjusting an electric current from the screen to distribute power into heating coil and wait until reaching the required temperature.

5. Starting time when temperature inside the reactor reaches the desired temperature. Collecting the product, separate liquid product from solid residues by vacuum filtration using glass filter and the separated liquid was used for further analysis.

6. Washing the reactor with toluene solution, wipe clean with pre-weighted soft paper. Then, solid and soft paper are dried in oven at 105 °C for 24 h, weight and calculate the overall yield.

7. The liquid product is analysed with Simulated Distillation Gas Chromatography to determine the compositions distribution of liquid product in various periodic boiling points and chemical compositions.

8. Calculating the percentage of liquid product.

CHAPTER IV

RESULTS AND DISCUSSIONS

This research studies the pyrolysis process of rapeseed oil with thermal and catalyst by using MgO, CaO, HZSM-5, 1%wt Fe/AC and 5%wt Fe/AC in order to synthesize the liquid product with value added compositions such as naphtha, kerosene and diesel. The cracking reaction in batch reactor was investigated the variables that affect the amount of gas, liquid product and solid. The variables are type of catalyst, initial hydrogen pressure, catalyst content, reaction temperature and reaction time. The optimum condition for thermal cracking of non-edible vegetable oil such as maximum amount of liquid product and naphtha yield were determined. The 2^k factorial experimental is designed by using Design Expert 7.0.0. The kinetics of three catalyst are also examined.

4.1. Properties of rapeseed oil

In this study rapeseed oil was used as raw material to study the catalytic pyrolysis process to produce liquid fuel. Before using as raw material, properties of rapeseed oil must be investigated to account for experimental results and compare the properties before and after the experiment. The properties studies were such as chemical composition and chemical properties of rapeseed oil.

4.1.1 The chemical composition of rapeseed oil

Chemical composition of rapeseed oil was studied by using gas chromatography-mass spectrometry as shown in Fig. 4.1 which showed the chromatogram of rapeseed oil composition. Four dominant peaks were observed at retention time of 9.689, 10.817, 15.323 and 15.766 min. The comparison of spectrum pattern showed that peaks at such retention time was cis-11-hexadecenal, Oleic acid , 4-Dehydroxy-N-(4,5-methylenedioxy-2-nitrobenzylidene) tyramine and 1-Propene, 3-(2-cyclopentenyl)-2-methyl-1,1-diphenyl respectively, as shown in Table 4.1.

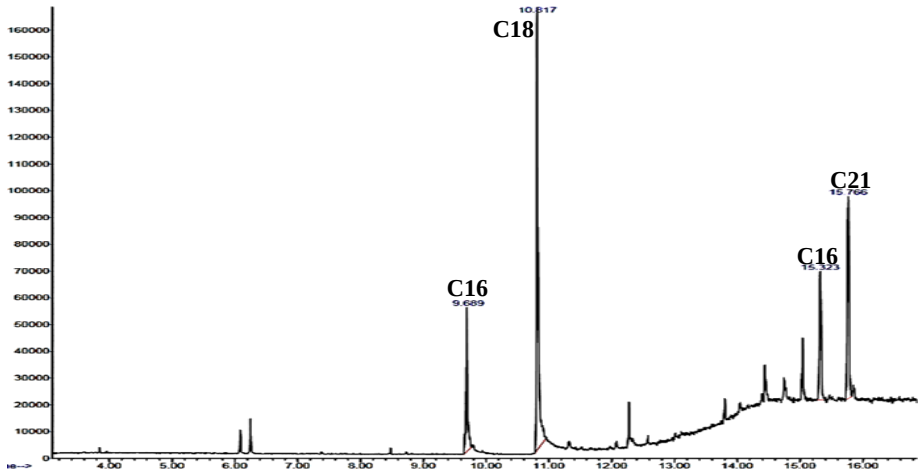

Fig. 4. 1 The chromatogram of rapeseed oil by GC-MS

Table 4. 1 The chemical composition of rapeseed oil by GC-MS

Peak (min)	Components	Formula	%
9.689	cis-11-hexadecenal	$C_{16}H_{30}O$	15.59
10.817	Oleic acid	$C_{18}H_{34}O_2$	45.45
15.323	4-Dehydroxy-N-(4,5-methylenedioxy-2-nitrobenzylidene)tyramine	$C_{16}H_{14}N_2O_4$	14.29
15.766	1-Propene, 3-(2-cyclopentenyl)-2-methyl-1,1-diphenyl-	$C_{21}H_{22}$	24.67

Table 4.2 showed the fatty acid profile of rapeseed oil. It was found that 5.91% was saturated fatty acid and 93.26% was unsaturated fatty acid. Table 4.2 showed that rapeseed oil consisted with 3.78% Palmitic acid (C16:0), 1.32% Stearic acid (C18:0), 0.58% Arachidic acid(C20:0), 40.67% Cis-9-Octadecenoic acid (C18:1 n-9), 21% Cis-13-Docosenoic acid (C20:1 n-9) and 14.95% Cis-9,12-Octadecadienoic acid(C18:2 n-6). This information was the main reason we chose rapeseed oil as raw material in producing liquid fuel by pyrolysis process. Rapeseed oil will be a good source of hydrocarbons with 16-20 carbon atoms, which catalytic pyrolysis could degrade into medium size hydrocarbon with 5-12 carbon atoms. The catalyst plays a role in selecting desired product which naphtha was the focus in this study.

Table 4. 2 The fatty acid profile of rapeseed oil.

Fatty acid composition	Percentage (%)
Myristic acid (C14:0)	0.05
Palmitic acid (C16:0)	3.78
Heptadecanoic acid (C17:0)	0.03
Stearic acid (C18:0)	1.32
Arachidic acid(C20:0)	0.58
Lignoceric acid (C24:0)	0.15
Total saturated fatty acid	**5.91**
Palmitoleic acid (C16:1 n-7)	0.17
Cis-10-Heptadecenoic acid (C17:1)	0.10
Cis-9-Octadecenoic acid (C18:1 n-9)	40.67
Cis-9,12-Octadecadienoic acid (C18:2 n-6)	14.95
Cis-9,12,15-Octadecatrienoic acid (C18:3 n-3)	7.92
Cis-11-Eicosenoic acid (C20:1 n-9)	7.60
Cis-11,14-Eicosadienoic acid (C20:2 n-6)	0.24
Cis-13-Docosenoic acid (C20:1 n-9)	21.00
Cis-13,16-Docosadienoic acid (C22:2)	0.16
Cis-15-Tetracosenoic acid (C24:1)	0.45
Total unsaturated fatty acid	**93.26**
Unidentified peak	0.83

4.1.2. The fuel composition of rapeseed oil by periodic boiling point.

Table 4.3 showed the fraction of distillation ranges by boiling points of fuel composition such as naphtha, kerosene, diesel and long residue. Fuel composition of rapeseed oil was analyzed according to American Society for Testing and Materials (ASTM) by using Standard Test Method for Boiling Range Distribution of Petroleum Fractions by Gas Chromatography, ASTM D 2887. The results were shown in Table 4.3. It was observed that rapeseed oil consisted of four main compositions: naphtha 7%, kerosene 1%, diesel 1% and residue 90% by weight. It could be observed that fuel composition of rapeseed oil mainly consisted of high content of long residue. It is not

suitable to be used directly as fuel. Therefore, it is interesting to change the large hydrocarbon molecules into smaller one by catalytic cracking into liquid fuels with properties similar to petroleum fuel.

Table 4. 3 The composition of rapeseed oil by the periodic boiling point

Boiling Point (°C)	Composition	% wt
IBP - 200	Naphtha (C_5 - C_{12})	7
200 - 250	Kerosene (C_{12} - C_{15})	1
250 - 350	Light gas oil (C_{15} - C_{25})	1
350 - 370	Gas oil (C_{25} - C_{33})	1
370 - FBP	Long Residue (>C_{33})	90

4.1.3. The analysis of the range of thermal cracking temperature of rapeseed oil by Thermogravimetric Analyzer (TGA)

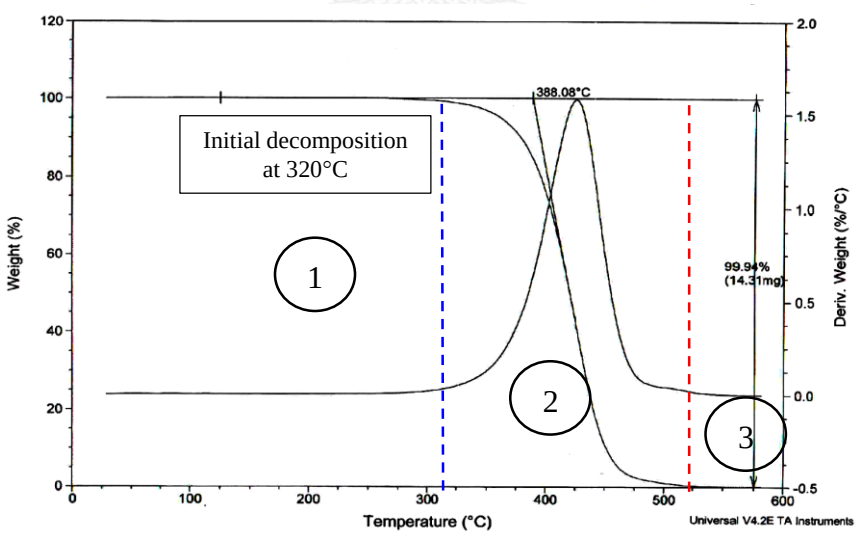

Fig. 4. 2 The thermal decomposition range of rapeseed oil by TGA

From Fig. 4.2 shows the thermogravimetric analysis and DTG curves for thermal degradation of Rapeseed oil in range of 50 – 600°C at heating rate of 20 °C/min under nitrogen atmosphere. The decomposition is found to take place in three steps. From ambient to about 320°C, mass loss of water and moisture in Rapeseed Oil, i.e. this part implies the depletion of Rapeseed Oil. The next part from 320-525°C, the main decomposition of Rapeseed Oil occurs in this zone. The last part i.e. 525-600°C, the completely decomposition and devolatilization occur in this zone. In Fig. 4.2, the maximum temperature that rapeseed oil decomposed is 388.08°C.

4.1.4. The ultimate analysis of rapeseed oil

The analysis of fuel composition of rapeseed oil could be performed by another method which was ultimate analysis of rapeseed oil. Table 4.4 showed the element composition of rapeseed oil. It was found that rapeseed oil consisted of 70.68% C, 11.11% H, 18.10 % O and 0.11% N by weight. It could be observed that rapeseed oil mainly consisted of oxygen which was the reason that heating value of rapeseed oil was lower than standard of common fuel. However, if rapeseed oil was pyrolysis, which resulted in lower oxygen content and the obtained liquid product was more suitable to use as fuel.

Table 4. 4 Elements component of rapeseed oil

Elements	**%wt**
Carbon	70.68
Hydrogen	11.11
Oxygen	18.1
Nitrogen	0.11

4.2 The composition of catalyst

Three types of catalysts were used in this study: basic (MgO and CaO), acidic (HZSM-5) and Fe/AC catalysts. The ultimate analysis was performed by using energy dispersive x-ray spectrometer. It was found that MgO content is 96.8% as shown in Table 4.5. In CaO catalyst, CaO purity is 95.85% as shown in Table 4.6.

Table 4. 5 The elements of magnesium oxide catalyst.

Magnesium oxide (Element)	Compound	Concentration (%weight)
Mg	MgO	96.8
Si	SiO_2	2.04
Ca	CaO	0.68
Fe	Fe_2O_3	0.44
P	P_2O_5	0.11

Table 4. 6 The elements of calcium oxide catalyst.

Calcium oxide (Element)	Compound	Concentration (%weight)
Ca	CaO	95.852
Si	SiO_2	0.052
P	P_2O_5	0.078
S	SO_3	0.28
K	K_2O	0.014
Mg	MgO	3.675
Sr	SrO	0.049

HZSM-5; Si was highest in SiO_2 form of 95.9%, as shown in Table 4.7. Amount of acid site is determined by Si/Al ratio. If there is low content of aluminium, zeolite will have more acid site which increase the hydrophobic properties of the zeolite. There is more substrate adsorbed on zeolite surface which may clog at the pores of the catalyst [18-20].

Table 4. 7 The elements of HZSM-5 catalyst.

HZSM-5 (Element)	Compound	Concentration (%weight)
Si	SiO_2	95.90
Al	Al_2O_3	4.05

1%wt Fe/AC; was analyzed by XRF which sample was burnt up in form as metal oxide. It was found 55.69% Fe_2O_3 followed by 18.29% CaO and form of 13.97% K_2O as shown in Table 4.8. It was observed several metal oxides which are the composition in ash of activated carbon made from biomass.

Table 4. 8 The elements of 1%wt Fe/AC catalyst.

1%wt Fe/AC (Element)	Compound	Concentration (%weight)
Fe	Fe_2O_3	55.69
Ca	CaO	18.29
K	K_2O	13.97
Si	SiO_2	8.99
S	SO_3	2.71
Mn	MnO	0.34

5%wt Fe/AC was found that there are 79.33% Fe, 8.37% CaO and 6.05% K_2O as shown in Table 4.9. It has more Fe_2O_3 content about 1.4 times in 5%wt Fe/AC than in 1%wt Fe/AC**.**

Table 4. 9 The elements of 5%wtFe/AC catalyst.

5%wt Fe/AC (Element)	Compound	Concentration (%weight)
Fe	Fe_2O_3	79.33
Ca	CaO	8.37
K	K_2O	6.05
Si	SiO_2	3.60
S	SO_3	1.50
Zn	ZnO	0.56
Cu	CuO	0.44
Mn	MnO	0.15

4.3 Surface area and pore volume of catalysts

The analysis of surface area, pore size and pore volume of MgO, CaO, HZSM-5, 1%wt Fe/AC and 5%wt Fe/AC by N_2 physisorption measurement as shown in Table 4.10 which showed surface area, pore size and pore volume of catalysts. It was found that basic catalysts had similar surface area, pore size and pore volume. MgO and CaO had surface area of 89 and 80.10 m^2/g and pore volume of 0.078 and 0.076 cm^3/g, respectively. Acidic catalyst (HZSM-5) had surface area of 421.78 m^2/g and pore volume of 0.48 cm^3/g. Neutral catalysts had similar surface area and pore volume. 1%wt Fe/AC and 5%wt Fe/AC had surface area of 613.40 and 549 m^2/g and pore volume of 0.1293 and 0.0978 cm^3/g, respectively. Activated carbon used in this study was produced from coconut shells. When Fe in form of $Fe(NO_3)_3 \bullet 9H_2O$ impregnated on activated carbon was calcined, $Fe(NO_3)_3 \bullet 9H_2O$ could act as activating agent to generate higher surface and pore volume at higher ratio of Fe on activated carbon whereas activated carbon prepared from coconut shell which is weaker structure than lignite therefore increasing the ratio of Fe on activated carbon, total surface area and pore volume were lower because Fe atom was accumulated in the structure.

Table 4. 10 Surface area and Pore volume

Catalyst	Sueface area (m^2/gram)	Pore volume (cm^3/gram)
MgO	89.00	0.078
CaO	80.10	0.076
HZSM-5	421.78	0.48
1%wt Fe/AC	613.40	0.1293
5%wt Fe/AC	549	0.0978

Fig. 4.3 (A-B) shows the picture of the outer surface of MgO using scanning electron microscope (SEM). At x 20,000 was seen that MgO connected small sheets. At x 50,000 was clearly seen that MgO was in irregular rod-shape and connected into small sheets. There are not widely opened surface so why it found the less specific surface area confirmed with small pore volume.

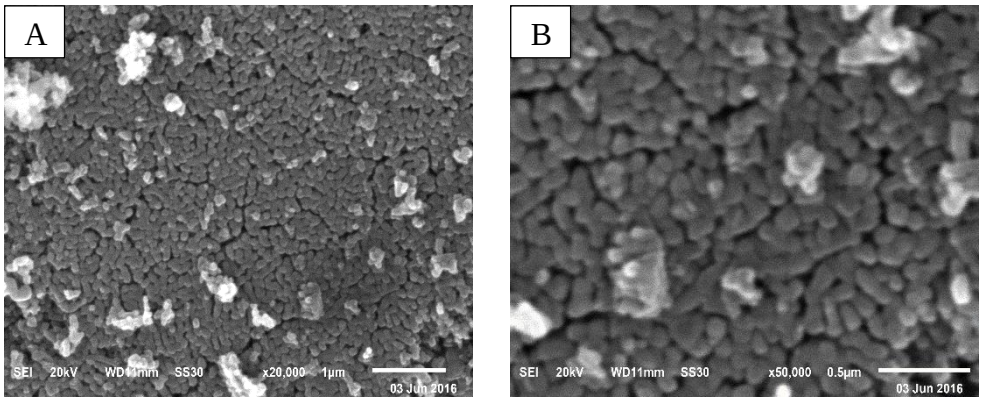

Fig. 4. 3 (A-B) MgO at x20,000 & x 50,000 magnification

Fig. 4.4 (A-B) showed the picture of surface area and particles of CaO using scanning electron microscope (SEM). At x 10,000 was seen that CaO particles were sheet stacked into clusters. At x 50,000 was clearly seen that CaO was obviously arranged in sheet form and there were white small particles of Mg. The outer surface of CaO looks like MgO, so why both catalyst has the same specific surface area and pore volume.

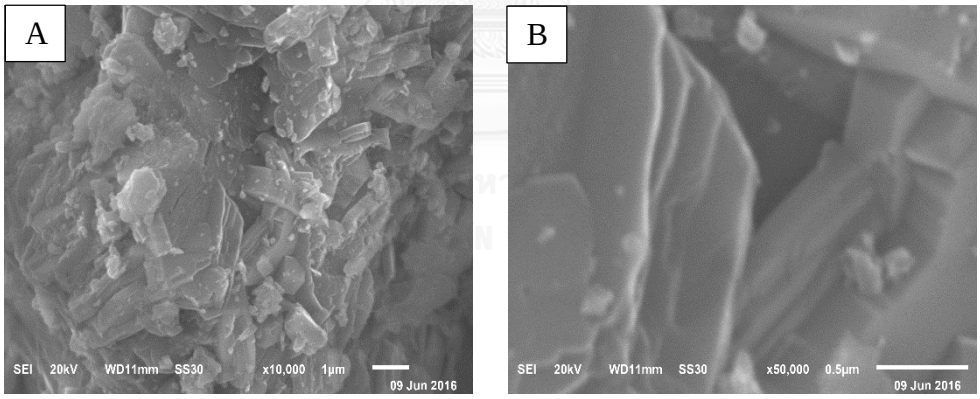

Fig. 4. 4 (A-B) CaO at x 10,000 & x 50,000 magnification

Fig. 4.5 (A-B) showed the picture of surface area and particles of HZSM-5 using scanning electron microscope (SEM). At x 10,000 was seen that HZSM-5 particles were regular rods arranged without direction. At x 50,000 was seen that HZSM-5 particles were clearly rectangular bars. It can see the deep and big holes that imply the existing of small pore developing inside the catalyst.

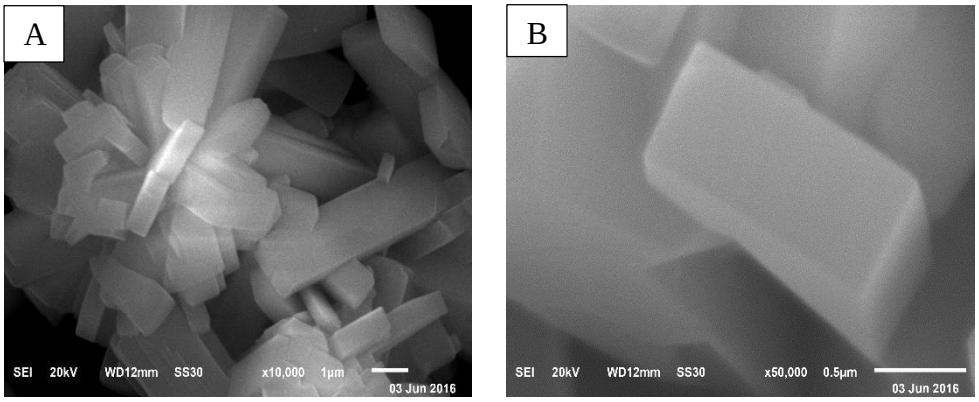

Fig. 4. 5 (A-B) HZSM-5 at x 10,000 and x 50,000 magnification

Fig. 4.6 and 4.7 show the picture of surface area and particles of 1%wt and 5% Fe/AC respectively using scanning electron microscope (SEM). At x 400 magnification it was found that activated carbon had stacked porous structure and Fe particles were within pores in Fig 4.7, it implies of using higher Fe impregnated on activated carbon.

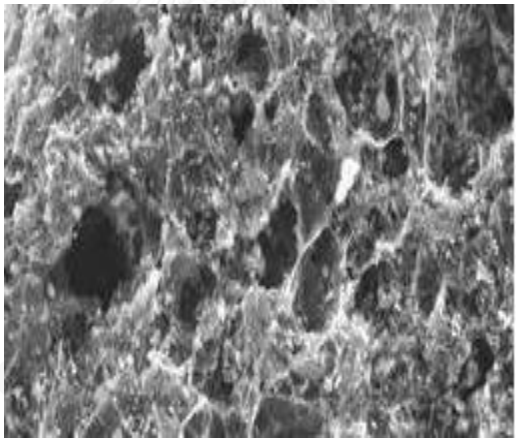

Fig. 4. 6 1%wt Fe/AC at x 4,000 magnification

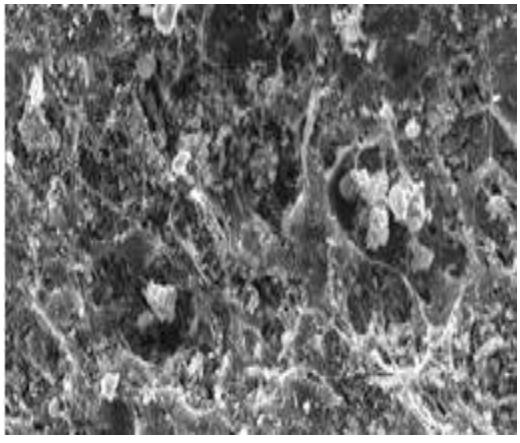

Fig. 4. 7 5%wt Fe/AC at x 4,000 magnification

4.4 The 2^k Experimental Design [23,24]

The 2^k experimental design is an efficient method to evaluate how various reaction factors influence the system. It is very beneficial in the primary experimental study when there are several variables effects to determine. This study investigated variables affecting percentage of liquid product. The distribution of liquid product was the result from catalytic pyrolysis of rapeseed oil by using MgO and CaO with 2^k factorial experimental design. The study of effects of variable on response will reduce the number of trials. Each studied variables could be divided into 2 levels, low and high level. In this study four variables were studied: reaction temperature, catalyst content, initial hydrogen pressure and reaction time.

A : Reaction temperature, Low at 390°C (-) High at 450°C (+)

B : Initial hydrogen pressure, Low at 1 bar (-) High at 5 bar (+)

C : Reaction time, Low at 30 min (-) High at 60 min (+)

D : Catalyst content, Low at 0.5%wt (-) High at 1%wt (+)

The above experimental design consisted of 16 trials in total and the trial at average value of variables which was reaction temperature (A) = 420 °C, initial hydrogen pressure (B) = 3 bar, reaction time (C) = 45 min and catalyst content (D) = 0.75%wt.

4.4.1 The effect of variables on percentage of liquid product and naphtha yield from catalytic pyrolysis of rapeseed oil using CaO.

From the study of catalytic pyrolysis of rapeseed oil by using CaO with 2^4 factorial experimental design and the experiment at an average value, the results were shown in Table 4.11. It was found that percentage of liquid product was in ranged of 62.10 – 86.53%wt and percentage of naphtha yield was in ranged of 5.19-35.71%wt.

Table 4. 11 Percentage of liquid product and naphtha from catalytic pyrolysis of rapeseed oil over CaO.

Run	Factor				%yield of Liquid	%yield of Naphtha		Factor Level	
	A	B	C	D				Low (-)	High (+)
1	390	1	30	0.5	86.53	5.19	A (°C)	390	450
2	450	1	30	0.5	67.75	31.84	B (bar)	1	5
3	390	5	30	0.5	83.46	5.42	C (min)	30	60
4	450	5	30	0.5	64.05	29.46	D (%wt)	0.5	1.0
5	390	1	60	0.5	82.28	30.03			
6	450	1	60	0.5	63.29	28.04			
7	390	5	60	0.5	81.48	30.15			
8	450	5	60	0.5	62.10	35.71			
9	390	1	30	1.0	85.62	6.85			
10	450	1	30	1.0	67.95	33.30			
11	390	5	30	1.0	82.58	6.61			
12	450	5	30	1.0	64.46	30.94			
13	390	1	60	1.0	81.64	25.72			
14	450	1	60	1.0	64.06	34.59			
15	390	5	60	1.0	80.33	25.71			
16	450	5	60	1.0	63.03	28.68			
17	420	3	45	0.75	71.61	31.51			

The procedure to examine the data from a single factorial design is providing through examination of a normal probability plot. The difference variables for the 2^4 design were determined and the normal probability plot of liquid and naphtha are illustrated in Appendix A (Fig. A-1 & A-2). From the normal probability plot, all of the variables that lie along the line are insignificant, whereas the larger variables depart from the straight line are significant. A study of the influence of reaction temperature (A), catalyst content (B), initial hydrogen pressure (C) and reaction time (D) by using the 2^k experimental design to investigate variables that affect on the liquid product and naphtha yield from catalytic pyrolysis of rapeseed oil using CaO, which are summarized in Table 4.12.

Table 4. 12 The variables affect on percentage of liquid product and naphtha yield.

	CaO		
	One variable	Two variables	Three variable
Liquid	A, D, C	CD, AB	
Naphtha	A, D, C, B	AD, BD, AB, CD	ABD, ACD

The analysis of variance (ANOVA) is considered the confidence interval of 95% or at of 0.05 significant interval. The variables with the P-value less than 0.05 as shown in Appendix B (Table B-1& B-2) Verified to determine whether the data are reliable or not by acting as Normal Plot of Residuals as shown in the Appendix A (Fig. A-3 & A-4) found that Residuals of percentage of liquid and naphtha yield tends to be straight is R^2 = 0.9998 & 0.9980, which is nearby 1 indicates that data are normally distributed.

4.4.2 The effect of variables on percentage of liquid product and naphtha yield from catalytic pyrolysis of rapeseed oil using MgO.

From the study of catalytic pyrolysis of rapeseed oil by using MgO with 2^4 factorial experimental design and the experiment at an average value the results were shown in Table 4.13. It was found that percentage of liquid product were in ranged of 63.10 – 88.98%wt and percentage of naphtha yield were in ranged of 4.82-40.32%wt.

Table 4. 13 Yield of liquid and naphtha product from catalytic pyrolysis of rapeseed oil over MgO.

Run	Factor				%yield of Liquid	%yield of Naphtha		Factor Level	
	A	B	C	D				Low (-)	High (+)
1	390	1	30	0.5	88.98	5.96	A (^{o}C)	390	450
2	450	1	30	0.5	68.66	32.27	B (bar)	1	5
3	390	5	30	0.5	88.96	7.12	C (min)	30	60
4	450	5	30	0.5	68.54	33.65	D (%wt)	0.5	1.0
5	390	1	60	0.5	84.77	27.97			
6	450	1	60	0.5	64.68	35.90			

7	390	5	60	0.5	84.54	30.01
8	450	5	60	0.5	64.16	39.14
9	390	1	30	1.0	87.59	4.82
10	450	1	30	1.0	67.28	33.98
11	390	5	30	1.0	87.46	7.87
12	450	5	30	1.0	67.18	34.93
13	390	1	60	1.0	83.44	29.37
14	450	1	60	1.0	63.10	37.23
15	390	5	60	1.0	83.49	31.31
16	450	5	60	1.0	63.49	40.32
17	420	3	45	0.75	73.41	32.30

The procedure to examine the data from a single factorial design is providing through examination of a normal probability plot. The difference variables for the 2^4 design were determined and the normal probability plot of liquid and naphtha are illustrated in Appendix A (Fig. A-5 & A-6). From the normal probability plot, all of the variables that lie along the line are insignificant, whereas the larger variables depart from the straight line are significant. A study of the influence of reaction temperature (A), catalyst content (B), initial hydrogen pressure (C) and reaction time (D) by using the 2^k experimental design to investigate variables that affect on the liquid product and naphtha yield from catalytic pyrolysis of rapeseed oil using MgO, which are summarized in Table 4.14.

Table 4. 14 The variables affect on percentage of liquid product and naphtha yield.

	MgO		
	One variable	Two variables	Three variable
Liquid	A, D, B		
Naphtha	A, D, C, B	AD	

The analysis of variance (ANOVA) is considered the confidence interval of 95% or at of 0.05 significant interval. The variables with the P-value less than 0.05 as shown in Appendix B (Table B-3 & B-4) Verified to determine whether the data are reliable or not by acting as Normal Plot of Residuals as shown in the Appendix A (Fig. A-7 & A-8) found that Residuals of percentage of liquid and naphtha yield tends to be straight is R^2 = 0.9991 & 0.9983, which is nearby 1 indicates that data are normally distributed.

4.4.3 The effect of variables on percentage of liquid product and naphtha yield from catalytic pyrolysis of rapeseed oil using HZSM-5.

From the study of catalytic pyrolysis of rapeseed oil over HZSM-5 using 2^4 factorial experimental design and the experiment at an average value the results were shown in Table 4.15. It was found that percentage of liquid product were in ranged of 34.17-78.88%wt and percentage of naphtha yield were in ranged of 4.13-34.71%wt.

Table 4. 15 Yield of liquid and naphtha product from catalytic pyrolysis of rapeseed oil over HZSM-5

Run	Factor				%yield of Liquid	%yield of Naphtha		Factor Level	
	A	B	C	D				Low (-)	High (+)
1	390	1	30	0.5	78.88	4.50	A (°C)	390	450
2	450	1	30	0.5	69.35	32.11	B (bar)	1	5
3	390	5	30	0.5	76.24	4.73	C (min)	30	60
4	450	5	30	0.5	68.42	31.54	D (%wt)	0.5	1.0
5	390	1	60	0.5	74.23	26.28			
6	450	1	60	0.5	57.95	34.71			
7	390	5	60	0.5	73.85	25.63			
8	450	5	60	0.5	34.17	34.63			
9	390	1	30	1.0	75.06	4.13			
10	450	1	30	1.0	65.81	29.88			
11	390	5	30	1.0	72.96	8.48			
12	450	5	30	1.0	64.51	29.29			

13	390	1	60	1.0	72.88	25.95
14	450	1	60	1.0	56.33	32.67
15	390	5	60	1.0	72.59	8.69
16	450	5	60	1.0	57.41	32.72
17	420	3	45	0.75	67.14	26.86

The procedure to examine the data from a single factorial design is providing through examination of a normal probability plot. The difference variables for the 2^4 design were determined and the normal probability plot of liquid and naphtha are illustrated in Appendix A (Fig. A-9 & A-10). From the normal probability plot, all of the variables that lie along the line are insignificant, whereas the larger variables depart from the straight line are significant. A study of the influence of reaction temperature (A), catalyst content (B), initial hydrogen pressure (C) and reaction time (D) by using the 2^k experimental design to investigate variables that affect on the liquid product and naphtha yield from catalytic pyrolysis of rapeseed oil using HZSM-5, which are summarized in Table 4.16.

Table 4. 16 The variables affect on percentage of liquid product and naphtha yield.

	HZSM-5		
	One variable	Two variables	Three variable
Liquid	A, D, B, C	AD, BD, AC	
Naphtha	A, D, B	AD, AB	

The analysis of variance (ANOVA) is considered the confidence interval of 95% or at of 0.05 significant interval. The variables with the P-value less than 0.05 as shown in Appendix B (Table B-5 & B-6) Verified to determine whether the data are reliable or not by acting as Normal Plot of Residuals as shown in the Appendix A (Fig. A-11 & A-12) found that Residuals of percentage of liquid and naphtha yield tends to be straight is $R^2 = 0.9995$ & 0.9991, which is nearby 1 indicates that data are normally distributed.

4.4.4 The effect of variables on percentage of liquid product and naphtha yield from catalytic pyrolysis of rapeseed oil using 1%wt Fe/AC.

From the study of catalytic pyrolysis of rapeseed oil by using 1%wt Fe/AC with 2^4 factorial experimental design and the experiment at an average value the results were shown in Table 4.17. It was found that percentage of liquid product were in ranged of 56.47-83.00%wt and percentage of naphtha yield were in ranged of 2.08-42.06%wt.

Table 4. 17 Yield of liquid and naphtha product from catalytic pyrolysis of rapeseed oil over 1 %wt Fe/AC

Run	Factor				%yield of Liquid	%yield of Naphtha		Factor Level	
	A	B	C	D				Low (-)	High (+)
1	390	1	30	0.5	83.00	2.08	A (°C)	390	450
2	450	1	30	0.5	70.28	34.79	B (bar)	1	5
3	390	5	30	0.5	82.23	3.29	C (min)	30	60
4	450	5	30	0.5	69.22	33.57	D (%wt)	0.5	1.0
5	390	1	60	0.5	80.33	11.25			
6	450	1	60	0.5	69.84	40.86			
7	390	5	60	0.5	79.53	12.33			
8	450	5	60	0.5	68.91	39.62			
9	390	1	30	1.0	80.76	3.63			
10	450	1	30	1.0	70.42	36.27			
11	390	5	30	1.0	79.97	4.40			
12	450	5	30	1.0	69.29	34.99			
13	390	1	60	1.0	80.83	12.48			
14	450	1	60	1.0	67.84	42.06			
15	390	5	60	1.0	79.63	13.54			
16	450	5	60	1.0	56.47	26.12			
17	420	3	45	0.75	66.95	40.84			

The procedure to examine the data from a single factorial design is providing through examination of a normal probability plot. The difference variables for the 2^4 design were determined and the normal probability plot of liquid and naphtha are illustrated in Appendix A (Fig. A-13 & A-14). From the normal probability plot, all of the variables that lie along the line are insignificant, whereas the larger variables depart from the straight line are significant. A study of the influence of reaction temperature (A), catalyst content (B), initial hydrogen pressure (C) and reaction time (D) by using the 2^k experimental design to investigate variables that affect on the liquid product and naphtha yield from catalytic pyrolysis of rapeseed oil using HZSM-5, which are summarized in Table 4.18.

Table 4. 18 The variables affect on percentage of liquid product and naphtha yield.

	1%wt Fe/AC		
	One variable	Two variables	Three variable
Liquid	A, D, B, C		ABD
Naphtha	A, D, B	AD, AB	

The analysis of variance (ANOVA) is considered the confidence interval of 95% or at of 0.05 significant interval. The variables with the P-value less than 0.05 as shown in Appendix B (Table B-5 & B-6) Verified to determine whether the data are reliable or not by acting as Normal Plot of Residuals as shown in the Appendix A (Fig. A-15 & A-16) found that Residuals of percentage of liquid and naphtha yield tends to be straight is R^2 = 0.9998 & 1.0000, which is nearby 1 indicates that data are normally distributed.

4.4.5 The effect of variables on percentage of liquid product and naphtha yield from catalytic pyrolysis of rapeseed oil using 5%wt Fe/AC.

From the study of catalytic pyrolysis of rapeseed oil by using 5%wt Fe/AC with 2^4 factorial experimental design and the experiment at an average value the results were shown in Table 4.19. It was found that percentage of liquid product were in ranged of 65.43-80.95%wt and percentage of naphtha yield were in ranged of 2.83-40.20%wt.

Table 4. 19 Yield of liquid and naphtha product from catalytic pyrolysis of rapeseed oil over 5 %wt Fe/AC

Run	Factor				%yield of Liquid	%yield of Naphtha		Factor Level	
	A	B	C	D				Low (-)	High (+)
1	390	1	30	0.5	80.80	2.83	A (°C)	390	450
2	450	1	30	0.5	69.73	33.47	B (bar)	1	5
3	390	5	30	0.5	75.37	14.51	C (min)	30	60
4	450	5	30	0.5	69.53	34.70	D (wt%)	0.5	1.0
5	390	1	60	0.5	79.03	8.85			
6	450	1	60	0.5	67.46	39.73			
7	390	5	60	0.5	80.22	7.62			
8	450	5	60	0.5	66.31	38.46			
9	390	1	30	1.0	80.56	2.98			
10	450	1	30	1.0	68.79	33.91			
11	390	5	30	1.0	80.95	3.89			
12	450	5	30	1.0	68.25	34.74			
13	390	1	60	1.0	78.05	8.74			
14	450	1	60	1.0	67.12	40.20			
15	390	5	60	1.0	78.98	7.98			
16	450	5	60	1.0	65.98	39.06			
17	420	3	45	0.75	65.43	30.10			

The procedure to examine the data from a single factorial design is providing through examination of a normal probability plot. The difference variables for the 2^4 design were determined and the normal probability plot of liquid and naphtha are illustrated in Appendix A (Fig. A-17 & A-18). From the normal probability plot, all of the variables that lie along the line are insignificant, whereas the larger variables depart from the straight line are significant. A study of the influence of reaction temperature (A), catalyst content (B), initial hydrogen pressure (C) and reaction time (D) by using the 2^k experimental design to investigate variables that affect on the liquid product and naphtha yield from catalytic pyrolysis of rapeseed oil using HZSM-5, which are summarized in Table 4.20.

Table 4. 20 The variables affect on percentage of liquid product and naphtha yield.

	5%wt Fe/AC		
	One variable	Two variables	Three variable
Liquid	A, D	AC, AD	ABD, ACD
Naphtha	A, D	CD	

The analysis of variance (ANOVA) is considered the confidence interval of 95% or at of 0.05 significant interval. The variables with the P-value less than 0.05 as shown in Appendix B (Table B-9 & B-10) Verified to determine whether the data are reliable or not by acting as Normal Plot of Residuals as shown in the Appendix A (Fig. A-15 & A-16) found that Residuals of percentage of liquid and naphtha yield tends to be straight is $R^2 = 0.9989$ & 0.9992, which is nearby 1 indicates that data are normally distributed.

Table 4. 21 The variables affecting on percentage of liquid product and naphtha yield of catalytic pyrolysis of rapeseed oil over all five catalysts.

Rapeseed Oil										
Variables	**CaO**		**MgO**		**HZSM-5**		**1%wt Fe/AC**		**5%wt Fe/AC**	
	Liq.	**Naph.**	**Liq.**	**Naph.**	**Liq.**	**Naph.**	**Liq.**	**Naph.**	**Liq.**	**Naph.**
Reaction temperature (A)	√	√	√	√	√	√	√	√	√	√
Catalyst content (B)	√	√			√	√	√	√	√	
Initial hydrogen pressure (C)		√	√		√		√			
Reaction time (D)	√	√	√	√	√	√	√	√	√	√

From Table 4.21 shown that the effects of reaction temperature and reaction time were highly significant. Increasing reaction temperature made large hydrocarbon cracked into medium and small hydrocarbon molecules. Further the increase of reaction temperature created small hydrocarbons and free radicals continuously until they became hydrogen gases. This resulted in lower percentage of liquid product while percentage of naphtha yield was higher with longer reaction time. Large hydrocarbon molecules are converted into small one and the cracking process continues which is affected by catalyst cracking under hydrogen atmosphere, due to the arrangement of small hydrocarbon molecules such as naphtha and higher percentage of naphtha yield.

4.5 The optimum condition of catalytic pyrolysis of rapeseed oil over CaO, MgO, HZSM-5, 1%wt Fe/AC and 5%wt Fe/AC

The effects of variables on catalytic pyrolysis of rapeseed oil over CaO, MgO, HZSM-5, 1%wt Fe/AC and 5%wt Fe/AC were studied by using 2^k factorial experimental design data. Design Expert version 7.0 was used to calculate the optimum condition which the range of variables were as shown in Table 4.22.

Table 4.22 shows the ranges of variables used to find the optimum condition. Five responses were considered: percentage of gas product, percentage of liquid product, percentage of solid, percentage of naphtha yield and percentage of diesel yield. The conditions with lowest percentage of gas product and percentage of solid product were considered and the remaining responses such as percetage of liquid product, percentage of naphtha yield and percentage of diesel yield were considered at highest values by using Design-Expert software in calculating the optimum condition. However, this research only considered two responses : percentage of liquid product and percentage of naphtha yield to study the performance of five catalysts.

Table 4. 22 The range of variables to determine the optimum conditions of catalytic pyrolysis of rapeseed oil over CaO, MgO, HZSM-5, 1%wt Fe/AC and 5%wt Fe/AC by using Design Expert program.

Name	Goal	Lower Limit	Upper Limit	Unit
Temperature (A)	is in range	390	450	°C
Catalyst (B)	is in range	0.5	1.0	%wt
Pressure (C)	is in range	1	5	Bar
Time (D)	is in range	30	60	Minute
Yield of gas	minimize	-	-	%wt
Yield of liquid	maximize	-	-	%wt
Yield of solid	minimize	-	-	%wt
Yield of naphtha	maximize	-	-	%wt
Yield of diesel	maximize	-	-	%wt

Table 4.23 showed the optimum conditions from the experiment compared with Design-Expert program. CaO: the optimum condition was reaction temperature of 390 °C, catalyst content of 1%wt (0.98%wt from program), initial hydrogen pressure of 3 bar (3.25 bar from program) and reaction time of 60 min gave percentage of liquid product and naphtha yield of 79.67%wt and 27.26%wt, respectively. MgO: the optimum condition was reaction temperature of 390 °C, catalyst content of 0.50%wt, initial hydrogen pressure of 3 bar (2.43 bar from program) and reaction time of 60 min gave percentage of liquid product and naphtha yield of 85.33%wt and 32.04%wt, respectively. HZSM-5: the optimum condition was reaction temperature of 390°C, catalyst content of 0.5%wt (0.51%wt from program), initial hydrogen pressure of 5 bar (4.99 bar from program) and reaction time of 60 min percentage of liquid product and naphtha yield of 73.56%wt and 27.61%wt, respectively. 1%wt Fe/AC: the optimum condition was reaction temperature of 400°C (407.10°C from program), catalyst content of 1.0%wt, initial hydrogen pressure of 1 bar and reaction time of 60 min gave percentage of liquid product and naphtha yield of 76.08%wt and 20.37%wt, respectively. 5%wt Fe/AC: the optimum condition was reaction temperature of 410°C (413.03°C from program), catalyst content of 0.50%wt, initial hydrogen pressure of 1 bar and reaction time of 60 min gave percentage of liquid product and naphtha yield of 75.03%wt and 20.25%wt, respectively.

Table 4. 23 The optimum conditions of catalytic pyrolysis of rapeseed oil over CaO, MgO, HZSM-5, 1%wt Fe/AC and 5%wt Fe/AC between Design-Expert program and the actual experiment.

Catalyst										
Variables	**CaO**		**MgO**		**HZSM-5**		**1%wt Fe/AC**		**5%wt Fe/AC**	
	Pro.	Exp.	Pro.	Exp.	Pro.	Exp.	Pro.	Exp.	Pro.	Exp.
Temperature (°C)	390	390	390	390	390	390	407.10	400	413.03	410

Catalyst										
Variables	**CaO**		**MgO**		**HZSM-5**		**1%wt Fe/AC**		**5%wt Fe/AC**	
	Pro.	Exp.	Pro.	Exp.	Pro.	Exp.	Pro.	Exp.	Pro.	Exp.
Catalyst (%wt)	0.98	1.00	0.50	0.50	0.51	0.50	1.0	1.00	0.50	0.50
Pressure (bar)	3.25	3	2.43	3	4.99	5	1	1	1	1
Time (Minute)	60	60	60	60	60	60	60	60	60	60
Yield of gas	9.39	9.77	7.48	7.78	16.68	18.26	16.49	16.13	16.08	15.65
Yield of solid	9.19	10.56	7.83	6.89	8.81	8.18	6.37	6.23	9.23	9.32
Yield of liquid	81.42	79.67	84.69	85.33	73.91	73.56	77.14	77.64	74.60	75.03
Yield of naphtha	25.94	27.26	30.93	32.04	26.13	27.61	20.91	20.37	20.75	20.25
Yield of diesel	22.60	18.99	25.31	23.79	22.76	21.98	34.49	35.16	27.62	28.45

From Table 4.23, it was found that each catalyst also reflected the remarks or important characteristics. Catalysts could be divided into 3 groups including base catalyst (CaO & MgO), acid catalyst (HZSM-5) and Fe/AC. All these catalyst had different reaction mechanisms which resulted in different product. For CaO & MgO, when radicals contacted with catalyst surface, H_2 transfer occurred on catalyst surface. Base catalysts also had overlapped surface which resulted in high surface area. H_2 transfer on surface increased steadily. The products were converted from long residue→diesel→kerosene→small hydrocarbon (naphtha). This could be concluded that base catalysts tended to have higher selectivity toward naphtha than diesel. While for HZSM-5, when radicals contacted with catalyst surface, H_2 transfer occurred within HZSM-5 pore. Only a small hydrocarbon molecule through micropore of

catalyst. Most products were small hydrocarbon such as naphtha and products were cracked further into gaseous hydrocarbon. From the Table 4.23, it could be observed that HZSM-5 gave high gas content. Fe/AC catalyst, activated carbon had large surface area. When radicals contacted with catalyst, H_2 transfer occurred on catalyst surface because Fe atom on activated carbon enhanced cracking of large hydrocarbon from long residue into medium and small hydrocarbon. From the Table 4.23, the higher %Fe, the better cracking of large hydrocarbon molecules into medium, small hydrocarbon molecules until small hydrocarbon molecules converted into gas hydrocarbon. It could be observed that at 5% wt Fe/AC the selectivity in diesel ranges was significantly lower compared to 1%wt Fe/AC. It can be observed that gas content is high, while %yield of naphtha was not significantly different.

4.6 Univariate study for the catalytic pyrolysis of rapeseed oil over five catalysts.

4.6.1 The effect of temperature

The effect of reaction temperature on the liquid product as shown in Fig. 4.8, when the temperature is increased from 390 °C to 450 °C, all catalysts result in lower liquid product yield. MgO, CaO and Fe/AC catalyst : Increasing reaction temperature increase energy for reactants or rapeseed oil which can breakdown large hydrocarbon compound into smaller chains [34, 55, 64, 65]. At higher reaction temperature, hydrocarbon molecules were cracked continuously until some of naphtha were converted into hydrocarbon gas which could be observed from significantly higher gas content at higher temperature. HZSM-5 has high acid catalyst which results in strong cracking reaction. For this reason, cracking of large hydrocarbon molecule could proceed very well from long residue $\rightarrow$ diesel $\rightarrow$ kerosene $\rightarrow$ naphtha. At higher temperature some of naphtha was further cracked into light gas oil while gas content increased at higher temperature.

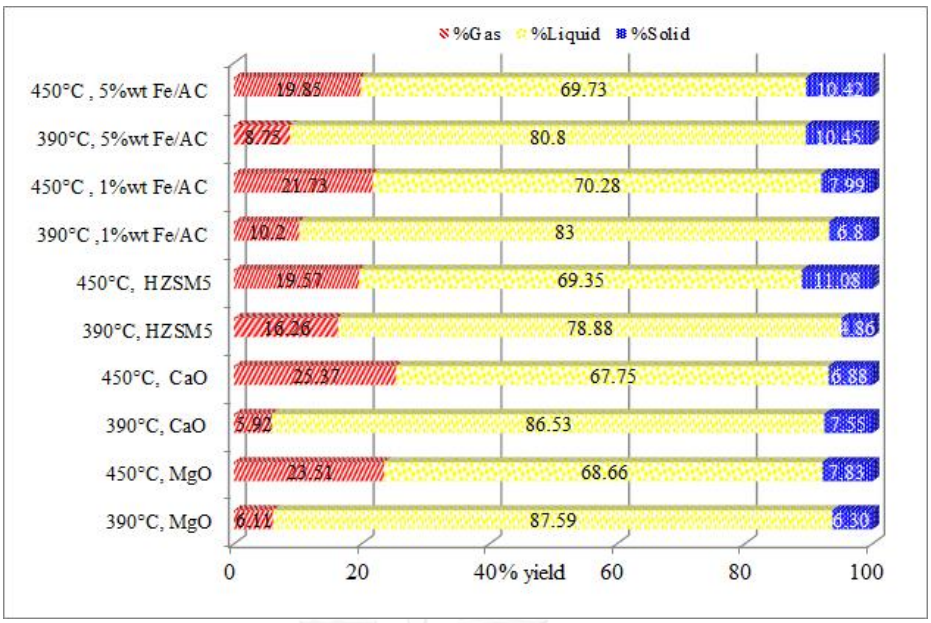

Fig. 4. 8 The effect of temperature on liquid product where initial hydrogen pressure of 1 bar, reaction time 60 minutes and 1%wt of catalyst content over five catalysts.

The effect of temperature on the naphtha yield as shown in Fig. 4.9, when the temperature is increased from 390 °C to 450 °C, all catalysts result in higher naphtha yield. MgO and CaO: At higher temperature, thermal cracking within system could thoroughly occur. Large hydrocarbon molecules cracked into medium hydrocarbon molecules. After that the catalyst played a role in the selectivity to produce small hydrocarbon molecules like naphtha which resulted in higher percentage of naphtha yield [55, 64, 65]. For Fe/AC catalyst, percentage of naphtha yield increased when reaction temperature was higher. Fe atom on activated carbon increased the active site of activated carbon and Fe atom could absorb hydrocarbon molecule. Therefore, Fe/AC had high catalytic activity. Large hydrocarbon molecules could be cracked into smaller hydrocarbon molecules significantly such as naphtha. HZSM5 : the higher temperature accelerated the thermal cracking and hence changing the long chain of hydrocarbon molecule from thermal cracking into a middle hydrocarbon molecule such as kerosene and diesel fraction. Thereafter kerosene, light gas oil and gas oil were catalytically cracked at the surface of HZSM-5, converting them into naphtha and gaseous (normally C_1-C_4).

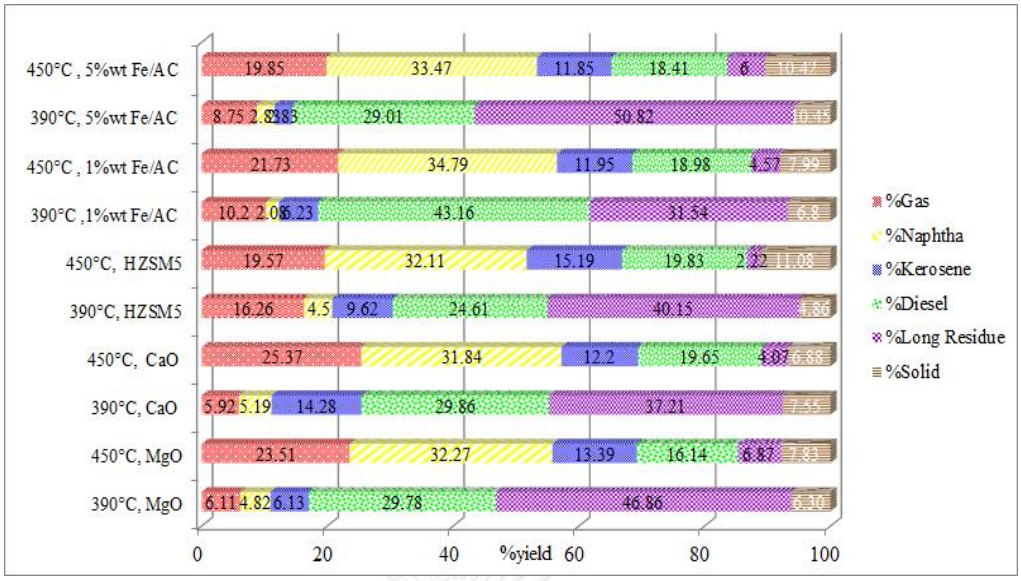

Fig. 4. 9 The effect of temperature on product distribution where initial hydrogen pressure of 1 bar, reaction time 60 minutes and 1%wt of catalyst content over five catalysts.

4.6.2 The effect of reaction time

Fig. 4.10 shows percentage of liquid product when reaction time is increased from 30 min to 60 min. All catalysts show the percentage of liquid product is lowered. Basic catalyst (MgO & CaO) and Fe/AC catalyst : Rapeseed oil begins crack and undergoes more cracking when the reaction time is continues, and hence, the light hydrocarbon molecules were produced in greater from the effect of thermal cracking [20, 21, 64, 66-68]. Therefore, percentage of liquid product was lower as shown in Fig 4.10. For acidic catalysts (HZSM-5), at longer reaction time the reactivity in cracking process was higher, small hydrocarbon molecules were further cracked into more gas contents. This resulted in lower percentage of liquid product.

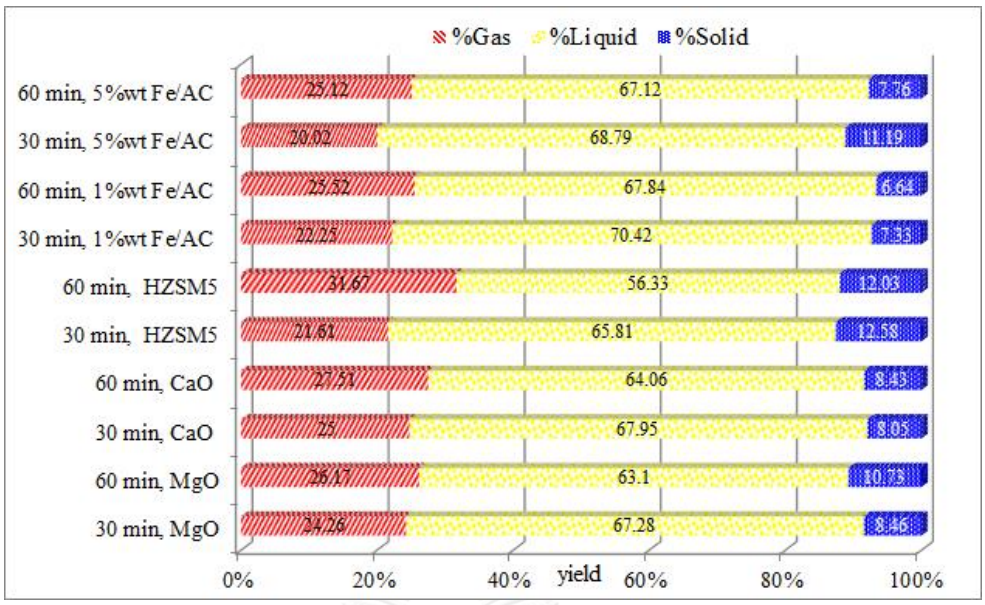

Fig. 4. 10 The effect of reaction time on liquid product where reaction temperature of 450 °C, initial hydrogen pressure of 1 bar and 1%wt of catalyst content over five catalysts.

Fig. 4.11 shows the effect of reaction time on the product distribution. When reaction time was increased from 30 to 60 mins it was found that all catalysts resulted in higher percentage of naphtha yield. For basic catalysts (MgO & CaO), at longer reaction time the thermal cracking within system thoroughly occur. Large hydrocarbon molecules are converted to smaller hydrocarbon molecules and continuously dissociated. Small hydrocarbon molecule was influenced by the catalyst disintegration in an atmosphere of hydrogen, the pore size of catalyst will select the proper size chains so the naphtha yield increased [20, 21, 55, 64, 65]. While Fe/AC catalyst, Fe atom can absorb hydrocarbon molecules which results in higher catalytic activity. At longer reaction time large hydrocarbon molecules cracked into smaller hydrocarbons which resulted in higher percentage of naphtha yield. HZSM-5, at longer reaction time the cracking could be better proceeded which made large hydrocarbon molecules cracked into more small hydrocarbon molecules such as naphtha. When the reaction time was further continued, some of naphtha was converted into gases which consistent with Fig 4.11.

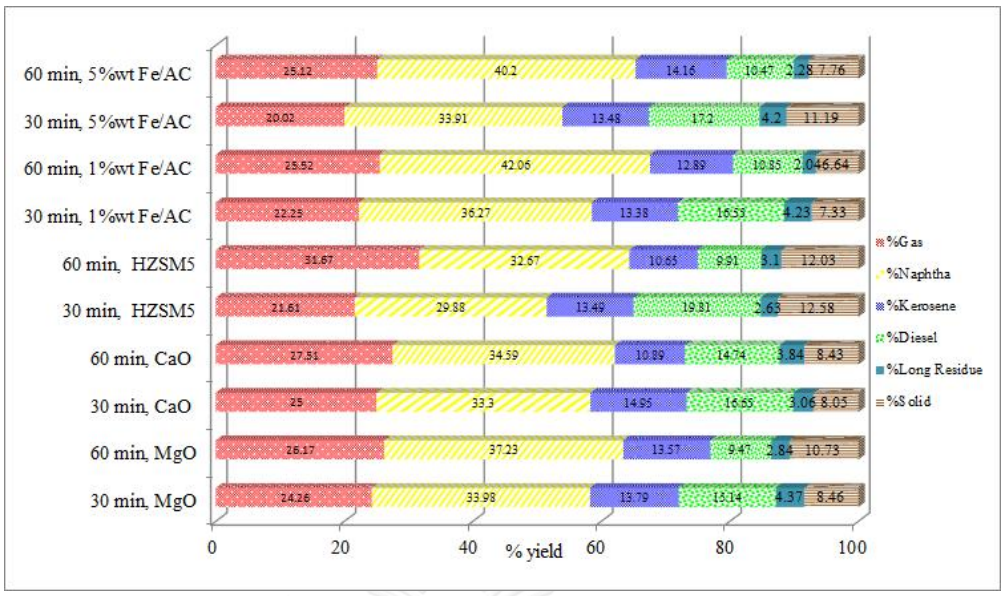

Fig. 4. 11 The effect of reaction time on product distribution where reaction temperature of 450 °C, initial hydrogen pressure of 1 bar and 1%wt of catalyst content over five catalysts.

4.6.3 The effect of initial hydrogen pressure

Fig. 4.12 shows the effect of initial hydrogen pressure on percentage of liquid product. It is found that increasing initial hydrogen pressure from 1 bar to 5 bar do not significantly influence on percentage of liquid product. For MgO & CaO, the increasing initial hydrogen pressure did not affect on the percentage of liquid product comparing with the effects of reaction temperature and reaction time. Fe/AC gave percentage of liquid product slightly decreased. It was possible that H_2 enhanced thermal cracking of large hydrocarbon molecules into small hydrocarbon molecules. The higher hydrogen pressure, the better cracking process. Therefore, the possibilities that small hydrocarbon molecules would crack into gases were higher. HZSM-5 resulted in slightly increasing of percentage of liquid product. This was because high acid catalyst resulted in very well cracking of large hydrocarbon molecules to small hydrocarbon molecules until hydrocarbon gases, as shown in Fig. 4.12.

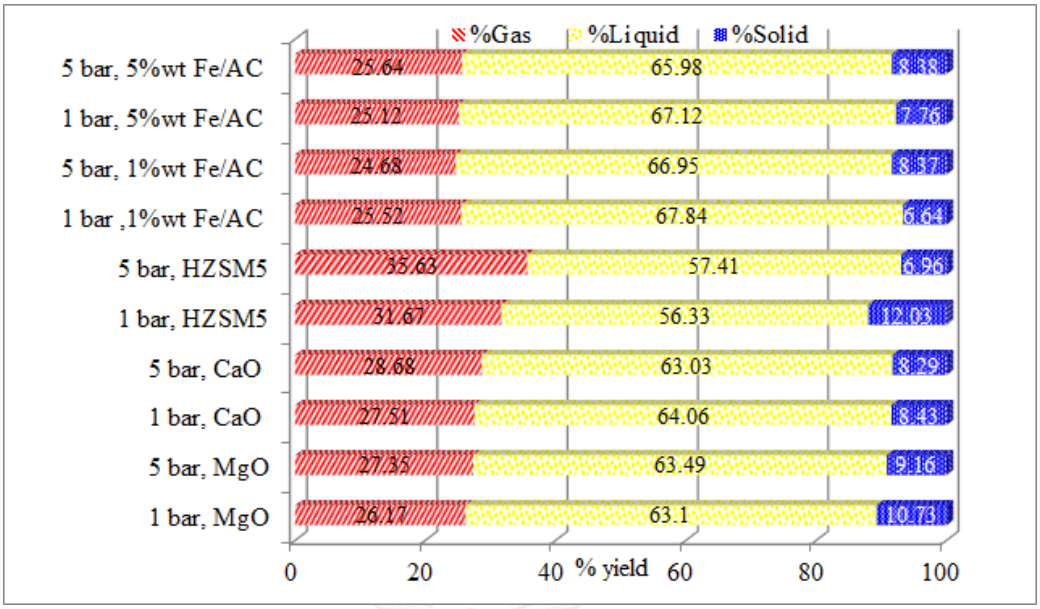

Fig. 4. 12 The effect of initial hydrogen pressure on liquid product where reaction temperature of 450 °C, reaction time of 60 minutes and 1wt% of catalyst content over five catalysts.

Fig. 4.13 shows product distribution of liquid product which is observed that when increase initial hydrogen pressure from 1 bar to 5 bar. It was found that percentage of naphtha yield slightly increased for basic catalysts (MgO & CaO), it was possible that H_2 enhanced the selectivity of product in naphtha range. While Fe/Ac catalyst gave percentage of naphtha yield slightly decreased. At higher H_2 pressure, small hydrocarbon molecules could be cracked better which made some of naphtha further cracked into more gases, as shown in Fig. 4.13. HZSM-5 found that percentage of naphtha yield was relatively stable. It could be said that H_2 did not significantly affect on naphtha fraction. However, it still had high catalytic activity in cracking process. It could be concluded that H_2 increased the selectivity of naphtha. MgO and CaO gave slightly higher percentage of naphtha yield, followed by HZSM-5 which gave stable percentage of naphtha yield and the last one was Fe/AC catalyst which resulted in slightly lower percentage of naphtha yield.

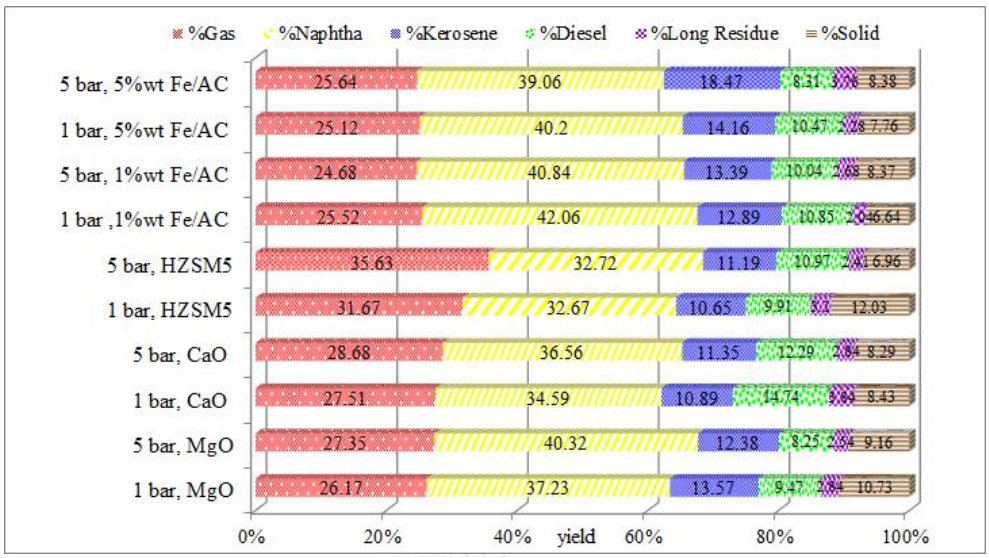

Fig. 4. 13 The effect of initial hydrogen pressure on product distribution where reaction temperature of 450 °C, reaction time of 60 minutes and 1wt% of catalyst content over five catalysts.

4.6.4 The effect of the catalyst content

From Fig. 4.14 observed that when increasing catalyst content from 0.5%wt to 1.0%wt, percentage of liquid product for all catalysts were not significantly different. This might be because catalyst was already thoroughly exposed to reactant no matter how much catalyst was increased. This was consistent with basic catalysts (MgO & CaO) which resulted in relatively stable percentage of liquid product at about 67-68% and Fe/AC catalyst resulted in relatively stable percentage of liquid product at about 68-70% while HZSM-5 resulted in significant reduction of percentage of liquid product. It indicated that with more catalyst content, the cracking reactivity was stronger and the possibility of gas content was higher.

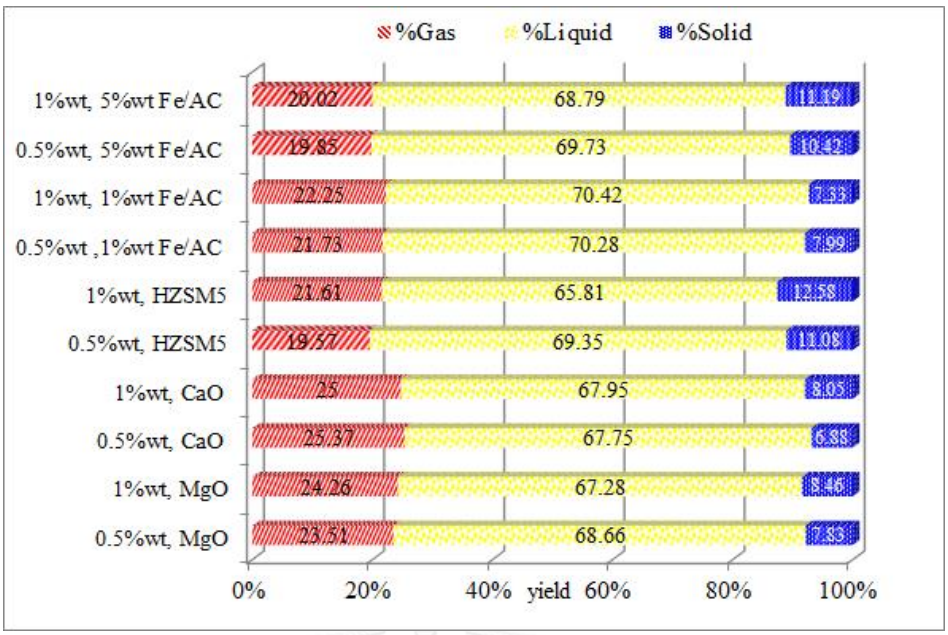

Fig. 4. 14 The effect of the catalyst content on liquid product where reaction temperature of 450 °C, reaction time of 30 minutes and initial hydrogen pressure of 1 bar over five catalysts.

Considering percentage of product distribution as shown in Fig. 4.15 found that all catalysts resulted in higher percentage of naphtha yield. The more catalyst content, the higher possibility that reactants contact with catalyst, and reached the equilibrium faster. In this case it was conversion of long residue into diesel, kerosene and naphtha which resulted in higher naphtha fraction. An another observation was higher catalyst content resulted in higher gas content. This was because catalyst enhanced cracking process by more contact between catalysts and reactants. It could be concluded that catalyst content increased percentage of naphtha yield in similar proportions for all catalysts.

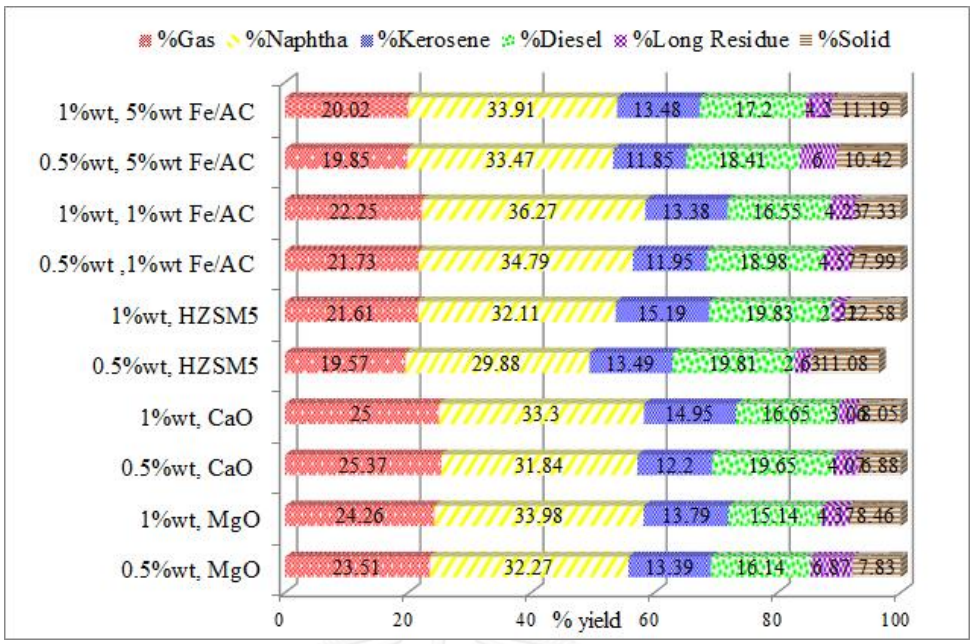

Fig. 4. 15 The effect of catalyst content on product distribution where reaction temperature of 450 °C, reaction time of 30 minutes and initial hydrogen pressure of 1 bar over five catalysts.

4.7 Kinetic Study

The effects of various variables affecting on percentage of liquid product and naphtha yield for all five catalysts by using Design Expert showed that MgO gave highest percentage of liquid product and naphtha yield, followed by HZSM-5 and 1wt% Fe/AC. Therefore, the kinetics of these three catalysts were selected. The kinetics variables were reaction temperature of 390, 410, 430 and 450 °C and reaction time of 0, 15, 25, 35, 45 and 60 minutes with constant initial hydrogen pressure and catalyst content. The kinetic variables condition of three catalysts were shown in Table 4.24

Table 4. 24 The kinetic condition of three catalysts.

Catalyst	Kinetics Study			
	Temperature (°C)	**Time** (min)	**Initial hydrogen pressure** (bar)	**Catalyst Content** (%wt)
MgO	390, 410, 430, 450	0, 15, 25, 35, 45, 60	1	0.5
HZSM-5	390, 410, 430, 450	0, 15, 25, 35, 45, 60	1	0.5
1%wt Fe/AC	390, 410, 430, 450	0, 15, 25, 35, 45, 60	1	0.5

4.7.1 The kinetic theory

The cracking mechanism was the mostly complex and slight in expression, then the assumption to expression the mechanism of catalytic pyrolysis of rapeseed oil to liquid product over three types of catalyst was occurred in batch reactor. Long Residue acted as reactant in rapeseed oil was followed with time for this kinetic study.

Fig. 4. 16 Schematic diagram represented of the batch reactor

The kinetics study for each experiment was performed in the batch reactor which could be represented by the following scheme Fig. 4.16. The assumption of kinetic model as following, the reaction is isothermal at the setting temperature for each batch of reaction under the initial pressure of hydrogen as indicated in Table 4.24 and constant of liquid volume. The conversion of Long Residue (LR) for each desired temperature could be calculated from the analysis of Long Residue, where the conversion at initial time is X_{B0} and at the time, t is X_B.

$$\% \text{ Conversion of long residue} = \left(\frac{X_{B0}-X_B}{X_{B0}}\right) \text{x } 100 \quad (1)$$

Thus, the gray part of the reactor (from Fig. 4.30) could be represented by the equation rate of disappearance of B = the rate of the conversion of B per volume

$$-r_B = \left(-\frac{1}{V}\right)\left(\frac{dn_B}{dt}\right) \quad (2)$$

It was assumed that N_{B0} is the beginning amount of LR in the reactor at time = 0 and N_B is the LR amount at time t. Then, the conversion of LR is defined.

$$X_B = \left(\frac{N_{B0}-N_B}{N_B}\right) = 1 - \frac{N_B/V}{N_{B0}/V} \quad (3)$$

$$X_B = 1 - \frac{C_B}{C_{B0}} \quad (4)$$

At the constant volume;

$$-r_B = (-dc_b/dt) = k_n C^n_B \quad (5)$$

If first order reaction is obtain the relationship between $-r_B$ and C_B from the equation 5 as follow

$$(-dc_B/dt) = k_1 C_B \quad (6)$$

$$-\int_{C_{B0}}^{C_B} dC_B / C_B = k_2 \int_0^t k_1 dt \quad (7)$$

Integrating

$$\ln(C_B) - \ln(C_{B0}) = -k_1 t \quad (8)$$

Thus

$$\ln(C_B) = \ln(C_{B0}) - k_1 t \quad (9)$$

A plotted of ln (C_B) versus t gives the straight line with slope = - k_1

If second order reaction is obtain the relationship between $-r_B$ and C_B from the equation 5 as follow

$$(-dc_B/dt) = k_2 C_B^2 \quad (10)$$

$$-\int_{C_{B0}}^{C_B} dC_B / C_B^{\,2} \quad = \quad k_2 \int_0^{t_B} dt \qquad (11)$$

Integrating

$$(1/C_B) - (1/C_{B0}) \quad = \quad k_2 t \qquad (12)$$

$$(1/C_B) \quad = \quad (1/C_{B0}) + k_2 t \qquad (13)$$

A plotted of $(1/C_B)$ versus t gives the straight line with slope = k_2

4.7.2 The kinetic of MgO

Table 4. 25 The conversion of Long Residue at the variation of reaction time where the catalytic pyrolysis of rapeseed oil over MgO

Temperature (°C)	Time (min)	Long Residue (%wt)	Conversion	ln(1-x)	x/(1-x)
390	0	57.45	0.0000	0.0000	0.0000
	15	54.40	0.0305	-0.0310	0.0315
	25	50.83	0.0661	-0.0684	0.0708
	35	48.94	0.0851	-0.0890	0.0930
	45	46.54	0.1091	-0.1155	0.1224
	60	44.75	0.1270	-0.1358	0.1455
410	0	55.64	0.0000	0.0000	0.0000
	15	50.86	0.0479	-0.0490	0.0503
	25	46.69	0.0895	-0.0938	0.0983
	35	42.88	0.1277	-0.1366	0.1463
	45	38.78	0.1686	-0.1847	0.2028
	60	34.99	0.2065	-0.2313	0.2603
430	0	54.55	0.0000	0.0000	0.0000
	15	48.83	0.0572	-0.0589	0.0607
	25	42.16	0.1240	-0.1324	0.1415
	35	37.20	0.1735	-0.1906	0.2099
	45	33.50	0.2105	-0.2364	0.2667

	60	30.20	0.2436	-0.2792	0.3220
450	0	52.92	0.0000	0.0000	0.0000
	15	45.36	0.0756	-0.0787	0.0818
	25	38.88	0.1404	-0.1513	0.1633
	35	32.02	0.2090	-0.2345	0.2643
	45	25.82	0.2710	-0.3160	0.3717
	60	20.61	0.3231	-0.3903	0.4774

From Table 4.25, column ln (1-x) and x/(1-x) were for first and second reaction order. When ln (1-x) [equation 8] and time were plotted as graph it was found that first reaction order crossed the negative axis, as shown in Fig.4.17 and when x(1-x) [equation 13] and time were plotted as graph it was found that the second reaction order crossed the positive axis as shown in Fig.4.18. Fig. 4.18 illustrated that the conversion of Long Residues to liquid product over MgO are validate at temperature 390, 410, 430 and 450˚C : reaction time at 0, 15, 25, 35, 45 and 60 minutes gave precisely a right line with a good regression constant near by 1.00.

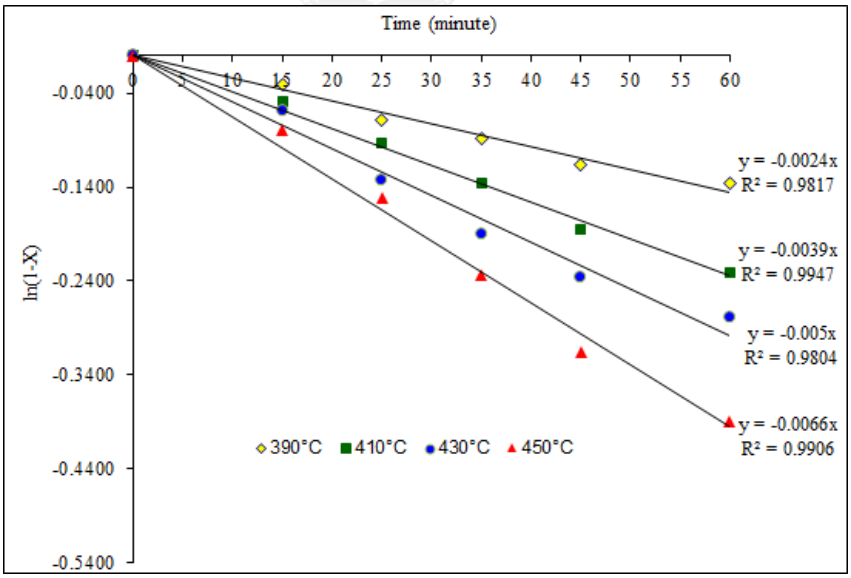

Fig. 4. 17 Conversion vs. Time of reaction for first order

[(◆) 390ºC; (■) 410ºC; (●) 430ºC ; (▲) 450ºC]

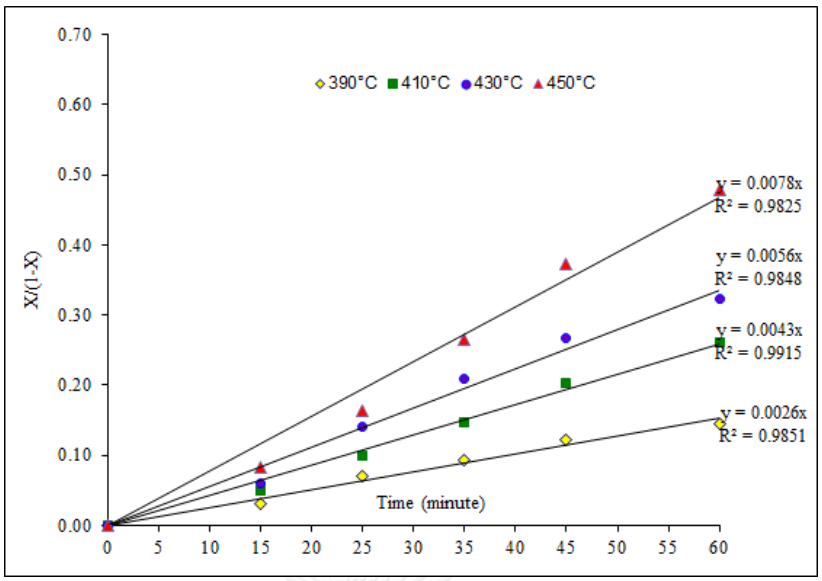

Fig. 4. 18 Conversion vs. Time of reaction for second order

[(◆) 390°C; (■) 410°C; (●) 430°C ; (▲) 450°C]

Hence, this reaction is the second order, thus the equation (5) become

$$(1/C_B) - (1/C_{B0}) = k_2t \quad (14)$$

$$(1/C_B) = (1/C_{B0}) + k_2t \quad (15)$$

Rearrange in term of conversion

$$X = 1 - (C_B/C_{B0}) \quad (16)$$

Thus

$$K_2C_{Bo}t = (1/(1-X)) - 1 \quad (17)$$

Consideration the rate constant at the various temperature and plot the relationship between $\ln(k_2)$ and 1/T from Arrhenius's equation

$$k_n = k_{(n0)}e^{(-E/RT)} \quad (18)$$

The equation is expression in term of logarithm as following

$$\ln(k_n) = \ln(k_{n0}) - (E/R)/T \quad (19)$$

A plotted of $\ln(k_n)$ versus 1/T gives the straight line with the slope as (-E/R) and the intercept = $\ln(k_{n0})$ which uses to determine the activation energy (Ea) and Pre-exponential (k_{n0}), respectively.

Table 4. 26 Represented of $\ln(k_n)$ versus 1/T at the variation of reaction temperature (MgO)

Temperature (°C)	1/T (K^{-1})	k_2C_{B0} (min^{-1})	$k_2\ C_{B0}$ (s^{-1})	$\ln(k_2)$
390	1.5080×10^{-3}	0.0026	4.33×10^{-5}	-10.0466
410	1.4638×10^{-3}	0.0043	7.17×10^{-5}	-9.5435
430	1.4222×10^{-3}	0.0056	9.33×10^{-5}	-9.2793
450	1.3828×10^{-3}	0.0078	1.3×10^{-4}	-8.9480

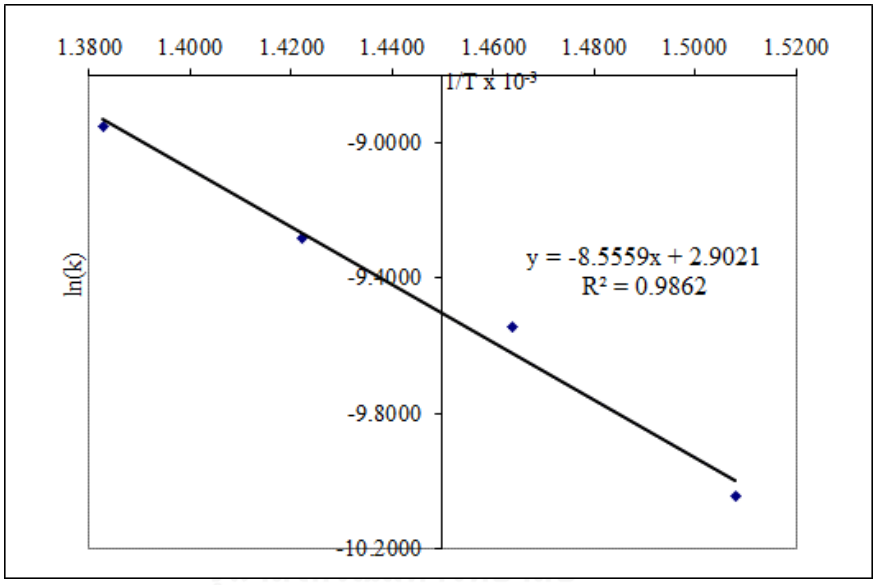

Fig. 4. 19 Plot of values of logarithmic specific reaction rate constant against the reciprocal of the reaction temperature (MgO)

From Fig. 4.19 shows ln k versus 1/T could be traced. So Ea, the activation energy could be obtained by the slope of the straight line and also, $\ln(k_0)$ as an intercept which determined the pre-exponential (k_0) from equation (19).

Thus

$$Ea = 71.134\ kJ\ mol^{-1} \quad ; \quad k_0 = 18.21\ s^{-1}$$

4.7.3 The kinetic of HZSM-5

Table 4. 27 The conversion of Long Residue at the variation of reaction time where the catalytic pyrolysis of rapeseed oil over HZSM-5

Temperature (°C)	Time (min)	Long Residue (%wt)	Conversion	ln(1-x)	x/(1-x)
390	0	52.56	0.0000	0.0000	0.0000
	15	46.30	0.0627	-0.0647	0.0669
	25	41.16	0.1140	-0.1210	0.1286
	35	36.83	0.1574	-0.1712	0.1867
	45	29.34	0.2322	-0.2642	0.3024
	60	22.81	0.2976	-0.3532	0.4236
410	0	51.55	0.0000	0.0000	0.0000
	15	42.41	0.0914	-0.0959	0.1006
	25	35.09	0.1646	-0.1798	0.1970
	35	28.50	0.2305	-0.2620	0.2996
	45	24.07	0.2748	-0.3213	0.3789
	60	20.85	0.3070	-0.3667	0.4430
430	0	50.57	0.0000	0.0000	0.0000
	15	41.24	0.0932	-0.0979	0.1028
	25	32.52	0.1805	-0.1990	0.2202
	35	26.01	0.2455	-0.2817	0.3254
	45	20.42	0.3014	-0.3587	0.4315
	60	15.20	0.3536	-0.4364	0.5471
450	0	49.42	0.0000	0.0000	0.0000
	15	37.23	0.1219	-0.1300	0.1388
	25	29.04	0.2037	-0.2278	0.2559
	35	22.38	0.2704	-0.3153	0.3706
	45	17.67	0.3175	-0.3820	0.4652
	60	12.56	0.3686	-0.4598	0.5838

From Table 4.27, column ln (1-x) and x/(1-x) were for first and second reaction order. When ln (1-x) [equation 8] and time were plotted as graph it was found that first reaction order crossed the negative axis, as shown in Fig.4.20 and when x(1-x) [equation 13] and time were plotted as graph it was found that the second reaction order crossed the positive axis as shown in Fig.4.21. Fig. 4.21 illustrated that the conversion of Long Residues to liquid product over HZSM-5 are validate at temperature 390, 410, 430 and 450°C, reaction time at 0, 15, 25, 35, 45 and 60 gave correctly a right line with a good regression constant nearby 1.00. Hence, this reaction is the second order.

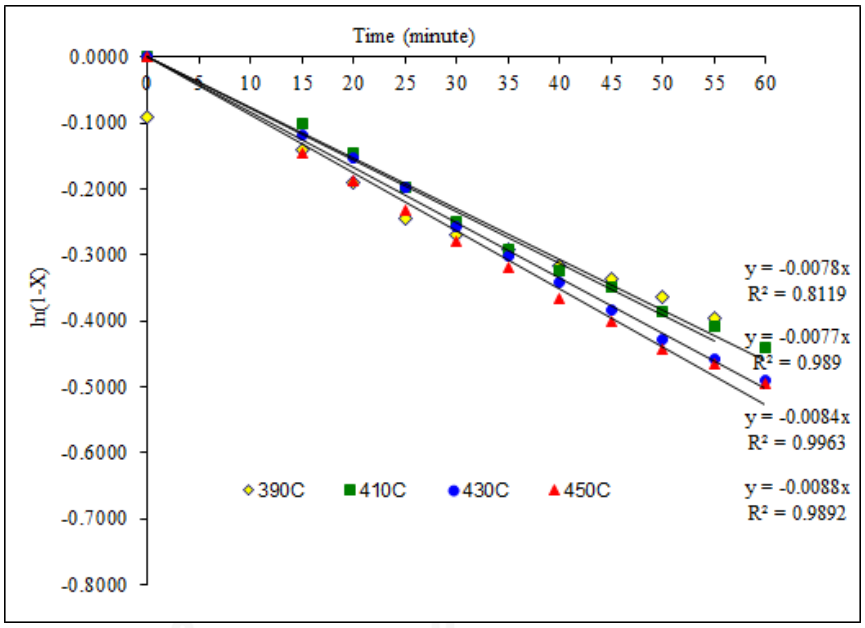

Fig. 4. 20 Conversion vs. Time of reaction for first order

[(◆) 390°C; (■) 410°C; (▲) 430°C ; (●) 450°C]

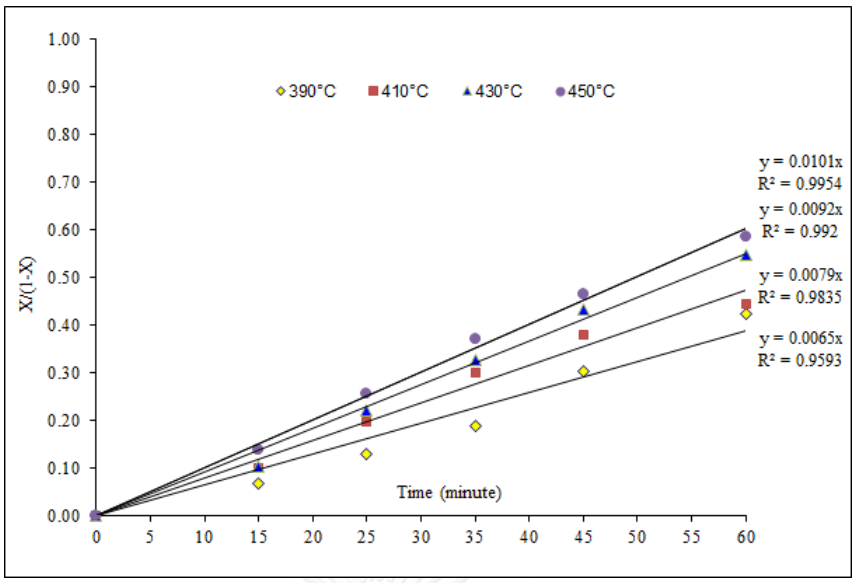

Fig. 4. 21 Conversion vs. Time of reaction for second order

[(◆) 390ºC; (■) 410ºC; (▲) 430ºC ; (●) 450ºC]

A plotted of $\ln(k_n)$ versus 1/T with the data in Table 4.28 gives the straight line with the slope as (-E/R) and the intercept = $\ln(k_{n0})$ which uses to determine the activation energy (Ea) and Pre-exponential (k_{n0}), respectively.

Table 4. 28 Represented of $\ln(k_n)$ versus 1/T at the variation of reaction temperature (HZSM-5)

Temperature (°C)	1/T (K^{-1})	k_2C_{B0} (min^{-1})	k_2 (s^{-1})	$\ln(k_2)$
390	1.5080×10^{-3}	0.0065	1.08×10^{-4}	-9.1303
410	1.4638×10^{-3}	0.0079	1.32×10^{-4}	-8.9352
430	1.4222×10^{-3}	0.0092	1.53×10^{-4}	-8.7829
450	1.3828×10^{-3}	0.0101	1.68×10^{-4}	-8.6896

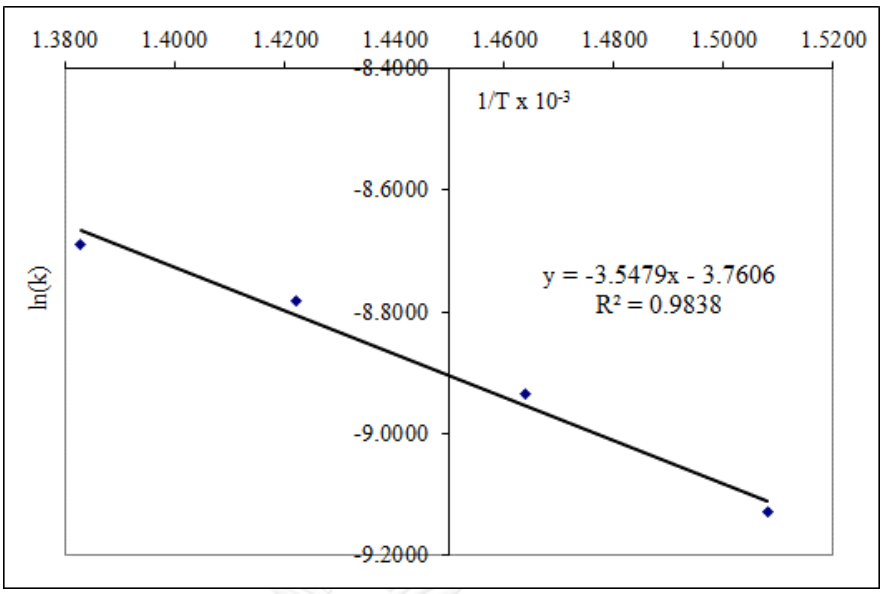

Fig. 4. 22 Plot of values of logarithmic specific reaction rate constant against the reciprocal of the reaction temperature (HZSM-5)

From Fig. 4.22 shows ln k versus 1/T could be traced. So Ea, the activation energy could be obtained by the slope of the straight line and also, $\ln(k_0)$ as an intercept which determined the pre-exponential (k_0) from equation (19).

Thus

$$Ea = 29.497 \text{ kJ mol}^{-1} ; \quad k_0 = 2.33 \times 10^{-2} \text{ s}^{-1}$$

4.7.4 The kinetic of 1%wt Fe/AC

The last kinetic study of catalytic pyrolysis of rapeseed oil was carried out on 1%wt Fe/AC. The conversion of LR with time was shown in Table 4.29.

Table 4. 29 The conversion of Long Residue at the variation of reaction time where the catalytic pyrolysis of rapeseed oil over 1%wt Fe/AC

Temperature (°C)	Time (min)	Long Residue (%wt)	Conversion	ln(1-x)	x/(1-x)
390	0	56.45	0.0000	0.0000	0.0000
	15	51.37	0.0508	-0.0521	0.0535
	25	46.61	0.0984	-0.1036	0.1092
	35	41.38	0.1508	-0.1634	0.1775
	45	38.40	0.1805	-0.1991	0.2203
	60	35.27	0.2118	-0.2380	0.2687
410	0	54.90	0.0000	0.0000	0.0000
	15	48.09	0.0680	-0.0704	0.0730
	25	41.81	0.1308	-0.1402	0.1505
	35	36.44	0.1846	-0.2040	0.2263
	45	31.40	0.2350	-0.2678	0.3071
	60	26.31	0.2858	-0.3366	0.4002
430	0	52.83	0.0000	0.0000	0.0000
	15	44.64	0.0819	-0.0854	0.0892
	25	38.15	0.1467	-0.1587	0.1720
	35	30.82	0.2201	-0.2486	0.2822
	45	25.78	0.2705	-0.3154	0.3707
	60	20.64	0.3218	-0.3884	0.4746
450	0	50.96	0.0000	0.0000	0.0000
	15	42.08	0.0888	-0.0930	0.0975
	25	34.09	0.1688	-0.1849	0.2031
	35	27.54	0.2342	-0.2668	0.3058
	45	21.36	0.2961	-0.3511	0.4206
	60	14.98	0.3599	-0.4461	0.5622

From Table 4.29, column ln (1-x) and x/(1-x) were for first and second reaction order. When ln (1-x) [equation 8] and time were plotted as graph it was found that first reaction order crossed the negative axis, as shown in Fig.4.23 and when x(1-x) [equation 13] and time were plotted as graph it was found that the second reaction order crossed the positive axis as shown in Fig.4.24. Fig. 4.24 illustrated that the conversion of Long Residues to liquid fuels over 1%wt Fe/AC are validate at temperature 390, 410, 430 and 450°C : time of reaction during 0 to 60 minutes gave correctly a right line with a good regression constant nearby 1.00. Hence, this reaction is the second order.

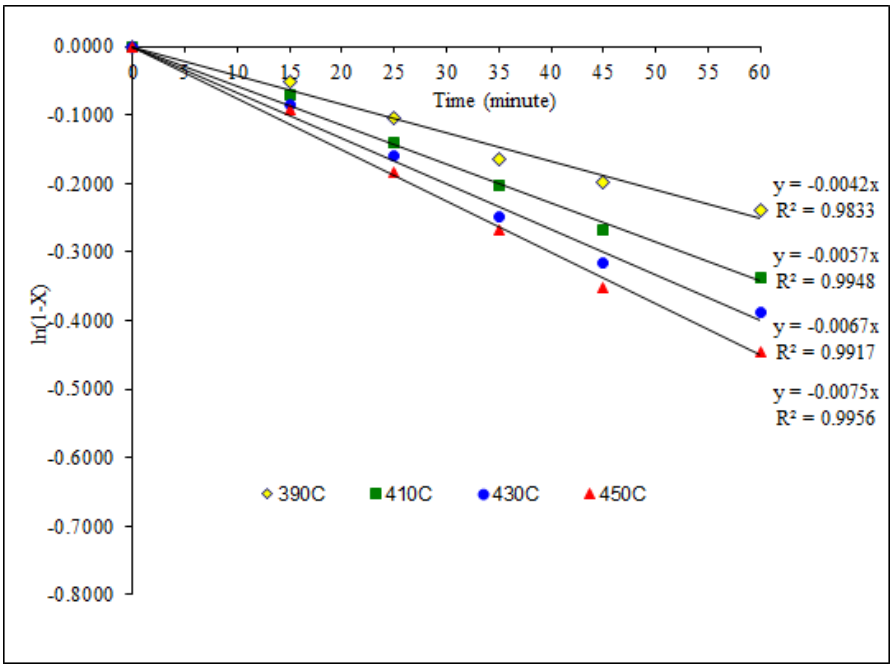

Fig. 4. 23 Conversion vs. Time of reaction for first order

[(◆) 390°C; (■) 410°C; (▲) 430°C ; (●) 450°C]

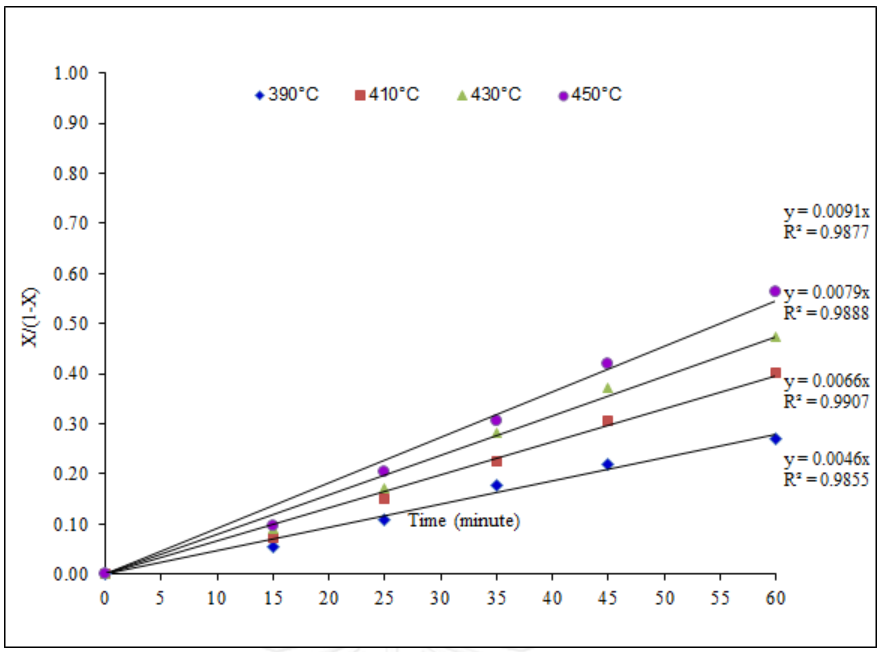

Fig. 4. 24 Conversion vs. Time of reaction for second order

[(◆) 390ºC; (■) 410ºC; (▲) 430ºC ; (●) 450ºC]

A plotted of $\ln(k_n)$ versus 1/T with the data in Table 4.30 gives the straight line with the slope as (-E/R) and the intercept = $\ln(k_{n0})$ which uses to determine the activation energy (Ea) and Pre-exponential (k_0), respectively.

Table 4. 30 Represented of $\ln(k_n)$ versus 1/T at the variation of reaction temperature (1%wt Fe/AC)

Temperature (°C)	1/T (K^{-1})	k_2C_{B0} (min^{-1})	k_2 (s^{-1})	$\ln(k_2)$
390	1.5080×10^{-3}	0.0046	7.67×10^{-5}	-9.4760
410	1.4638×10^{-3}	0.0066	1.1×10^{-4}	-9.1150
430	1.4222×10^{-3}	0.0079	1.32×10^{-4}	-8.9352
450	1.3828×10^{-3}	0.0091	1.52×10^{-4}	-8.7938

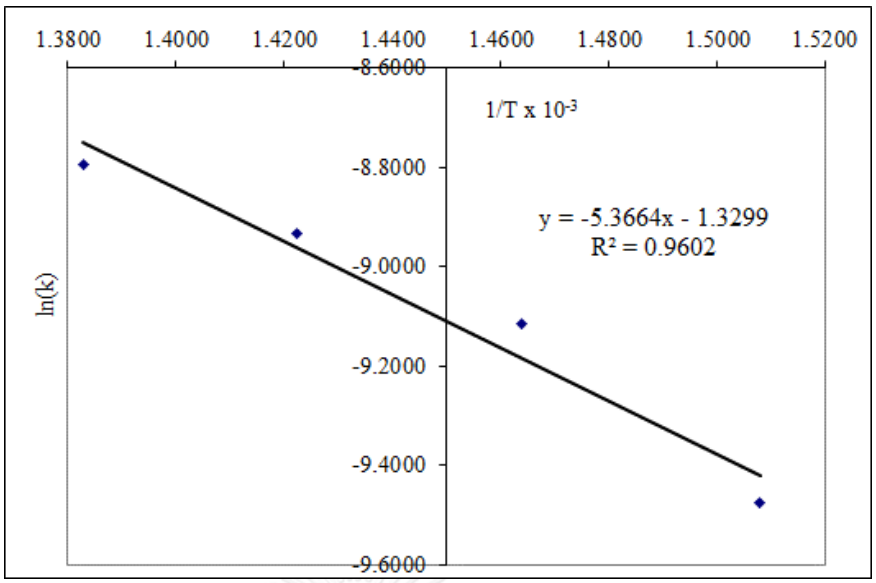

Fig. 4. 25 Plot of values of logarithmic specific reaction rate constant against the reciprocal of the reaction temperature (1%wt Fe/AC)

From Fig. 4.25 shows ln k versus 1/T traced. So Ea, the activation energy could be obtained by the slope of the right line and also, k_0 the pre-exponential factor ;

Thus,

$$Ea = 44.616 \text{ kJ mol}^{-1} ; \quad k_0 = 2.65 \times 10^{-1} \text{ s}^{-1}$$

The overview conclusion of kinetics study of three type catalysts was expressed in Table 4.31. It can be noted that HZSM-5 has lowest activation energy. It was confirmed higher activity of cracking reaction that it was found in the experiment.

Table 4. 31 The reaction order, activation energy and pre-exponential factor from kinetic study of three types of catalyst.

Catalyst	**Reaction Order**	**Activation Energy : (Ea) kJ/mol**	**Pre-exponential (s^{-1})**
MgO	2	77.134	18.21
HZSM-5	2	29.497	2.33×10^{-2}
1%wt Fe/AC	2	44.616	2.65×10^{-1}

4.8 The study of variables that effects the catalytic pyrolysis of rapeseed oil over MgO in continuous reactor

The optimum condition from Design Expert program found that MgO gave best percentage of liquid product and naphtha yield. Thus we study the catalytic pyrolysis of rapeseed oil over MgO in 3-L continuous reactor by studying the effects of temperature of 390°C and 450°C, feeding rate of 3 ml/min and 9 ml/min, N_2 gas flow rate of 50 ml/min and 150 ml/min, catalyst content of 30%V/V and 60%V/V. Using 2k experimental design to determine all of four variables on two responses, percentage of liquid product and percentage of naphtha in liquid product.

4.8.1 Percentage of liquid product

From 2-level factorial experimental design to determine variance of variables affecting on percentage of liquid product from catalytic pyrolysis process of rapeseed oil over MgO in continuous reactor, the results are shown in Table 4.32.

Table 4.32 shows percentage of liquid product from catalytic pyrolysis of rapeseed oil over MgO in continuous. It is found that the main variables are likely to deviate from linear relationship are reaction temperature (A), interaction between N_2 gas flow and feeding rate (CD), interaction between reaction temperature and feeding rate (AD) and catalyst content (B) as shown in Fig. 4.26. The ANOVA results are consistent with Half Normal probability plot of percentage of liquid product as shown in Table 4.33. It indicates that such variables significantly affect on percentage of liquid product from catalytic pyrolysis of rapeseed oil over MgO in continuous reactor.

Table 4. 32 Percentage of liquid product from catalytic pyrolysis of rapeseed oil over MgO in continuous reactor.

Run	Variable				liquid yield (%wt)
	Temperature : A (°C)	Cat. Content. : B (%V/V)	N_2 gas Flow Rate : C (ml/min)	Feeding Rate : D (ml/min)	
1	390	60	150	3	33.42
2	390	30	150	3	41.97
3	450	60	50	9	80.14
4	450	30	50	3	69.01
5	450	30	50	9	84.21
6	390	60	50	3	25.14
7	450	60	150	3	69.04
8	450	60	150	9	71.50
9	390	30	150	9	25.73
10	450	30	150	3	78.11
11	390	30	50	9	34.43
12	390	60	150	9	21.84
13	450	60	50	3	69.00
14	450	30	150	9	79.45
15	390	60	50	9	31.01
16	390	30	50	3	33.45
17	420	45	100	6	80.24

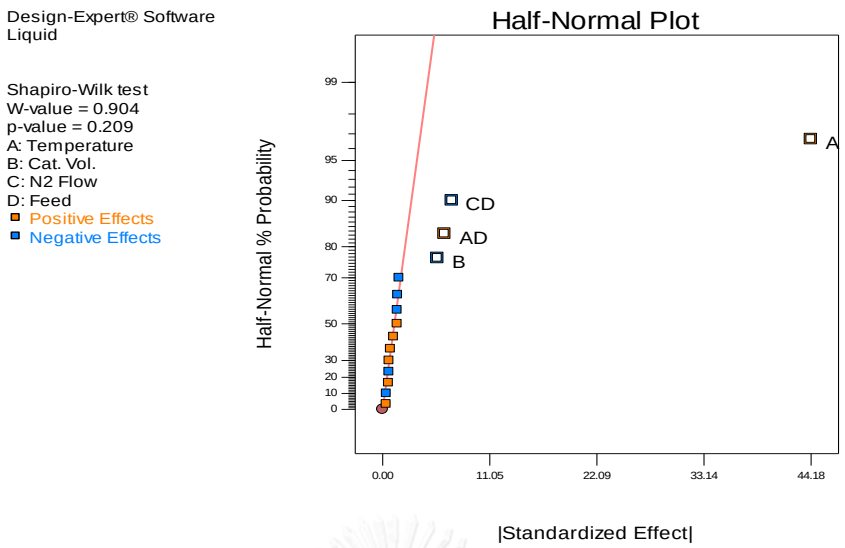

Fig. 4. 26 Half normal probability plot of percentage of liquid product from catalytic pyrolysis of rapeseed oil over MgO in continuous reactor.

Table 4. 33 ANOVA of variables affecting on percentage of liquid product from catalytic pyrolysis of rapeseed oil over MgO in continuous reactor.

Source	Sum of Squares	df	Mean Square	F Value	p-value	
Model	8304.73	4	2076.18	420.69	< 0.0001	significant
A-Temperature	7808.82	1	7808.82	1582.27	< 0.0001	
B-Cat. Con.	128.09	1	128.09	25.95	0.0003	
AD	163.26	1	163.26	33.08	0.0001	
CD	204.56	1	204.56	41.45	< 0.0001	
Curvature	700.13	1	700.13	141.87	< 0.0001	significant
Residual	54.29	11	4.94			
Cor Total	9059.15	16				

The normal plot of residuals as shown in Fig. 4.27 percentage of liquid product from catalytic pyrolysis of rapeseed oil over MgO in continuous reactor shows the linear relationship (R^2 = 0.9935).

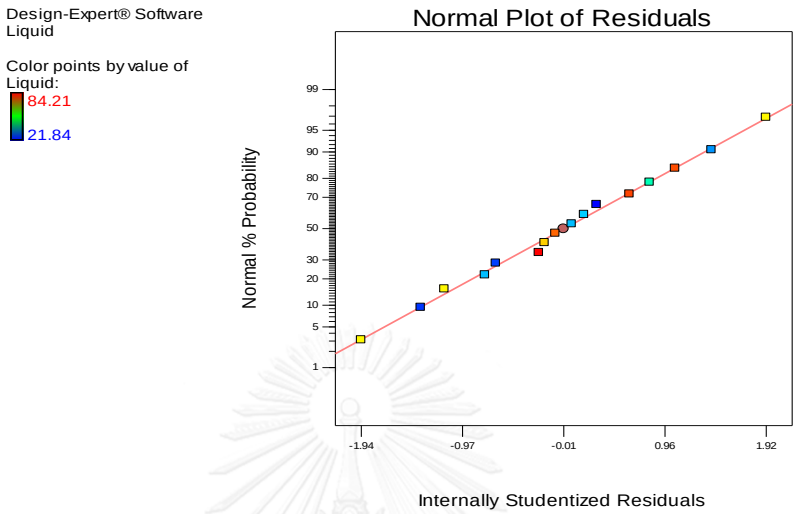

Fig. 4. 27 Normal plot of residuals of percentage of liquid product from catalytic pyrolysis of rapeseed oil over MgO in continuous reactor.

After the ANOVA analysis which determine the main variables affecting on percentage of liquid product from catalytic pyrolysis of rapeseed oil over MgO in continuous reactor, the effects of these variables were further studied by comparing the results between lower value and higher value of each variable as shown in Fig 4.28.

Fig. 4.28 showed the effect of reaction temperature on percentage of liquid product from the catalytic pyrolysis of rapeseed oil over MgO in continuous reactor. Increasing reaction temperature increased percentage of liquid product because heavy oil were cracked into large amount of medium and small hydrocarbon products. It implies that temperature significantly influenced thermal cracking. This was because increasing reaction temperature increased energy of reactants or rapeseed oil which made rapeseed oil had higher energy and cracked into smaller hydrocarbon compounds, via decarboxylation and decarbonylation [34]. When rapeseed oil was heated further it cracked into smaller hydrocarbon compounds which increased percentage of liquid product [65].

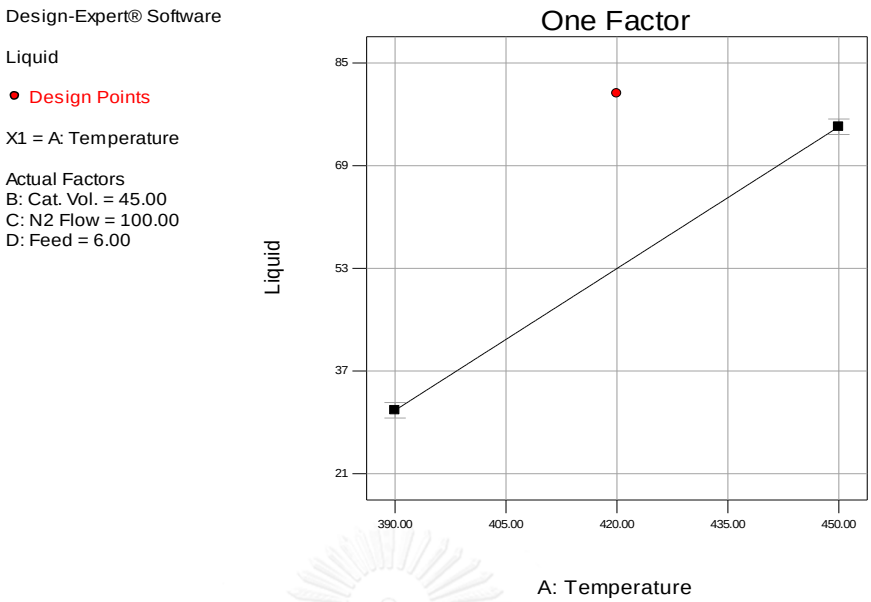

Fig. 4. 28 The effect of reaction temperature on percentage of liquid product

Fig 4.29 showed the interaction between reaction temperature and feeding rate on percentage of liquid product from catalytic pyrolysis of rapeseed oil over MgO in continuous reactor. It confirmed that when increasing reaction temperature, reactant had more energy therefore large hydrocarbon molecules were more cracked into medium and small hydrocarbons. This was corresponded with increased feeding rate which made the reaction proceed forward and resulted in higher percentage of liquid product [55]. From Fig. 4.29 observed that when reaction temperature was increased from 390 °C to 450 °C and feeding rate from 3 mL/min to 9 mL/min, percentage of liquid product increased from 68.29% to 81.83%. Considering the relationship between reaction temperature-feeding rate-N_2 gas flow rate it was found that when reaction temperature was increased from 390°C to 450 °C, feeding rate from 3 mL/min to 9 mL/min and N_2 gas flow rate from 50 mL/min to 150 mL/min, percentage of liquid product decreased from 81.83% to 74.68% as shown in Fig. 4.46. This indicated that N_2 gas flow rate did not significantly affect on percentage of liquid product.

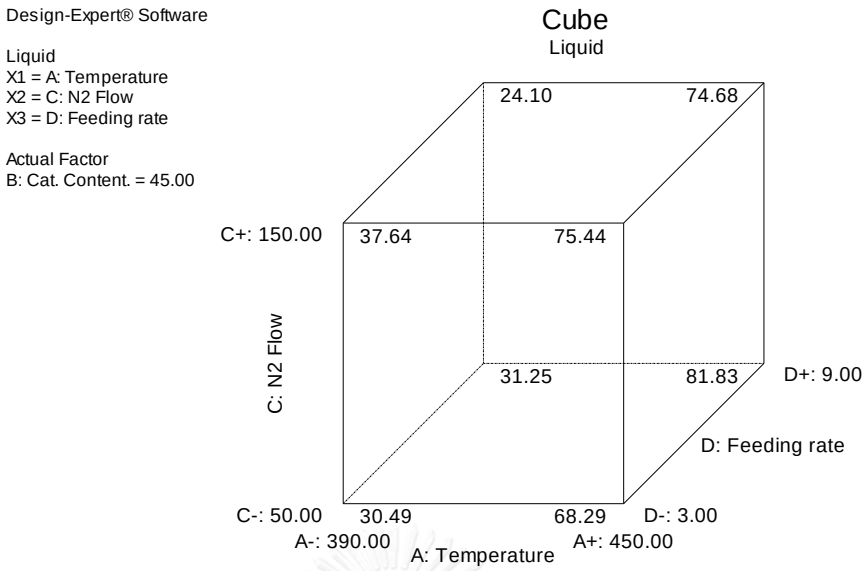

Fig. 4. 29 Cube surface of interaction between reaction temperature and feeding rate affect on percentage of liquid product

Considering the catalyst content (B), it was found that percentage of liquid product was changed in the opposite direction which was slightly decreased. This is because higher amount of catalyst made the reaction faster and facilitated the decarboxylation [34, 55]. Long chain hydrocarbon compounds were cracked into large amount of smaller hydrocarbon compounds. These small hydrocarbons could be further cracked into hydrocarbon gases which resulted in slightly lower percentage of liquid product as shown in Fig. 4.30.

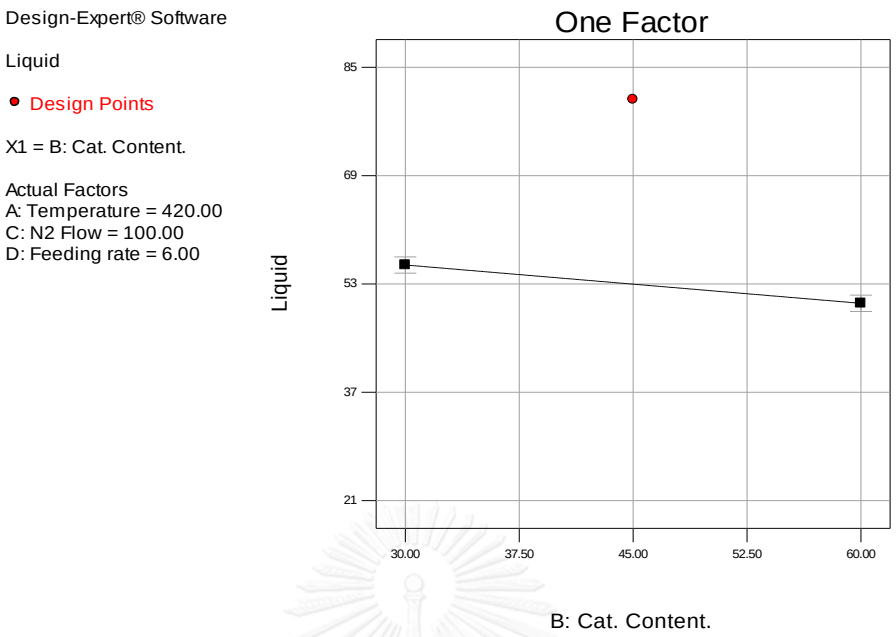

Fig. 4. 30 The effect of catalyst content on percentage of liquid product

For the interaction between N_2 gas flow rate and feeding rate (CD) it was found that percentage of liquid product gradually increased at a particular point. (N_2 gas flow rate of 100 mL/min and feeding rate of 6 mL/min). After that percentage of liquid product gradually decreased (N_2 gas flow rate of 150 mL/min and feeding rate of 9 mL/min). It can be explained that at an initial phase the cracking in reactor could proceed very well when increasing N_2 gas flow rate and feeding rate. However, when N_2 gas flow rate and feeding rate were further increased, percentage of liquid product decreased. It was possible that heavy oil needed some time to be cracked into small hydrocarbon molecules. Increasing N_2 gas flow rate might make heavy oil was not cracked and percentage of liquid product decreased as shown in Fig. 4.31. It could be observed that percentage of liquid product decreased from 31.25% to 24.10%.

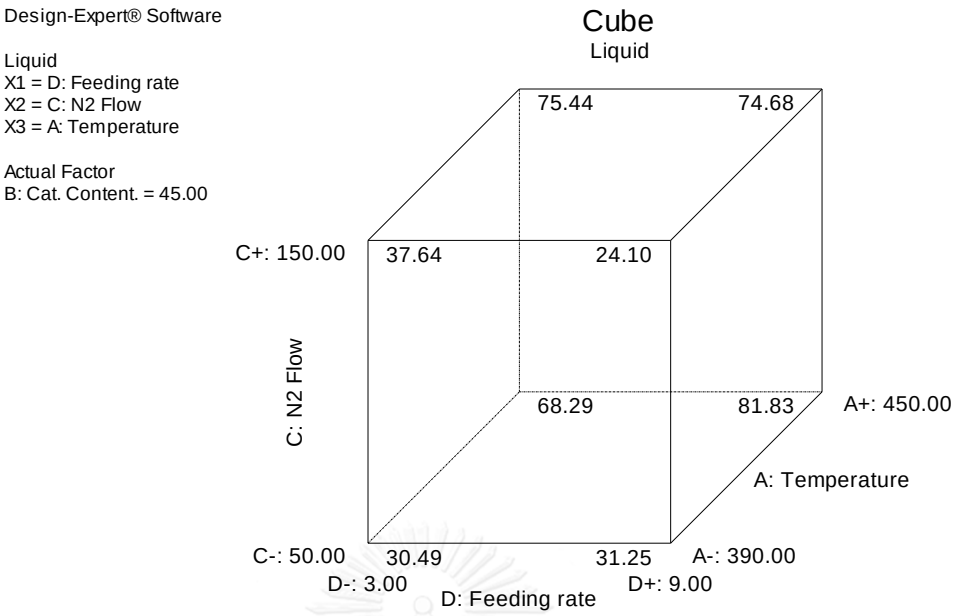

Fig. 4. 31 Cube Surface of interaction between reaction N_2 gas flow rate and feeding rate affect on percentage of liquid product

4.8.2 Percentage of naphtha in liquid product

The objectives of this study were to study the effect of variables affecting on naphtha in liquid products from catalytic pyrolysis of rapeseed oil over MgO in continuous reactor. Percentage of naphtha in liquid product from Table 4.34 was analyzed by The ANOVA. Table 4.35 showed ANOVA analysis of variables affecting on percentage of naphtha in liquid product. It was observed that the main variables were the catalyst content (B), N_2 gas flow rate (C), feeding rate (D). It was also found that the interaction between three factors (BCD, BC and BD) also affected on percentage of naphtha in liquid product as well. The ANOVA results were consistent with half normal probability plot of percentage of naphtha in liquid product as shown in Fig 4.32 which showed the half normal probability of percentage of naphtha in liquid product. It could be observed that the variables likely to deviate from linear relationship were B, C, D, BCD, BC and BD which indicated that such variables and interaction of variables significantly influenced percentage of naphtha in liquid product

Table 4. 34 Percentage of naphtha in liquid product from catalytic pyrolysis of rapeseed oil over MgO in continuous reactor.

Run	Variable				Naphtha yield (%wt)
	Temperature : A (°C)	Cat. Content. : B (%V/V)	N_2 gas Flow rate : C (ml/min)	Feeding Rate : D (ml/min)	
1	390	60	150	3	49.8
2	390	30	150	3	30.7
3	450	60	50	9	52.4
4	450	30	50	3	41.6
5	450	30	50	9	52
6	390	60	50	3	46.5
7	450	60	150	3	50
8	450	60	150	9	49.8
9	390	30	150	9	39.5
10	450	30	150	3	45.3
11	390	30	50	9	43.3
12	390	60	150	9	42.5
13	450	60	50	3	46.8
14	450	30	150	9	50.2
15	390	60	50	9	44.3
16	390	30	50	3	45.3
17	420	45	100	6	53.9

Table 4. 35 ANOVA of variables affecting on percentage of naphtha in liquid product from pyrolysis of rapeseed oil over MgO in continuous reactor.

Source	Sum of Squares	df	Mean Square	F Value	p-value	
Model	550.39	6	91.73	418.55	< 0.0001	significant
B-Cat. Content.	219.04	1	219.04	999.42	< 0.0001	
C-N_2 gas Flow rate	166.41	1	166.41	759.29	< 0.0001	
D-Feeding rate	91.20	1	91.20	416.13	< 0.0001	
BC	24.01	1	24.01	109.55	< 0.0001	
BD	18.92	1	18.92	86.34	< 0.0001	
BCD	30.80	1	30.80	140.54	< 0.0001	
Curvature	10.56	1	10.56	48.19	< 0.0001	significant
Residual	1.97	9	0.22			
Cor Total	562.92	16				

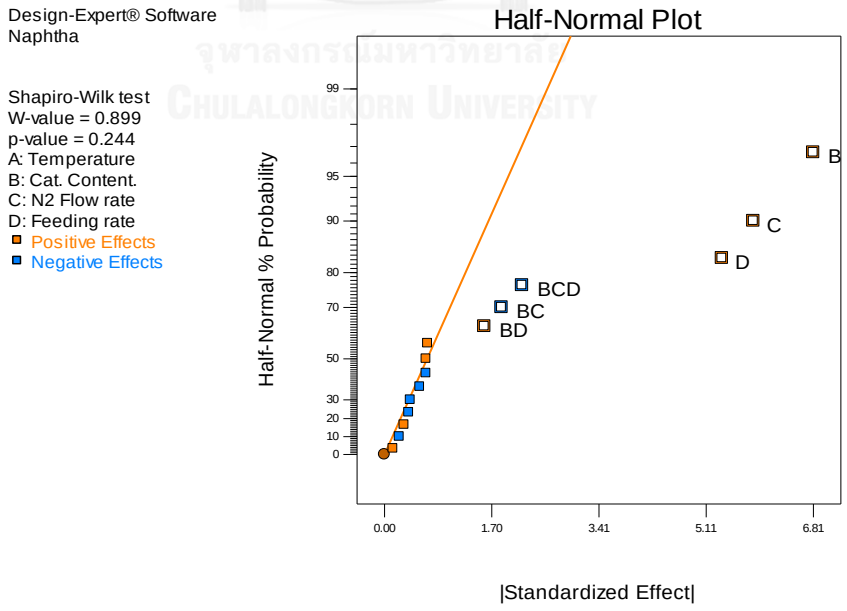

Fig. 4. 32 Half normal probability plot of percentage of naphtha in liquid product from catalytic pyrolysis of rapeseed oil over MgO in continuous reactor.

The normal plot of residuals as shown in Fig. 4.33 percentage of naphtha in liquid product from catalytic pyrolysis of rapeseed oil over MgO in continuous reactor shows the linear relationship ($R^2 = 0.9964$).

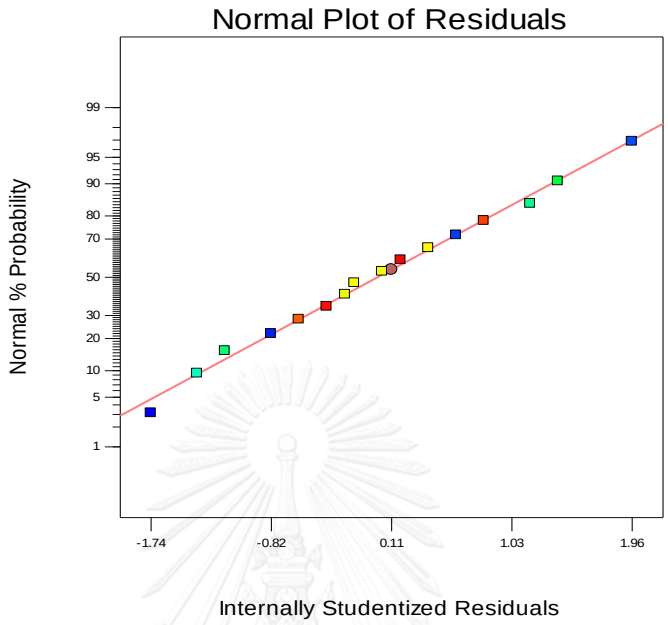

Fig. 4. 33 Normal plot of residuals of percentage of naphtha in liquid product from pyrolysis of rapeseed oil over MgO in continuous reactor.

Fig. 4.34 showed the effect of the catalyst content on percentage of naphtha in liquid product from catalytic pyrolysis of rapeseed oil over MgO in continuous reactor. It was seen that higher amount of catalyst increased percentage of naphtha in liquid product because increasing catalyst content made reactant particles thoroughly contacted with catalyst which resulted in better reaction and heavy oil was cracked into medium hydrocarbon molecules until smaller hydrocarbon molecules so naphtha fraction was higher yield.

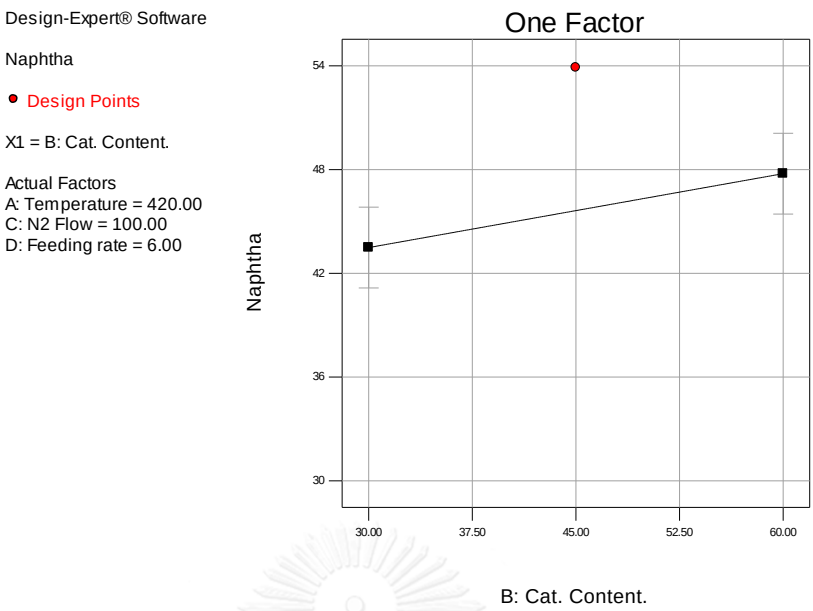

Fig. 4. 34 The effect of catalyst content on percentage of naphtha in liquid product

Fig. 4.35 showed the effect of the N_2 gas flow rate on percentage of naphtha in liquid product from catalytic pyrolysis of rapeseed oil over MgO in continuous reactor. It was found that higher N_2 gas flow rate increased percentage of naphtha in liquid product because N_2 gas would help in producing naphtha by cracking from long residue to diesel, kerosene and naphtha, respectively.

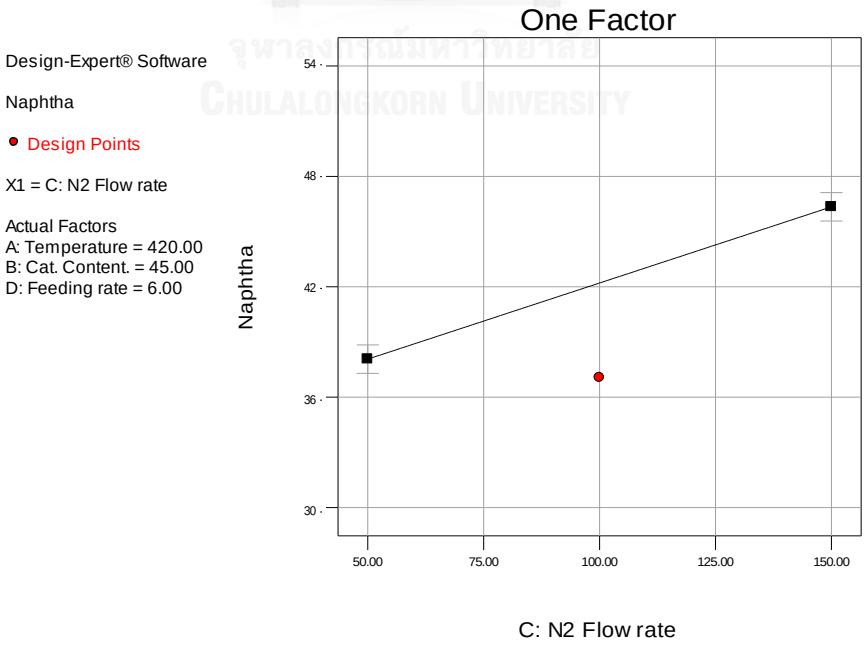

Fig. 4. 35 The effect of N_2 gas flow rate on percentage of naphtha in liquid product

Fig. 4.36 showed the effect of feeding rate of rapeseed oil on percentage of naphtha in liquid product from catalytic pyrolysis of rapeseed oil over MgO in continuous reactor. It was found that percentage of naphtha tend to increased when increasing feeding rate of rapeseed oil. As mentioned above that the reactor could provide enough heat for reactants, so increasing oil feeding rate increased the amount of reactants which resulted in better reaction. Enough heat made reactants cracked even more. In addition, if the amount of catalyst was increased, the reaction could occur better. Higher degradation of rapeseed oil directly affected to free radical, which increased the amount of free radical. Since free radicals were unstable and highly reactive, so products in reactor could be cracked further and gave higher percentage of naphtha yield.

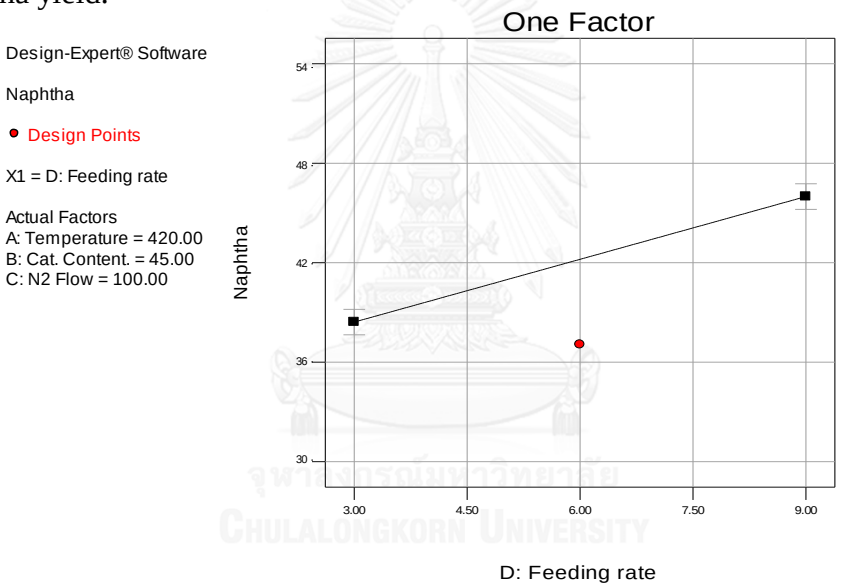

Fig. 4. 36 The effect of feeding rate on percentage of naphtha in liquid product

4.9 The optimum condition of catalytic pyrolysis of rapeseed oil to obtain the highest percentage of liquid product and naphtha yield over MgO in continuous reactor.

The ANOVA results could determine the variables affecting on percentage of liquid product and naphtha yield from catalytic pyrolysis of rapeseed oil over MgO in continuous reactor and could also determine the interaction between variables affecting on percentage of liquid product and naphtha yield. This made us could not choose the optimum condition by considering each variables separately because the interaction between variables affected on percentage of naphtha yield inconsistent with each variable. Therefore, choosing optimum condition by each variable separately might not the actual optimum condition. In this study the optimum condition for catalytic pyrolysis of rapeseed oil to obtain highest percentage of liquid product and naphtha yield over MgO in continuous was chosen by using mathematical model in conjunction with response surface methodology [69]. Table 4.36 showed the range of optimum condition from Design-Expert program of catalytic pyrolysis of rapeseed oil over MgO in continuous reactor. The analysis results were shown as relationship equation between percentage of liquid product, naphtha in liquid product and four variables that affecting on percentage of naphtha in liquid product. The coefficients of different variables depend on the effect size of variable on percentage of naphtha in liquid product as shown in equation 4.1 and 4.2

$$\text{Liquid} = +52.97 + 22.09*A - 2.83*B + 3.19*A*D - 3.58*C*D \quad (4.1)$$

$$\text{Naphtha} = +30.35 + 3.70*B + 3.22*C + 2.39*D - 1.22*B*C + 1.09*B*D - 1.39*B*C*D \quad (4.2)$$

Table 4. 36 The range of optimum condition from Design-Expert program of catalytic pyrolysis of rapeseed oil over MgO in continuous reactor.

Variables	Goal	Lower Limit	Upper Limit
Temperature	in range	390°C	450°C
Feeding rate	in range	3 ml/min	9 ml/min
Catalyst content	in range	30%V/V	60%V/V
N_2 flow rate	in range	50 ml/min	150 ml/min
Percentage of liquid product	maximize	21.84%wt	84.21%wt
Percentage of naphtha yield	maximize	30.70%wt	53.90%wt

Table 4.37 shows the optimum condition from Design-Expert program compared with the experiment. The optimum condition from Design expert program is reaction temperature of 450°C, feeding rate of 5.21 ml/min, catalyst content of 52.99 %V/V and N_2 gas flow rate of 150 ml/min gave percentage of liquid product and naphtha yield of 73.65% and 36.58%, respectively. The optimum condition calculated from Design Expert program was used in actual experiment in order to compare. The actual experiment condition is reaction temperature of 450°C, feeding rate of 5 ml/min, catalyst content of 50 %V/V and N_2 gas flow rate of 150 ml/min gave percentage of liquid product and naphtha yield of 75.44 % and 36.62 %, respectively. It found that the percentage of liquid product was higher, while the percentage of naphtha yield was similar.

Table 4. 37 The optimum conditions of catalytic pyrolysis of rapeseed oil over MgO in continuous reactor between Design-Expert program and the actual experiment

Variables	**Rapeseed Oil**	
	Design Expert Program	**Actual Experiment**
Reaction temperature	450°C	450°C
Feeding rate	5.21 ml/min	5 ml/min
N_2 gas flow rate	150 ml/min	150 ml/min
Catalyst content	52.99%V/V	50%V/V
Percentage of liquid product :	73.65%wt	75.44%wt
Percentage of naphtha yield :	36.58%	36.62%

Table 4.38 shows the reaction results from the actual experiment. Products were 75.44% of liquid hydrocarbon, 16.81% of gas and 10.93% of solid. The amount of solid was determined as the weight difference between weight of the catalyst before and after use. The unreacted triglyceride was not detected in the liquid product, perhaps it did not come out of the reactor as well as the high boiling reaction products, because of their high boiling point. These materials are designated as “solid”. In addition, There is also analyzed the gas composition by GC-TCD and GC-FID. It proves that the catalytic pyrolysis of rapeseed oil over MgO in continuous reactor reacted through decarboxylation of free fatty acid resulted in hydrocarbon compound and CO_2. $MgCO_3$ enhanced the decarboxylation reaction. $MgCO_3$ could decompose into MgO which results in continuous catalysis. Decarbonylation of ketone results in hydrocarbon compound and CO. Hydrocarbon compounds from decarboxylation and decarbonylation were in form of paraffins and olefins which would go through cracking, hydrogen transfer and isomerization processes and resulted in smaller hydrocarbon compound product.

Table 4. 38 Material balance of pyrolysis rapeseed oil from the actual experiment

Catalyst	Product yield [%wt]				
	Oil	Gaseous H.C	CO_2	CO	Solid
MgO	75.44	4.52	9.08	3.21	10.93

4.10 Physico-chemical of pyrolysis rapeseed oil

Fig. 4.37 - 4.39 shows simulation distillation chart of rapeseed oil, pyrolysis rapeseed oil and gasoline 95 which all composition such as naphtha (gasoline), kerosene, diesel and long residue are expressed in Table 4.39. Considering the composition of liquid product which is consisted of naphtha, kerosene, diesel and long residue, it was found that pyrolysis rapeseed oil had 48% naphtha, 8% kerosene, 37% diesel and 7% Long residue. Comparing with rapeseed oil which had only 7% naphtha, it confirmed that catalytic pyrolysis could improve the quality of liquid product to be close to standard fuel although %naphtha might not as high as gasoline 95 which has 59% naphtha as shown in Table 4.39. The quality of liquid product depend on many factors such as temperature, type of catalyst, catalyst quality, catalyst content, gas flow rate, feeding rate even the size of system. The larger production system, the more obtaining the specific compositions and at desired quantity product oil.

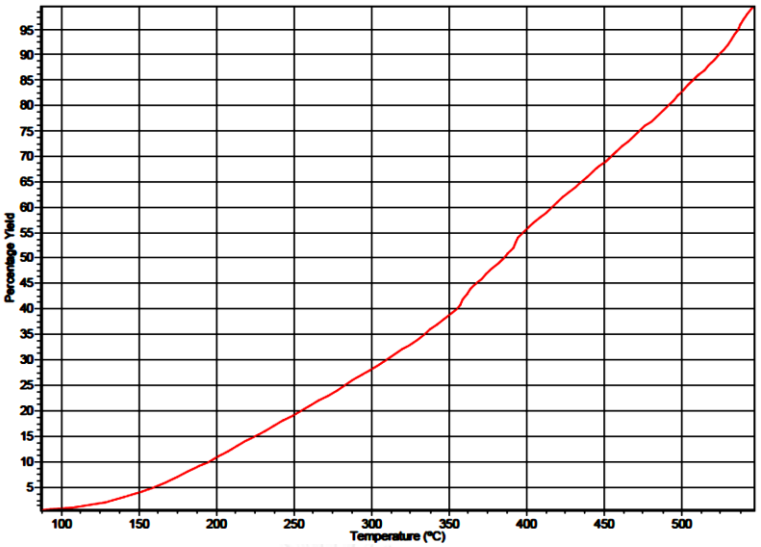

Fig. 4. 37 Distillation graph of rapeseed oil

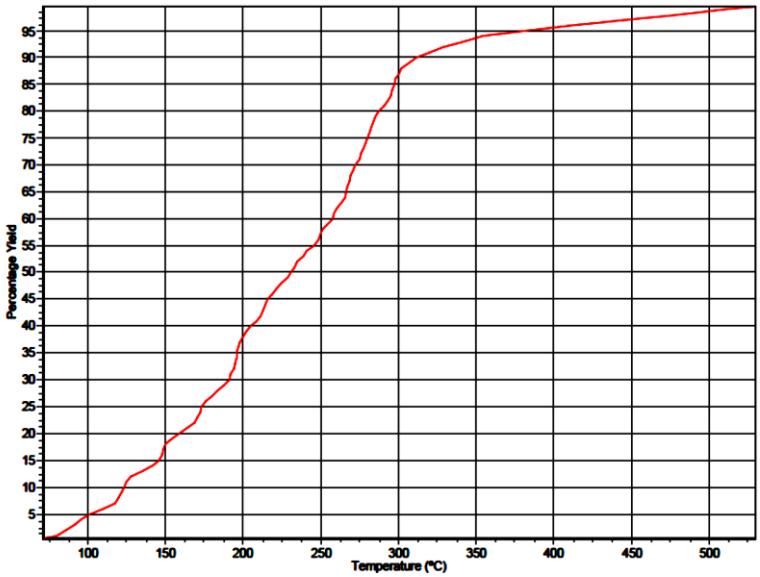

Fig. 4. 38 Distillation graph of pyrolysis rapeseed oil where reaction temperature of 450°C, feeding rate of 5 ml/min, N_2 gas flow rate of 150 ml/min and catalyst content of 50%V/V.

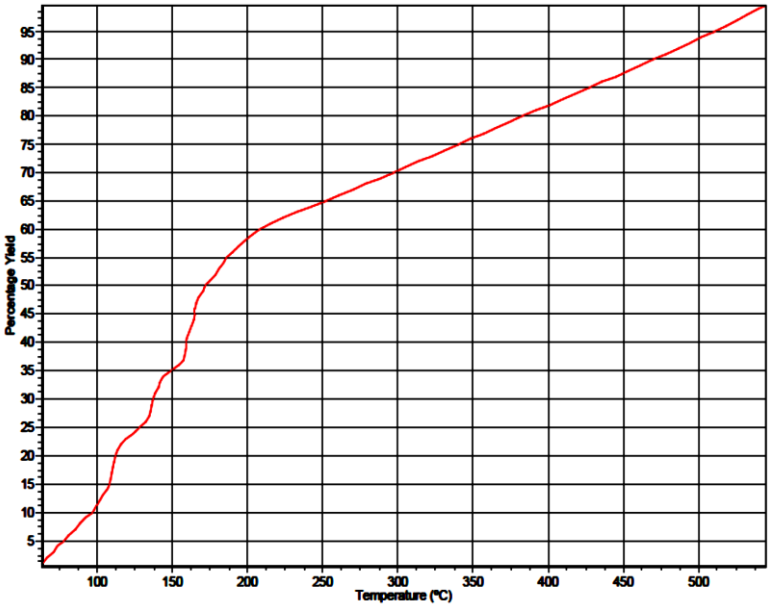

Fig. 4. 39 Distillation graph of Gasoline 95

The ultimate analysis (C, H, O, N) of three oils which is the analysis of four elements: carbon, hydrogen, oxygen and nitrogen in %wt is found that the elemental composition of rapeseed oil is 70.8%wt C, 11.11%wt H, 18.1%wt O and 0.11%wt N. It is also found that the composition of pyrolysis rapeseed oil has 84.67%wt C, 13.64%wt H, 1.4%wt O and 0.29%wt N. Oxygen content of pyrolysis rapeseed oil is lower than oxygen value of rapeseed oil. It indicates that pyrolysis of vegetable oil effectively decreases oxygen content due to decarboxylation. Decreasing of oxygen content directly affect heating value. Heating value increases when oxygen content is decreased. As shown in Table 4.39 it is found that heating value of pyrolysis rapeseed oil increase from 39.13 to 45 KJ/kg. While heating value of gasoline 95 is only 37 KJ/kg, which can be clearly seen that the pyrolysis rapeseed oil has better potential to provide heat energy.

From acid value as shown in Table 4.39 it is found that acid value of rapeseed oil, pyrolysis rapeseed oil and gasoline 95 are 25.26, 1.49 and 1.16 mg KOH/g, respectively. This indicates that using MgO catalyst can decrease acid value of pyrolysis rapeseed oil. It is consistent with Junming, X. et al.[7] which observed that using basic catalyst can decrease acid value of pyrolysis waste palm oil [34] also explain the reaction when using basic catalyst as shown in equation 4.3 that metal oxide such as MgO will react with fatty acid produced from cracking of triglyceride in

vegetable oil into $MgCO_3$. This makes fatty acid decompose further into hydrocarbon compound which results in lower acid value. Carbonate will decompose into oxide again as shown in equation 4.4. These reactions can occur in the same reactor.

$$RCOOH+MgO \rightarrow RH+MgCO_3 \qquad (4.3)$$

$$MgCO_3 \rightarrow MgO+CO_2 \qquad (4.4)$$

In the same way, the comparison of viscosity (Table 4.49) of pyrolysis rapeseed oil shows that the viscosity is decreased from 8.97 to 0.99 cSt. Although the viscosity of pyrolysis rapeseed oil is higher than viscosity of gasoline 95 (0.33 cSt) but still is in the acceptable threshold

Table 4. 39 Comparison the physical chemical between rapeseed oil, pyrolysis rapeseed oil and gasoline 95

	Rapeseed Oil	**MgO**	**Gasoline 95****
Components (wt. %)			
• Naphtha	7.00	48	59
• Kerosene	1.00	8	9
• Diesel	2.00	37	14
• Long Residue	90.00	7	17.5
Ultimate analysis (wt. %)			
• C	70.68	84.67	82.95
• H	11.11	13.64	14.24
• O	18.1	1.6	1.78
• N	0.11	0.09	1.03
Fuel Properties			
• HV (MJ/kg)	39.13	45	37
• Acidity (mgKOH/g)	25.26	1.49	1.16
• Kinematic Viscosity (cSt)	8.97	0.99	0.39

** Gasoline 95 is liquid fuels that sold in the gas station.

Fig. 4.40 shows the chromatogram of liquid product from catalytic pyrolysis of rapeseed oil over MgO in continuous reactor under the optimum condition to obtain the highest naphtha fraction and Table 4.50 shows the compositions of liquid product analyzed by using gas chromatography-mass spectrometry. It was found that the liquid product was mainly composed of alkanes and alkenes hydrocarbon. Alkanes combined with alkenes which had 5-12 C atoms were accounting for 43.85 of total peak area (excluding solvents). Such peaks were in range of naphtha because the compositions of rapeseed were mainly composed of cis-9-octadecenoic acid (C18:1 n-9), cis-13-docosenoic acid (C20:1 n-9) and cis-9,12-octadecadienoic acid (C18:2 n-6) which had 18-20 C atoms. These three fatty acids were unsaturated fatty acid which had double bonds in their molecules. It could be observed that double bond position of cis-9-octadecenoic acid was C9, of cis-13-docosenoic acid was C13 and of 12-octadecadienoic acid were C9 and C12 which were unstable positions and could be easily degraded as shown in Fig. 4.41-4.43 During decarboxylation, carbon in carboxylic group was degraded into carbon dioxide and obtained many of other different hydrocarbons as shown in Table 4.40.

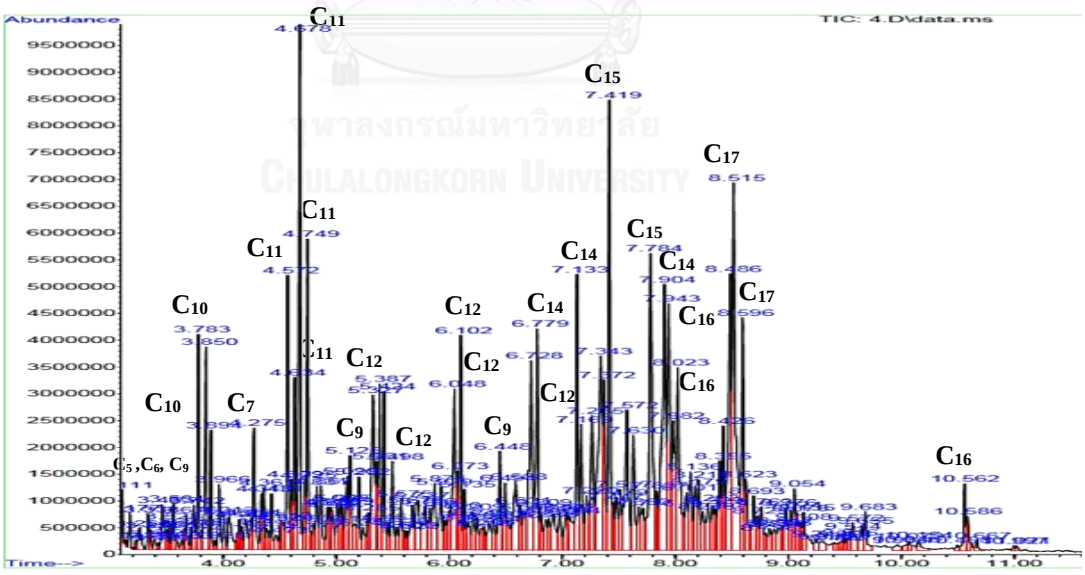

Fig. 4. 40 Chromatogram of pyrolysis rapeseed oil where reaction temperature of 450°C, feeding rate of 5 ml/min, N_2 gas flow rate of 150 ml/min and catalyst content of 50%V/V.

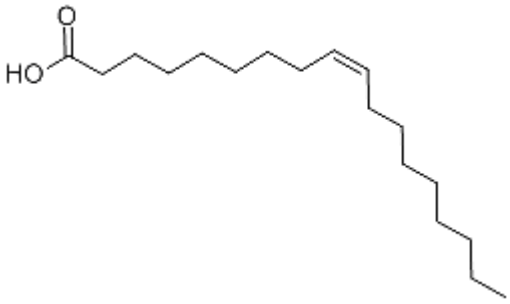

Fig. 4. 41 Cis-9-Octadecenoic acid structure [70]

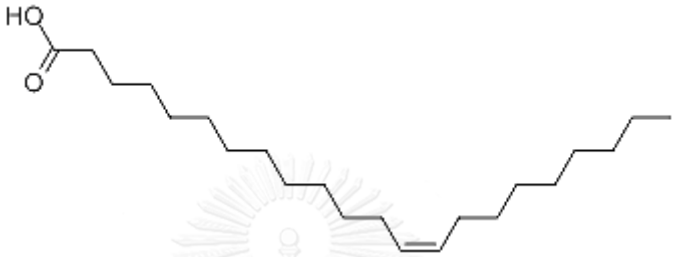

Fig. 4. 42 Cis-13-Docosenoic acid structure [71]

Fig. 4. 43 Cis-9,12-Octadecadienoic acid structure [72]

Considering Table 4.40 the important composition for explaining the mechanism of decarboxylation was observed. The composition of 8-heptadecene (at 8.515 min) was observed as shown in Fig 4.44. The structure of 8-heptadecene (Fig. 4.44) consisted of methyl group on both carbon ends and there was double bond at C8. 8–heptadecene had 17 carbon atoms close to cis-9-octadecenoic acid, the main composition of rapeseed oil. The presence of this composition could reveal and confirm the degradation of triglyceride. For the degradation of triglyceride, each ester group was degraded separately and produced free fatty acid which consisted of carboxylic acid [73]. This was followed by decarboxylation which gave product, carbon dioxide and hydrocarbon without oxygen in molecules. Decarboxylation occurred via two main reaction mechanisms which were β-elimination of triglyceride which gave carboxylic acid as product. After that carboxylic acid undergone γ-hydrogen transfer and gave

alkane or alkene hydrocarbons and carbon dioxide. In addition, γ-hydrogen transfer reaction of carboxylic acid might also produce methyl compounds but methyl compound might further cracked into alkane or alkene and carbon monoxide [32]. Therefore, from Table 4.40 methyl composition (8-heptadecene) was observed which resulted from incomplete cracking of fatty acid.

Fig. 4. 44 8-Heptadecene structure [74]

Table 4. 40 Main compounds present in the pyrolysis rapeseed oil.

Compound	Molecular formula	Reaction Time (min)	Probability (%)
1,3-Nonadiene, (E)-	C_5H_8	3.265	0.22
Cyclopentene, 1-butyl-	C_9H_{16}	3.464	0.89
Cyclohexene,1-propyl-	C_9H_{16}	3.564	0.30
Benzene, 1-ethyl-3-methyl-	C_9H_{12}	3.741	0.36
1-Decene	$C_{10}H_{20}$	3.785	1.13
Decane	$C_{10}H_{22}$	3.850	1.32
4-Decene	$C_{10}H_{20}$	3.893	0.61
2-Decene, (Z)-	$C_{10}H_{20}$	3.967	0.46
4,6-Decadiene	$C_{10}H_{18}$	4.054	0.45
Phenol, 2-methyl-	C_7H_8O	4.275	0.82
1-Undecene	$C_{11}H_{22}$	4.574	1.74
Undecane	$C_{11}H_{24}$	4.635	1.08
5-Undecene	$C_{11}H_{22}$	4.678	3.31
5-Undecene	$C_{11}H_{22}$	4.749	1.68
Cyclooctene	C_8H_{14}	4.830	0.45
2,4-Nonadiene, (E,E)-	C_9H_{16}	5.098	0.61
Benzene, pentyl-	C_9H_{16}	5.124	0.73
4-Methylphenyl acetone	$C_{10}H_{12}O$	5.202	0.51

Compound	Molecular formula	Reaction Time (min)	Probability (%)
1-Dodecene	$C_{12}H_{24}$	5.328	1.56
Dodecane	$C_{12}H_{26}$	5.385	0.99
3-Dodecene, (Z)-	$C_{12}H_{24}$	5.424	1.50
2-Dodecene, (Z)-	$C_{12}H_{24}$	5.497	0.63
Phenol, 2,3,6-trimethyl-	$C_{12}H_{26}$	5.675	0.52
Cyclopentane, decyl-	$C_{15}H_{30}$	5.727	0.63
5-Octen-1-ol, (Z)-	$C_8H_{16}O$	5.788	0.60
Benzene, hexyl-	$C_{12}H_{18}$	5.874	0.70
Benzene, (1,3-dimethylbutyl)-	$C_{12}H_{18}$	5.931	0.64
1-Tridecene	$C_{13}H_{26}$	6.048	1.45
Tridecane	$C_{13}H_{28}$	6.104	1.28
Cyclopentane, (2-methylpropyl)-	C_9H_{18}	6.447	0.76
Cyclopentene, 1-octyl-	$C_{13}H_{24}$	6.494	0.57
Bicyclo[3.3.1]nonan-3-one, 7-methylene-	$C_{10}H_{14}O$	6.590	1.03
2-Tetradecene, (E)-	$C_{14}H_{28}$	6.729	1.84
Tetradecane	$C_{14}H_{30}$	6.781	1.67
1H-Imidazole, 2-ethyl-	$C_5H_8N_2$	6.928	0.53
Cyclopentane, nonyl-	$C_{14}H_{28}$	7.133	1.75
Cyclopentene, 1-octyl-	$C_{13}H_{24}$	7.171	0.94
1-Methyl-2-methylenecyclohexane	C_8H_{14}	7.717	1.51
n-Octylidencyclohexane	$C_{14}H_{26}$	7.266	1.30
Cyclopentadecane	$C_{15}H_{30}$	7.343	2.67
1-Pentadecene	$C_{15}H_{30}$	7.370	1.25
Pentadecane	$C_{15}H_{32}$	7.418	2.94
Naphthalene, decahydro-2-methyl-	$C_{11}H_{20}$	7.479	0.56
Cyclobutane, (1-methylethylidene)-	C_7H_{12}	7.570	1.66

Compound	Molecular formula	Reaction Time (min)	Probability (%)
Dodeca-1,6-dien-12-ol, 6,10-dimethyl-	$C_{14}H_{26}O$	7.630	0.99
n-Nonylcyclohexane	$C_{15}H_{30}$	7.784	3.23
Cyclohexene, 1-octyl-	$C_{14}H_{26}$	7.903	3.38
7-Hexadecene, (Z)-	$C_{16}H_{32}$	7.942	2.08
Cetene	$C_{16}H_{32}$	7.981	1.42
Hexadecane	$C_{16}H_{34}$	8.023	1.72
Oxalic acid, cyclohexylmethyl propyl ester	$C_{12}H_{20}O_4$	8.137	0.71
6-Methyloctahydrocoumarin	$C_{10}H_{16}O_2$	8.176	0.63
12-Heptadecyn-1-ol	$C_{17}H_{32}O$	8.210	0.53
Cyclohexane, 1,1'-(1,2-dimethyl-1,2-ethanediyl)bis-, (R*,R*)-(.+/-.)-	$C_{16}H_{30}$	8.395	0.79
8-Heptadecene	$C_{17}H_{34}$	8.426	0.94
8-Heptadecene	$C_{17}H_{34}$	8.486	2.54
8-Heptadecene	$C_{17}H_{36}$	8.515	3.89
Heptadecane	$C_{17}H_{36}$	8.596	1.53
Cyclopentane, 1,2-dibutyl-	$C_{13}H_{26}$	8.623	0.70
Cyclohexane, 1-(cyclohexylmethyl)-2-ethyl-, trans-	$C_{15}H_{28}$	8.693	0.47
2-Heptadecanone	$C_{17}H_{34}O$	9.683	0.31
1,15-Hexadecadiene	$C_{16}H_{30}$	10.562	0.46
Z,E-3,13-Octadecadiene-1-ol	$C_{18}H_{34}O$	10.586	0.24

Fig. 4.45 and 4.46 show the adsorption peak of rapeseed oil and pyrolysis rapeseed oil. It was found that the main functional group found in rapeseed oil and pyrolysis rapeseed oil was C-H in aliphatic at 2850-3000 cm^{-1}. Thermal cracking using MgO catalyst showed that C=O group (carbonyl) was degraded and C=O content was significantly decreased. It was concluded that the triglyceride molecule undergoes dehydration (H_2O), decarboxylation (CO_2), decarbonylation (CO), recombination and rearrangement reactions [75] to generate different hydrocarbons.

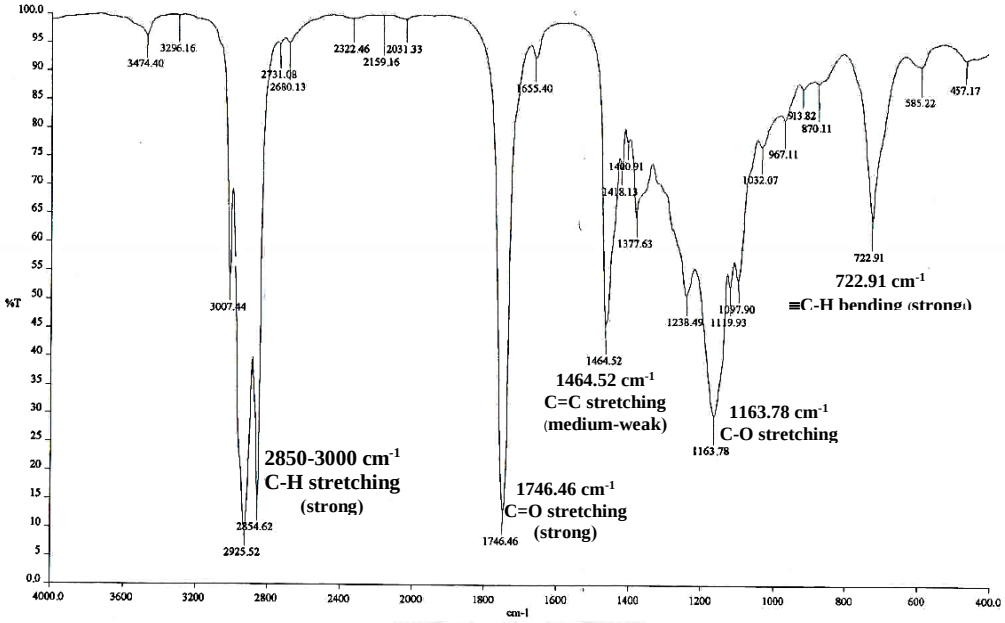

Fig. 4. 45 FTIR absorption peaks of rapeseed oil.

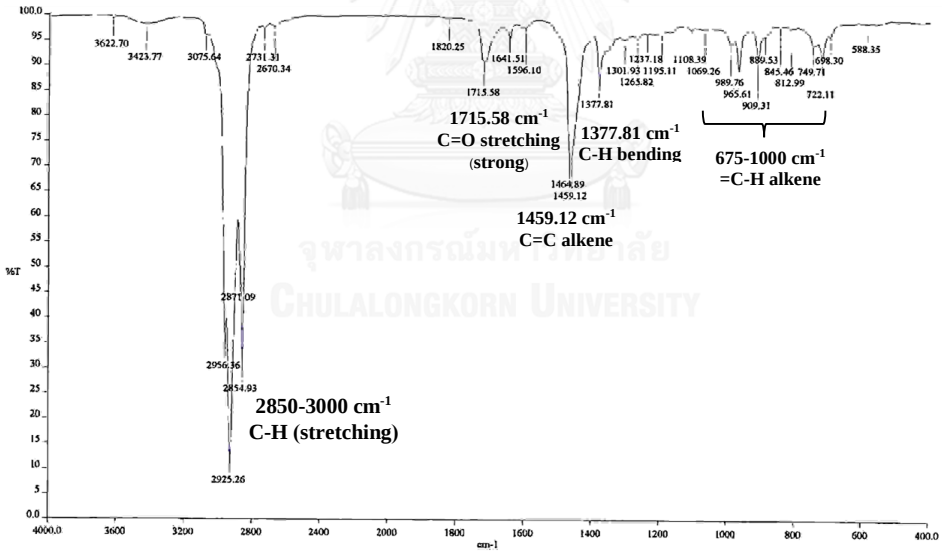

Fig. 4. 46 FTIR absorption peaks of pyrolysis rapeseed oil where reaction temperature of 450°C, feeding rate of 5 ml/min, N_2 gas flow rate of 150 ml/min and catalyst content of 50%V/V.

CHAPTER V

CONCLUSIONS AND SUGGESTIONS

Conclusions of the pyrolysis of rapeseed oil into liquid product in continuous reactor were divided into two parts. The first part was for the pyrolysis of rapeseed oil into liquid product in batch reactor by using five catalysts including such as CaO, MgO, HZSM-5, 1%wt Fe/AC and 5%wt Fe/AC in order to investigate the variables affecting to liquid product and naphtha yield and determine the kinetics of cracking of long residues. The second part was for the pyrolysis of rapeseed oil into liquid product in continuous bench reactor in order to investigate the variables affecting to liquid product and naphtha yield and determine the optimum condition of production.

5.1 Conclusions in the first part

The variables affecting on percentage of liquid product and naphtha yield of catalytic pyrolysis of rapeseed oil over five catalysts are following.

MgO :

The main variables effecting the liquid yield are temperature (A), reaction time (D), initial hydrogen pressure (C), initial hydrogen pressure- reaction time interaction (CD) and reaction temperature-catalyst content of CaO interaction (AB).

The major variables effecting the naphtha yield are temperature (A), time of reaction (D), temperature-time of reaction interaction (AD), catalyst content of CaO time of reaction interaction (BD), temperature- catalyst content of CaO interaction (AB), temperature- catalyst content of CaO-time of reaction interaction (ABD), hydrogen pressure-time of reaction interaction (CD) and temperature-hydrogen pressure-time of reaction interaction (ACD).

CaO :

The main variables effecting the liquid yield are reaction temperature (A), reaction time (D) and catalyst content of MgO (B).

The major variables effecting the naphtha yield are reaction temperature (A), reaction reaction (D), reaction temperature- reaction time interaction (AD), initial hydrogen pressure (C) and catalyst content of MgO (B).

HZSM-5:

The main variables effecting the liquid yield are reaction temperature (A), reaction time (D), temperature-time of reaction interaction (AD), catalyst content of HZSM-5 (B), catalyst content of HZSM-5- time of reaction interaction (BD), initial hydrogen pressure-time of reaction interaction (CD), initial hydrogen pressure (C) and temperature- initial hydrogen pressure interaction (AC).

The major variables effecting the naphtha yield are temperature (A), reaction time (D), reaction temperature- reaction time interaction (AD), catalyst content of HZSM-5 (B) and reaction temperature- catalyst content of HZSM-5 (AB).

1%wt Fe/AC :

The main variables effecting the liquid yield are reaction temperature (A), reaction time (D), reaction temperature- catalyst content of 1wt%Fe/AC- reaction tme interaction (ABD), catalyst content of 1wt%Fe/AC (B) and initial hydrogen pressure (C).

The major variables effecting the naphtha yield are reaction temperature (A), reaction time(D), reaction temperature-reaction time interaction (AD), catalyst content of 1% wt Fe/AC (B) and reaction temperature- initial hydrogen pressure interaction (AC).

5%wt Fe/AC :

The main variables effecting the liquid yield are reaction temperature (A), reaction time (D), reaction temperature-initial hydrogen pressure interaction (AC), catalyst content of 5%wt Fe/AC (B), reaction temperature- catalyst content of 5wt%Fe/AC- reaction time interaction (ABD), reaction temperature-initial hydrogen pressure- reaction time interaction (ACD) and reaction temperature- reaction temperature interaction (AD).

The major variables effecting the naphtha yield are reaction temperature (A), reaction time (D) and initial hydrogen pressure-time of reaction interaction (CD).

Table 5. 1 The variables affecting on percentage of liquid product and naphtha yield of catalytic pyrolysis of rapeseed oil over all five catalysts

Rapeseed Oil										
Variables	**CaO**		**MgO**		**HZSM-5**		**1%wt Fe/AC**		**5%wt Fe/AC**	
	Liq.	**Naph.**	**Liq.**	**Naph.**	**Liq.**	**Naph.**	**Liq.**	**Naph.**	**Liq.**	**Naph.**
Reaction temperature (A)	√	√	√	√	√	√	√	√	√	√
Catalyst content (B)	√	√			√	√	√	√	√	
Initial hydrogen pressure (C)		√	√		√		√			
Reaction time (D)	√	√	√	√	√	√	√	√	√	√

The results of each variable affecting percentage of liquid product and naphtha were concluded in Table 5.1. It was observed that the effects of reaction temperature and reaction time were highly significant. Increasing reaction temperature made large hydrocarbon cracked into medium and small hydrocarbon molecules. Further heating made small hydrocarbons and free radicals continuously cracked until they became hydrogen gases. This resulted in lower percentage of liquid product while percentage of naphtha yield was higher with longer reaction time. Large hydrocarbon molecules are converted into small one and the cracking process continues which is affected by catalyst cracking under hydrogen atmosphere. This results in the arrangement of small hydrocarbon molecules such as naphtha and higher percentage of naphtha yield.

Table 5. 2 The optimum conditions of catalytic pyrolysis of rapeseed oil all five catalysts between Design-Expert program and the actual experiment.

Catalyst										
Variables	**CaO**		**MgO**		**HZSM-5**		**1%wt Fe/AC**		**5%wt Fe/AC**	
	Pro.	Exp.	Pro.	Exp.	Pro.	Exp.	Pro.	Exp.	Pro.	Exp.
Temperature (°C)	390	390	390	390	390	390	407.10	400	413.03	410
Catalyst (%wt)	0.98	1.00	0.50	0.50	0.51	0.50	1.0	1.00	0.50	0.50
Pressure (bar)	3.25	3	2.43	3	4.99	5	1	1	1	1
Time (Minute)	60	60	60	60	60	60	60	60	60	60
Yield of liquid	81.42	79.67	84.69	85.33	73.91	73.56	77.14	77.64	74.60	75.03
Yield of naphtha	25.94	27.26	30.93	32.04	26.13	27.61	20.91	20.37	20.75	20.25

From Table 5.2, it was found that each catalyst also reflected the remarks or important characteristics. Catalysts could be divided into 3 groups including base catalyst (CaO & MgO), acid catalyst (HZSM-5) and Fe/AC. All these catalyst had different reaction mechanisms which resulted in different product. For CaO & MgO, when radicals contacted with catalyst surface, H_2 transfer occurred on catalyst surface. Base catalysts also had overlapped surface which resulted in high surface area. H_2 transfer on surface increased steadily. The products were converted from long residue→diesel→kerosene→small hydrocarbon (naphtha). This could be concluded that base catalysts tended to have higher selectivity toward naphtha than diesel. While for HZSM-5, when radicals contacted with catalyst surface, H_2 transfer occurred within HZSM-5 pore. Only a small hydrocarbon molecule through micropore of

catalyst. Most products were small hydrocarbon such as naphtha and products were cracked further into gaseous hydrocarbon. From the Table 4.23, it could be observed that HZSM-5 gave high gas content. Fe/AC catalyst, activated carbon had large surface area. When radicals contacted with catalyst, H_2 transfer occurred on catalyst surface because Fe atom on activated carbon enhanced cracking of large hydrocarbon from long residue into medium and small hydrocarbon. From the Table 4.23, the higher %Fe, the better cracking of large hydrocarbon molecules into medium, small hydrocarbon molecules until small hydrocarbon molecules converted into gas hydrocarbon. It could be observed that at 5% wt Fe/AC the selectivity in diesel ranges was significantly lower compared to 1%wt Fe/AC. It can be observed that gas content is high, while %yield of naphtha was not significantly different.

Table 5. 3 The reaction order, activation energy and pre-exponential factor from kinetic study of three types of catalyst.

Catalyst	**Reaction Order**	**Activation Energy : (Ea) kJ/mol**	**Pre-exponential (s^{-1})**
MgO	2	71.134	18.21
HZSM-5	2	29.497	2.33×10^{-2}
1%wt Fe/AC	2	44.616	2.65×10^{-1}

The kinetics of catalytic pyrolysis of rapeseed oil over MgO HZSM-5, and 1%wt Fe/AC were determined. It was found that the second order of long residue was observed for all catalysts. The activated energy and pre-exponential were shown in Table 5.3. The activation energy of HZSM-5 is lowest showing that HZSM-5 promote the cracking reaction very well.

5.2 Conclusions in the second part

The variables affecting on percentage of liquid product and naphtha yield of catalytic pyrolysis of rapeseed oil over MgO operation in continuous reactor.

The variables affecting on percentage of liquid product were temperature (A), interaction between N_2 gas flow rate and feeding rate (CD), interaction between reaction time and feeding rate (AD) and catalyst content (B). Considering the above variables it was found that each variable was related. Increasing reaction temperature increased the energy of reactants. Better cracking into smaller hydrocarbon compound was related with catalyst content in system. The higher catalyst content was related the faster reaction acheived. Increasing feeding rate and N_2 gas flow rate in system pushed reaction forward and resulted in higher percentage of liquid product.

The variables affecting on percentage of naphtha yield were catalyst content (B), N_2 gas flow rate (C), feeding rate (D) and interaction between three factors (BCD, BC and BD) were different, because the effect of reaction temperature was not significant. Increasing reaction temperature promotes cracking into more medium and small hydrocarbon molecules and even hydrocarbon gases. The retention times of products should not too long which means higher N_2 gas flow rate must was needed to obtain higher percentage of naphtha yield.

Table 5. 4 The optimum condition of catalytic pyrolysis of rapeseed oil over MgO using Design Expert Program and experiment is followed.

Variables	**Rapeseed Oil**	
	Design Expert Program	**Experimental**
Reaction temperature	450°C	450°C
FeedING rate	5.21 ml/min	5 ml/min
N_2 gas flow rate	150 ml/min	150 ml/min
Catalyst content	52.99%V/V	50%V/V
Percentage of liquid product :	73.65%wt	75.44%wt
Percentage of naphtha yield :	36.58%	36.62%

The physico-properties between pyrolyzed rapeseed oil is close to gasoline 95 as shown in Table 5.5. The fuel properties of liquid product had heating value of 44.95 MJ/kg, acid value of 1.49 mg KOH/g and viscosity of 0.99 cSt. While gasoline had heating value of 37 MJ/kg, acid value of 1.19 mg KOH/g and viscosity of 0.39 cSt. The ultimate analysis showed that pyrolyzed rapeseed oil and gasoline 95 had similar carbon content of 85.69 and 82.95% by weight, respectively. In addition the composition of rapeseed oil showed that the prominent peaks were of aliphatic hydrocarbon (C-H stretching) at 2850-3000 cm^{-1} similar to gasoline 95.

Table 5. 5 Comparison the physical chemical between, pyrolysis rapeseed oil and gasoline 95.

	Pyrolysis rapeseed oil	**Gasoline 95**
Components (wt. %)		
• Naphtha	48	59
• Kerosene	8	9
• Diesel	37	14
• Long Residue	7	17.5
Ultimate analysis (wt. %)		
• C	84.67	82.95
• H	13.64	14.24
• O	1.6	1.78
• N	0.09	1.03
Fuel Properties		
• HV (MJ/kg)	45	37
• Acidity (mgKOH/g)	1.49	1.16
• Kinematic Viscosity (cSt)	0.99	0.39

5.3 Suggestions

1. The experiment was divided into two parts. For the first part the batch reactions were studied to determine the optimum condition for five catalysts at reaction time of 390 and 450 °C, catalyst content of 0.5 and 1.0%wt, initial hydrogen pressure of 1 and 5 bar, reaction time of 30 and 60 minutes that affected percentage of liquid product and naphtha yield. The optimum conditions from above experiments might not the actual optimum condition because the ranges of some variables were not significantly different. Catalyst content and initial hydrogen pressure should be change to the obvious ranges in order to reflect the actual variables on percentage of liquid product and naphtha yield. This was in order to use the optimum conditions from the experiment in continuous system as the guideline for commercial liquid fuel production in future.

2. Study other basic catalysts which may give better percentage of liquid product and naphtha and also lower acid value of liquid product.

3. Improve the quality of liquid product to practically use in various engines in order to reduce the use of petroleum-based fuel and to encourage using biomass fuel which is more suitable.

4. Study the feasibility of commercial production of naphtha from rapeseed oil.

REFERENCES

1. Charusiri, W., *Fast Pyrolysis of Residues from Paper Mill Industry to Bio-oil and Value Chemicals: Optimization Studies* Energy Procedia 2015. **74**: p. 933-941.
2. Zhou, L., et al., *Catalytic pyrolysis of rice husk by mixing with zinc oxide: Characterization of bio-oil and its rheological behavior.* Fuel Processing Technology, 2013. **106**: p. 385-391.
3. Thangalazhy-Gopakumara, S., et al., *Production of hydrocarbon fuels from biomass using catalytic pyrolysis under helium and hydrogen environments.* Bioresource Technology, 2011. **102**(12): p. 6742-6749.
4. Knutson, A., *What's the Difference Between Canola and Rapeseed?*
5. Wikipedia, *Rapeseed*. 2016.
6. Junming X., et al., *Biofuel production from catalytic cracking of woody oil.* Bioresource Technology, 2010. **101**: p. 5586-5591.
7. Junming, X., et al., *Production of hydrocarbon fuels from pyrolysis of soybean oils using a basic catalyst.* Bioresource Technology, 2010. **101**(24): p. 9803-9806.
8. Junming, X., et al., *Liquid hydrocarbon fuels obtained by the pyrolysis of soybean oils.* Bioresource Technology, 2009. **100**(20): p. 4867-4870.
9. Wang, D., et al., *Comparison of catalytic pyrolysis of biomass with MCM-41 and CaO catalysts by using TGA–FTIR analysis.* Journal of Analytical and Applied Pyrolysis, 2010. **89**: p. 171-177.
10. Sedighi, M., K. Keyvanloo, and J. Towfighi, *Kinetic study of steam catalytic cracking of naphtha on a Fe/ZSM-5 catalyst.* Fuel, 2013. **109**: p. 432-438.
11. Bielansky, P., A. Reichhold, and C. Schonberger, *Catalytic cracking of rapeseed oil to high octane gasoline and olefins.* Chemical Engineering and Processing, 2010. **49**: p. 873-880.
12. Foster, A.J., et al., *Optimizing the aromatics yield and distribution from catalytic fast pyrolysis of biomass over ZSM-5.* Applied Catalysis A: General, 2012. **423-424**: p. 154-161.
13. Gollakota, A.R.K., et al., *A review on the upgradation techniques of pyrolysis oil.* Renewable and Sustainable Energy Reviews, 2016. **58**: p. 1543-1568.
14. Liu, C., et al., *Catalytic fast pyrolysis of lignocellulosic biomass* Chemical Society Reviews, 2014. **43**: p. 7594-7623.
15. Stefanidis, S., et al., *Mesopore-modified mordenites as catalysts for catalytic pyrolysis of biomass and cracking of vacuum gasoil processes.* Green Chemistry, 2013. **15**: p. 1647-1658.
16. Shi, J.W., *Preparation of Fe(III) and Ho(III) co-doped TiO2 films loaded on activated carbon fibers and their photocatalytic activities.* Chemical Engineering Journal, 2009. **151**: p. 241-246.
17. Choochuay, P., *Cracking of polybutene-1 to liquid fuels on Fe/Activated carbon catalyst*, in *Department of chemical technology*. 2001, Chulalongkorn University: Faculty of Science.
18. Insuk, S., *Catalytic cracking of acrylonitrile-butadiene-styrene and used-lubricating oil with Fe/activated carbon*, in *Department of chemical technology*. 2004, Chulalongkorn University: Faculty of Science.

19. Sumarin, J., *Hydrocracking of used lubricating oil on iron/activated carbon catalyst using a tubular reactor*, in *Department of chemical technology*. 2006, Chulalongkorn University: Faculty of Science.
20. Charusiri, W., *Thermal cracking of used plastics, used vegetable oil and used lubricating oil to gasoline and liquid fuels in a continuous reactor*, in *Research reports*. 2008, Chulalongkorn University: Energy Research Institute.
21. Jansopapitr, K., *Catalytic cracking of beef tallow on Fe/activated carbon*, in *Department of chemical technology*. 2009, Chulalongkorn University: Faculty of Science.
22. Panprasong, T., *Guidelines for management of frying oil deterioration*. 2016.
23. Tamunaidu, P. and S. Bhatia, *Catalytic cracking of palm oil for the production of biofuels: Optimization studies.* Bioresource Technology, 2007. **98**(18): p. 3593-3601.
24. Wikimedia, *Brassica napus*. 2016.
25. Wikipedia, *Vegetable oils* 2016.
26. oxford-instruments, *Triglycerides*. 2016.
27. Shahidi, F., *Fatty acids found in most vegetable oils*. 2005.
28. Naik, S.N., et al., *Production of first and second generation biofuels: A comprehensive review.* Renewable and Sustainable Energy Reviews 2010, 2010. **14**(578-597).
29. Morrison, R.T. and R.N. Boyd, *Organic Chemistry*, ed. t. ed. 1992, Englewood Cliffs,Prentice Hall, New Jersey.
30. Solomons, T.W.G., *Organic Chemistry*, ed. t. ed. 1992, John Wiley & Sons, New York.
31. Raber, D.J. and N.K. Raber, *Organic Chemistry*, ed. W.P. Company. 1988, St. Paul, Minnesota.
32. Maher, K.D. and D.C. Bressler, *Pyrolysis of triglyceride materials for the production of Renewable fuels and chemicals.* Bioresource Technology, 2007. **98**: p. 2351–2368.
33. Tani, H., et al., *Development of direct process of diesel fuel from vegetable oils.* The Japan institute of energy 90, 2011: p. 466-470.
34. Tani, H., et al., *Selective catalytic decarboxy-cracking of triglyceride to middle-distillate hydrocarbon.* CatalysisToday 2011. **164**: p. 410-414.
35. K.D. Maher and D.C. Bressler, *Pyrolysis of triglyceride materials for the production of Renewable fuels and chemicals.* Bioresource Technology 98, 2007: p. 2351-2368.
36. Chaiwet, P. and N. Kritdanurak, *Technology of Petroeum*. 1994, Bangkok: Chulalongkorn University.
37. Basu, P., *Biomass gasification and pyrolysis: practical design and theory*. 2010, Elsevier, USA.
38. Panpranot, J., *Basic knowledge of heterogeneous*. 2009, Department pf chemical engineering: Chulalongkorn University.
39. Chatuporn Wittayakun and Nurak Kritsadanurak, *Infrastructure and application of catalyst* 2004, Bangkok.
40. Refaat, A.A., *Biodiesel production using solid matal oxide catalysts.* Int. J. Environ. Sci. Tech, 2011. **8**(1): p. 203-221.

41. Chorkendorff, I. and J.W. Niemantsverdriet, *Concepts of Modern Catalysis and Kinetics*. 2003, The Federal Republic of Germany: WILEY-VCH Verlag GmbH & Co. KGaA, Weinheim.
42. Catalyst, H., *http://share.psu.ac.th/blog/eng-biodiesel/21511*. 2011.
43. Lee, D.-W., Y.-M. Park, and K.-Y. Lee, *Heterogeneous Base Catalysts for Transesterification in Biodiesel Synthesis.* Catalysis Surveys from Asia, 2009. **13**(2): p. 63-77.
44. WebElement, *Calcium Oxide*. 2016.
45. Zabeti, M., et al., *Activity of solid catalysts for biodiesel production: A review.* Fuel Processing Technology, 2009. **90**(6): p. 770-777.
46. Verziu, M., et al., *Sunflower and rapeseed oil transesterification to biodiesel over different nanocrystalline MgO catalysts.* Green Chemistry, 2008. **10**(4): p. 373-381.
47. Bruce C. Gates, *Catalytic Chemistry*. University of Delaware,John Wiley & Sons.
48. Zeolite, *http://scitechdaily.com/zeolite-catalyst-creates-p-xylene-from-biomass/* 2013.
49. patents/EP0711601A2, *Bronsted to Lewis acid*. 2016.
50. Szostak, R., *Molecular Sieve Principle of Synthesis and Identification*. 1989, New York. Norstand Reinhold.
51. W., P., *Fuel & Petroleum*. 1991, Department of Chemistry, Chiangmai University.
52. Srisuwong, T., *Catalytc cracking of Tung oil to liquid fuel on heterogeneous base catalyst*, in *Department of chemical technology*. 2011, Chulalongkorn University: Bangkok.
53. Pütün, E., *Catalytic pyrolysis of biomass : Effects of pyrolysis temperature, sweeping gas flow rate and MgO catalyst.* Energy. **35**: p. 2761-2766.
54. Idem, et al., *Thermal cracking of canola oil: Reaction products in the presence and absence of steam.* Energy Fuels, 1996. **10**(6): p. 1150-1162.
55. Jungjaroenpanit, C., *Catalytic pyrolysis of used cooking oil by MgO and Acitvated carbon in continuous reactor*, in *Department of chemical technology*. 2012, Chulalongkorn University: Bangkok.
56. Buzetzki, E., et al., *The influence of zeolite catalysts on the products of rapeseed oil cracking.* . Fuel Processing Technology, 2011. **92**: p. 1623-1631.
57. Thanh-An Ngo, et al., *Pyrolysis of Soybean oil with HZSM-5 and MCM41 catalysts fixed bed reactor.* Energy, 2010. **35**.
58. Lima, D., et al., *Diesel-like fuel obtained by pyrolysis of vegetable oils* Anal. Appl. Pyrolysis 2004. **71**(987-996).
59. Sawasraksa, S., *Catalytic cracking of Jatropha oil to liquid fuels on HZSM-5*, in *Department of chemical technology*. 2009, Chulalongkorn University: Faculty of Science.
60. Chookiert, D.e.a., *Catalytic cracking of used vegetable oils to liquid fuels using HZSM-5* in *Department of chemistry*. 2010, Latkrabong Technology University: Bangkok.
61. Mongkol, M., *Catalytic cracking of used vegetable oil to liquid fuel using Fe/active carbon and HZSM-5*, in *Department of chemical technology*. 2003, Chualongkorn University: Bangkok.

62. Sekine, Y., et al., *Reaction control in Radical -Transforming Catalytic Degradation of Polypropylene using Fe supported Activated carbon catalyst under high hydrogen pressure*, in *Department of applied chemistry*. Unversity of Tokyo: Japan.
63. Taepakdee, P., *Catalytic cracking of polypropylene, polystyrene and used-lubricating oil with Fe/activated carbon* in *Department of chemical technology*. 2004, Chulalongkorn University: Bangkok.
64. Palavat, S., *Effects of base catalysts on pyrolysis of soybean oil*, in *Department of chemical technology*. 2012, Chulalongkorn Unuversity: Bangkok.
65. Natakaranakul, J., *Continouos pyrolysis of crude palm oik to liquid fuels on dolomite catalyst*, in *Department of Chemical Technology, Faculty of Science*. 2013, Chulalongkorn University.
66. Kaewchingduang, P., *Catalytic cracking of rapeseed oil on magnesium oxide and FCC catalysts*, in *Department of chemical technology*. 2012, Chulalongkorn University: Bangkok.
67. Adjaye, J.D., *Catalytic conversion of a biofuel to hydrocarbon of mixtures of HZSM-5 and silica-alumina catalysts on product distribution.* Fuel Processing Technology, 1996. **48**: p. 115-143.
68. Twaiq, F.A., *Liquid hydrocarbon fuels from palm oil by catalytic cracking over aluminosilicate mesoporous catalysts with various Si/Al ratios.* Microporous and Mesoporous materials, 2003. **64**: p. 95-107.
69. Montgomery, D.C., *Design and Analysis of Experiment*, ed. edition. 2009: John Wiley & Sons, Inc.
70. chemicalbook.com, *Cis-9-Octadecenoic acid structure*. 2016.
71. chemicalbook.com/CAS/GIF/112-86-7.gif, *Cis-13-Docosenoic acid structure*. 2016.
72. webbook.nist.gov, *Cis-9,12-Octadecadienoic acid structure* 2016.
73. Benson, T.J., *Elucidation of the catalytic cracking pathway for unsaturated mono-, di-, and triacylglycerides on solid acid catalysts.* Journal of Molecular Catalysis A: Chemical, 2009. **303**(1-2): p. 117-123.
74. webbook.nist.gov, *8-Heptadecene structure*. 2016.
75. Biswas, S. and D.K. Sharma, *Studies on cracking of Jatropha oil.* Journal of Analytical and Applied Pyrolysis, 2013. **99**: p. 122-129.

APPENDIX

APPENDIX A

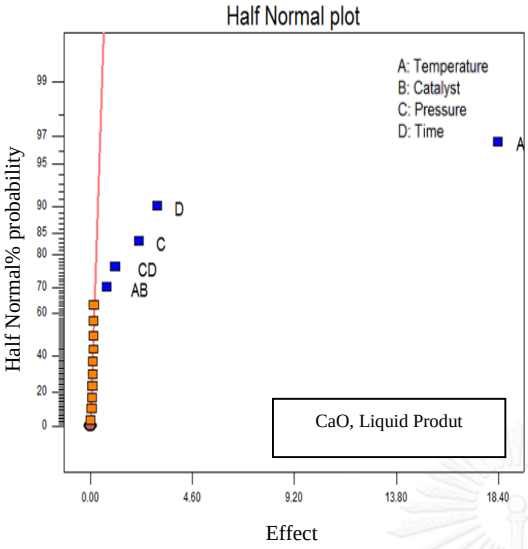

Fig. A-1 Normal probability plot of liquid product of CaO

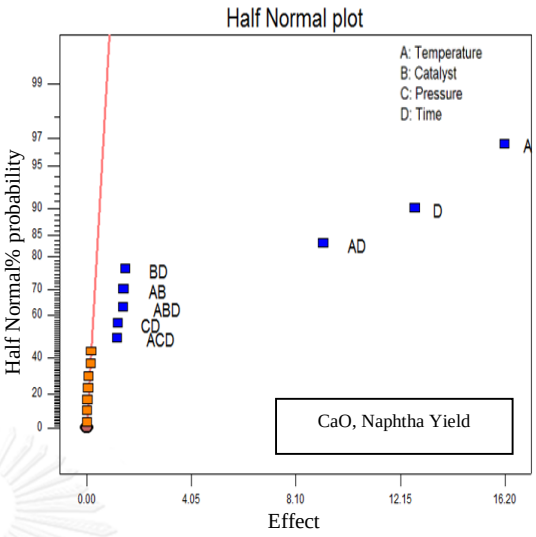

Fig. A-2 Normal probability plot of naphtha yield of CaO

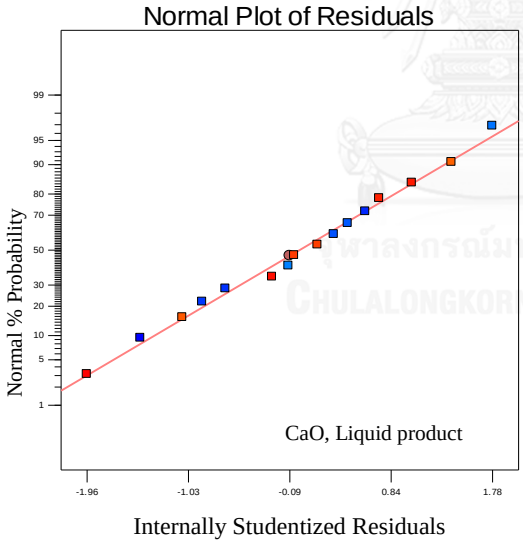

Fig. A-3 The relationship between Normal % Probability and the residual of percentage of liquid product of CaO

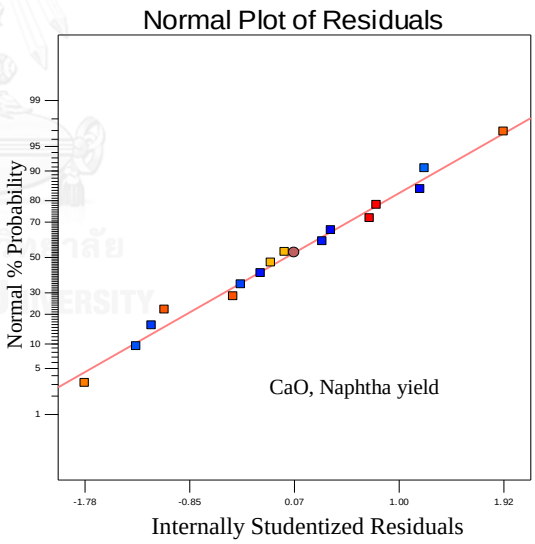

Fig. A-4 The relationship between Normal % Probability and the residual of percentage of naphtha yield of CaO

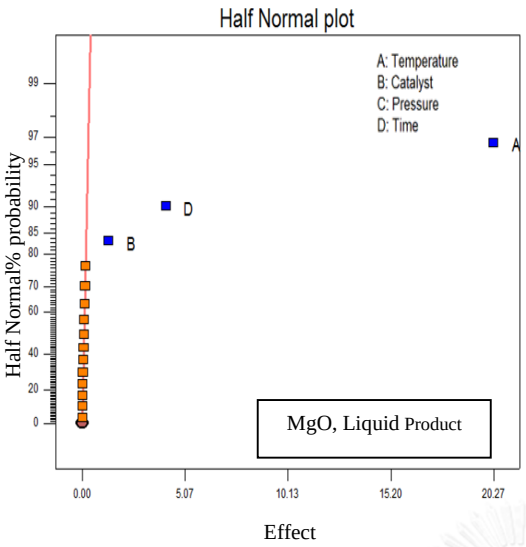

Fig. A-5 Normal probability plot of liquid product of MgO

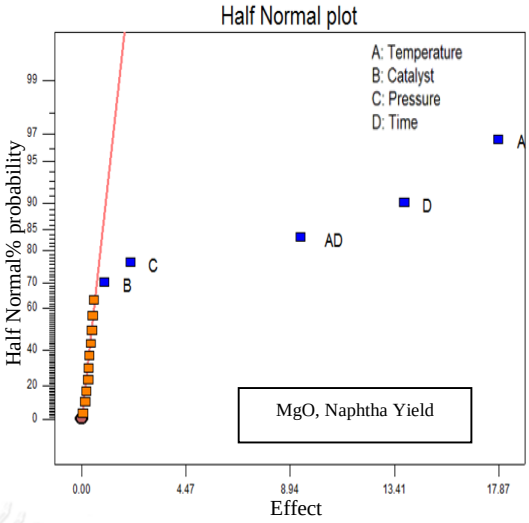

Fig. A-6 Normal probability plot of naphtha yield of MgO

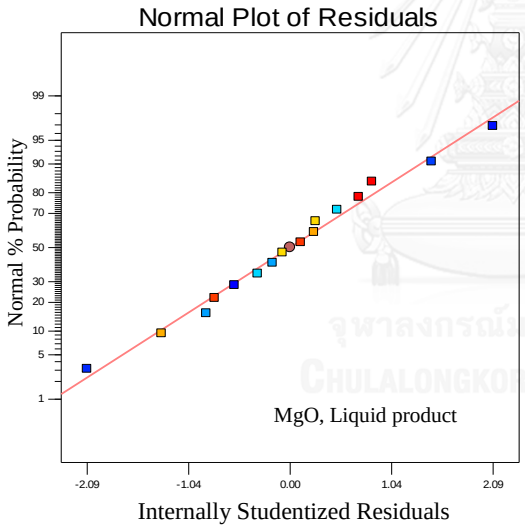

Fig. A-7 The relationship between Normal % Probability and the residual of percentage of liquid product of MgO

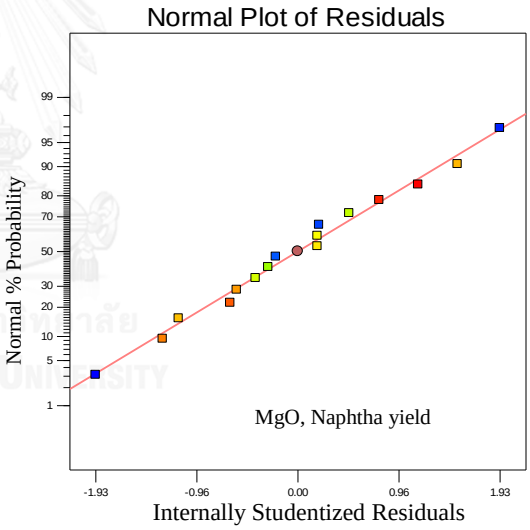

Fig. A-8 The relationship between Normal % Probability and the residual of percentage of naphtha yield of MgO

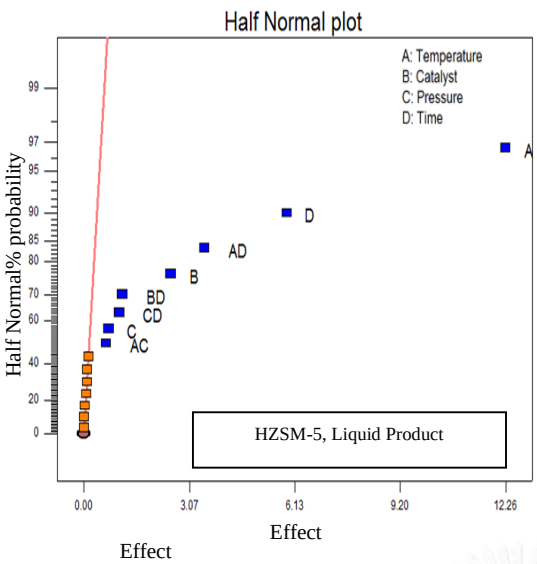

Fig. A-9 Normal probability plot of liquid product of HZSM-5

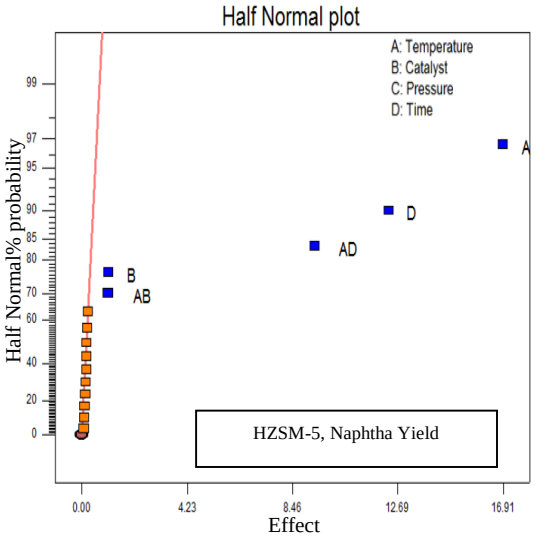

Fig. A-10 Normal probability plot of naphtha yield of HZSM-5

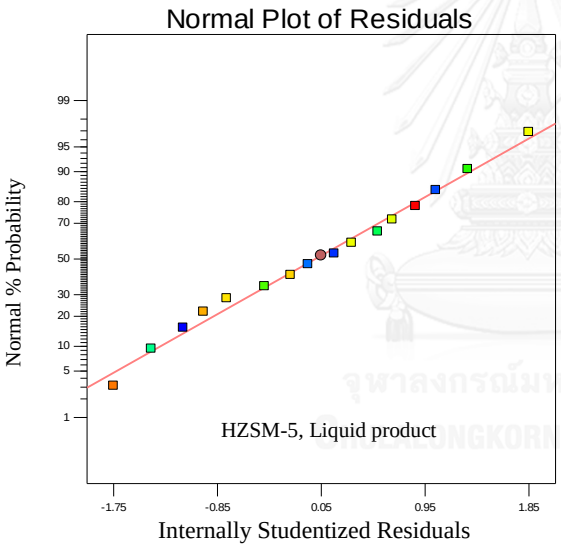

Fig. A-11 The relationship between Normal % Probability and the residual of percentage of liquid product of HZSM-5

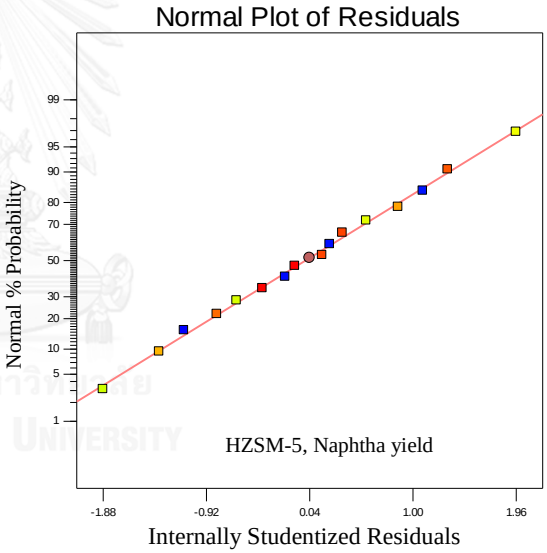

Fig. A-12 The relationship between Normal % Probability and the residual of percentage of naphtha yield of HZSM-5

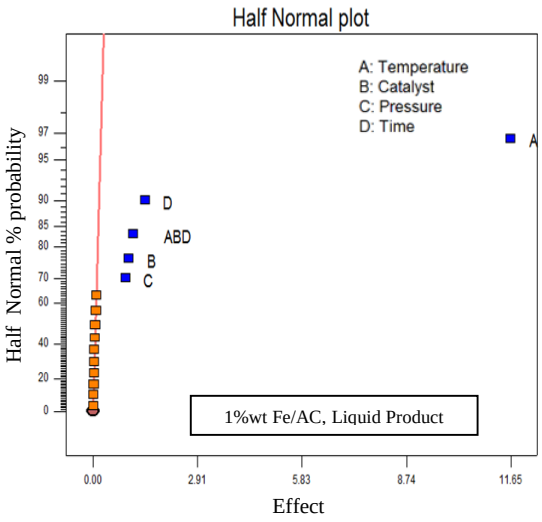

Fig. A-13 Normal probability plot of liquid product of 1%wt Fe/AC

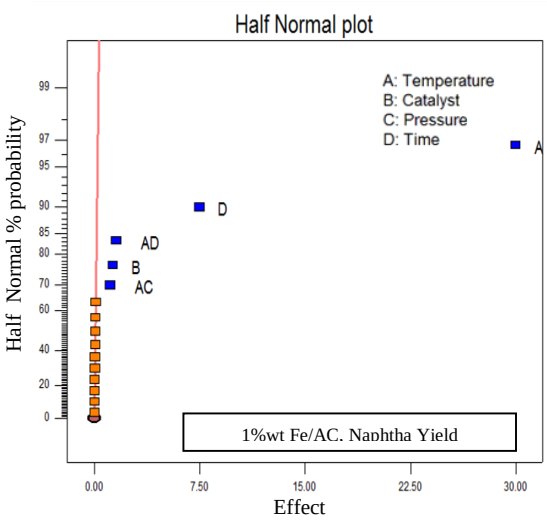

Fig. A-14 Normal probability plot of naphtha yield of 1%wt Fe/AC

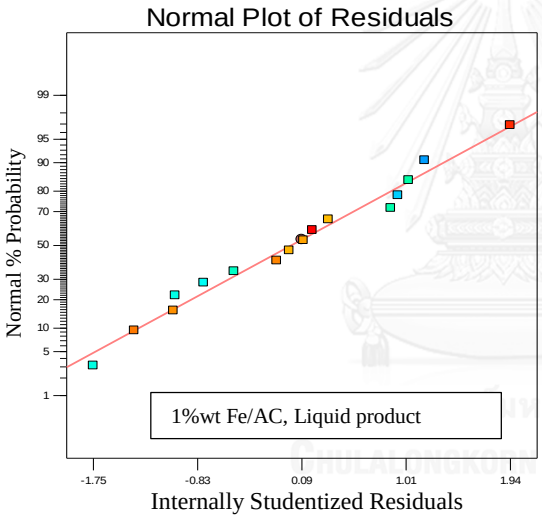

Fig. A-15 The relationship between Normal % Probability and the residual of percentage of liquid product of 1%wt Fe/AC

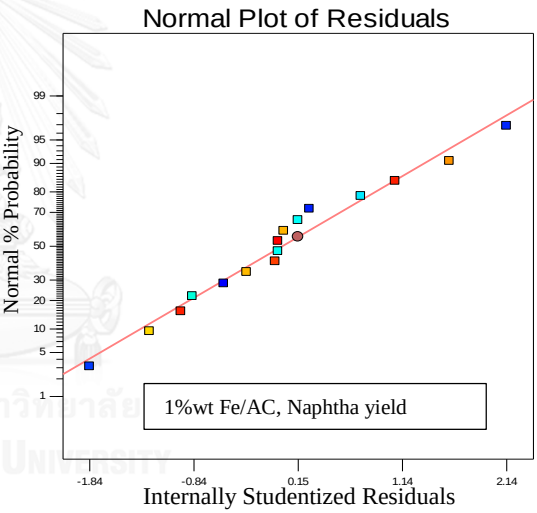

Fig. A-16 The relationship between Normal % Probability and the residual of percentage of naphtha yield of 1%wt Fe/AC

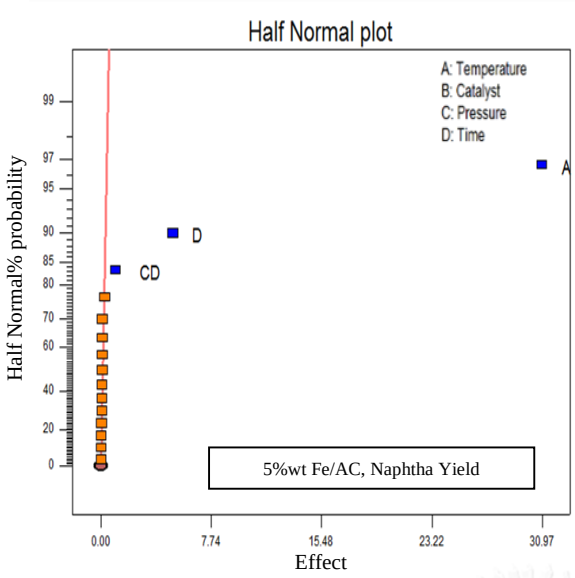

Fig. A-17 Normal probability plot of liquid product of 5%wt Fe/AC

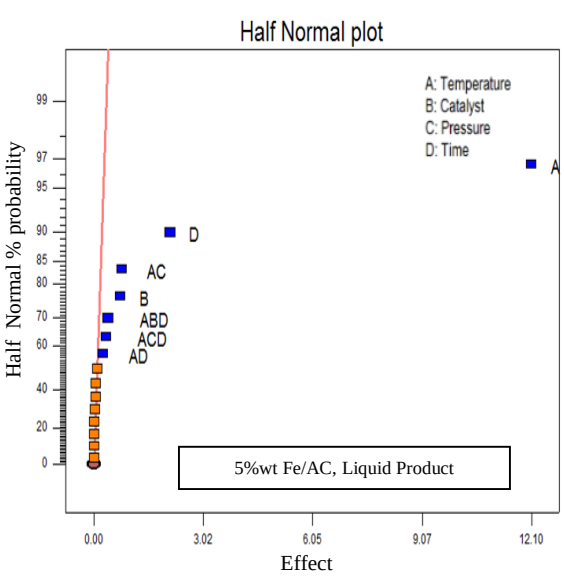

Fig. A-18 Normal probability plot of naphtha yield of 5%wt Fe/AC

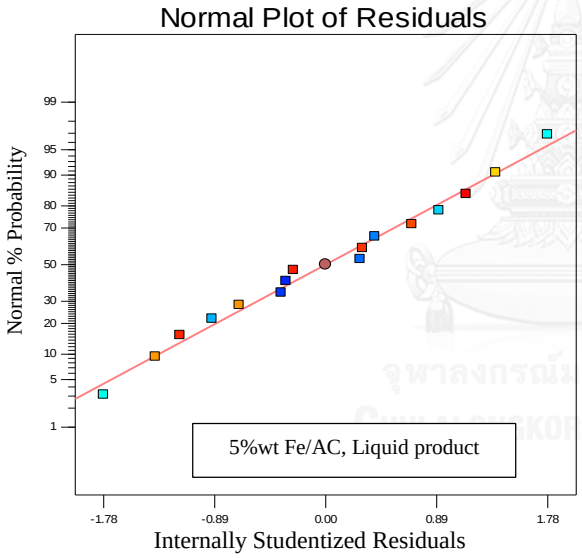

Fig. A-19 The relationship between Normal % Probability and the residual of percentage of liquid product of 5%wt Fe/AC

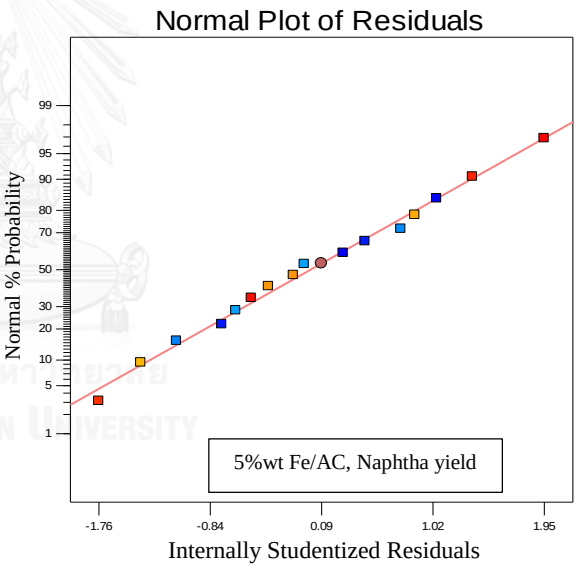

Fig. A-20 The relationship between Normal % Probability and the residual of percentage of naphtha yield of 5%wt Fe/AC

APPENDIX B

Table B-1 Analysis of Variance for 2^k experimental design in catalytic pyrolysis of rapeseed oil over CaO.

Source	Sum of Squares	Degree of Freedom	Mean Squares	F Value	Prob> F Value	
Model	1417.99	5	283.60	5532.40	<0.0001	significant
A	1354.79	1	1354.79	26429.17	<0.0001	
D	36.57	1	36.57	713.45	<0.0001	
C	19.43	1	19.43	378.96	<0.0001	
CD	5.03	1	5.03	98.10	<0.0001	
AB	2.17	1	2.17	42.30	<0.0001	
Curvature	4.47	1	4.47	87.11	<0.0001	significant
Residual	0.51	10	0.051			
Total	1422.97	19				

Table B-2 Analysis of Variance for 2^k experimental design in catalytic pyrolysis of rapeseed oil over CaO.

Source	Sum of Squares	Degree of Freedom	Mean Squares	F Value	Prob> F Value	
Model	2069.69	8	258.71	7401.01	<0.0001	significant
A	1050.25	1	1050.25	30044.59	<0.0001	
D	647.32	1	647.32	18518.03	<0.0001	
AD	335.90	1	335.90	9609.08	<0.0001	
BD	9.02	1	9.02	257.89	<0.0001	
AB	8.08	1	8.08	231.14	<0.0001	
ABD	7.83	1	7.83	223.88	<0.0001	
CD	5.80	1	5.80	165.81	<0.0001	
ACD	5.51	1	5.51	157.65	<0.0001	
Curvature	39.13	1	39.13	1119.47	<0.0001	significant
Residual	0.24	7	0.035			
Total	2109.07	16				

Table B-3 Analysis of Variance for 2^k experimental design in catalytic pyrolysis of rapeseed oil over MgO.

Source		Sum of Squares	Degree of Freedom	Mean Squares	F Value	Prob> F Value	
Model		1717.65	3	572.55	19965.37	<0.0001	significant
	A	1643.09	1	1643.09	57296.14	<0.0001	
	D	67.98	1	67.98	2370.53	<0.0001	
	B	6.58	1	6.58	229.42	<0.0001	
Curvature		6.41	1	6.41	223.57	<0.0001	significant
Residual		0.34	12	0.029			
Total		1724.40	16				

Table B-4 Analysis of Variance for 2^k experimental design in catalytic pyrolysis of rapeseed oil over MgO.

Source		Sum of Squares	Degree of Freedom	Mean Squares	F Value	Prob> F Value	
Model		2417.44	5	483.49	1001.82	<0.0001	significant
	A	1277.88	1	1277.88	2647.85	<0.0001	
	D	765.21	1	765.31	1585.57	<0.0001	
	AD	352.78	1	352.78	730.99	<0.0001	
	C	17.75	1	17.75	36.77	<0.0001	
	B	3.81	1	3.81	7.90	<0.0001	
Curvature		26.53	1	26.53	54.97	<0.0001	significant
Residual		4.93	10	0.48			
Total		2448.79	16				

Table B-5 Analysis of Variance for 2^k experimental design in catalytic pyrolysis of rapeseed oil over HZSM-5.

Source		Sum of Squares	Degree of Freedom	Mean Squares	F Value	Prob> F Value	
Model		828.32	8	103.54	4579.25	<0.0001	significant
	A	601.72	1	601.72	26612.20	<0.0001	
	D	139.24	1	139.24	6158.14	<0.0001	
	AD	2170.21	1	49.07	2170.21	<0.0001	
	B	1123.43	1	25.4	1123.43	<0.0001	
	BD	220.92	1	5.0	220.92	<0.0001	
	CD	4.22	1	4.22	186.77	<0.0001	
	C	2.04	1	2.04	90.44	<0.0001	
	AC	1.63	1	1.63	71.90	<0.0001	
Curvature		1.62	1	1.62	71.84	<0.0001	significant
Residual		0.16	7	0.023			
Total		830.1	16				

Table B-6 Analysis of Variance for 2^k experimental design in catalytic pyrolysis of rapeseed oil over HZSM-5.

Source		Sum of Squares	Degree of Freedom	Mean Squares	F Value	Prob> F Value	
Model		2111.83	5	422.37	3744.17	<0.0001	significant
	A	1144.3	1	1144.3	10143.94	<0.0001	
	D	608.49	1	608.49	5394.08	<0.0001	
	AD	350.16	1	350.16	3104.06	<0.0001	
	B	4.48	1	4.48	39.75	<0.0001	
	AB	4.40	1	4.40	39	<0.0001	
Curvature		9.18	1	9.18	81.38	<0.0001	significant
Residual		1.13	10	0.11			
Total		2122.13	16				

Table B-7 Analysis of Variance for 2^k experimental design in catalytic pyrolysis of rapeseed oil over 1%wt Fe/AC.

Source		Sum of Squares	Degree of Freedom	Mean Squares	F Value	Prob> F Value	
Model		563.95	5	112.79	11171.40	<0.0001	significant
	A	543.24	1	543.24	53806.07	<0.0001	
	D	8.43	1	8.42	834.42	<0.0001	
	ABD	5.03	1	5.03	498.09	<0.0001	
	B	3.95	1	3.95	391.25	<0.0001	
	C	3.30	1	3.30	327.18	<0.0001	
Curvature		112.24	1	112.24	11117.47	<0.0001	significant
Residual		0.10	10	0.010			
Total		676.29	16				

Table B-8 Analysis of Variance for 2^k experimental design in catalytic pyrolysis of rapeseed oil over 1%wt Fe/AC.

Source		Sum of Squares	Degree of Freedom	Mean Squares	F Value	Prob> F Value	
Model		3846.31	5	769.26	57035.20	<0.0001	significant
	A	3600.00	1	3600.00	26690.05	<0.0001	
	D	224.70	1	224.70	16659.88	<0.0001	
	AD	9.67	1	9.67	717.12	<0.0001	
	B	6.79	1	6.79	503.13	<0.0001	
	AC	5.15	1	5.15	382.05	<0.0001	
Curvature		48.86	1	48.86	3622.49	<0.0001	significant
Residual		0.13	10	0.013			
Total		3895.30	16				

Table B-9 Analysis of Variance for 2^k experimental design in catalytic pyrolysis of rapeseed oil over 5%wt Fe/AC.

Source		Sum of Squares	Degree of Freedom	Mean Squares	F Value	Prob> F Value	
Model		608.96	7	86.99	10942.63	<0.0001	significant
	A	585.52	1	585.52	73650.19	<0.0001	
	D	17.70	1	17.70	2226.80	<0.0001	
	AC	2.33	1	2.33	293.49	<0.0001	
	B	2.08	1	2.08	261.74	<0.0001	
	ABD	0.60	1	0.60	76.04	<0.0001	
	ACD	0.46	1	0.46	57.74	<0.0001	
	AD	0.26	1	0.26	32.40	<0.0001	
Curvature		68.25	1	68.25	8584.93	<0.0001	significant
Residual		0.064	8	0.008			
Total		677.27	16				

Table B-10 Analysis of Variance for 2^k experimental design in catalytic pyrolysis of rapeseed oil over 5%wt Fe/AC.

Source		Sum of Squares	Degree of Freedom	Mean Squares	F Value	Prob> F Value	
Model		3941.84	3	1313.95	26546.62	<0.0001	significant
	A	3835.32	1	3835.32	77487.83	<0.0001	
	D	102.31	1	102.31	2067.11	<0.0001	
	CD	4.20	1	4.20	84.91	<0.0001	
Curvature		72.86	1	72.86	1472.12	<0.0001	significant
Residual		0.59	12	0.049			
Total		4015.30	16				

APPENDIX C

THE BATCH EXPERIMENTAL RESULT

Table C-1 The 2^k experimental design of catalytic pyrolysis of rapeseed oil over CaO in micro-reactor

Experiment no.	Parameter				Product yield (%wt)			Product distribution (%wt)			
	Temperature (°C)	Catalyst (%wt)	Pressure (bar)	Time (Min)	Gas (%wt)	Solid (%wt)	Liquid (%wt)	Naphtha (%wt)	Kerosene (%wt)	Diesel (%wt)	Long residue (%wt)
1	420.00	0.75	3.00	45.00	17.33	11.06	71.61	31.51	9.31	24.35	6.44
2	390.00	1.00	5.00	60.00	10.4	9.27	80.33	25.71	16.47	24.5	13.66
3	450.00	0.50	1.00	30.00	25.37	6.88	67.75	31.84	12.2	19.65	4.07
4	450.00	1.00	1.00	30.00	25	7.05	67.95	33.3	14.95	16.65	3.06
5	390.00	0.50	5.00	60.00	9.79	8.73	81.48	30.15	14.67	23.63	13.04
6	390.00	1.00	1.00	60.00	8.36	10.00	81.64	25.72	22.04	20.82	13.06
7	450.00	0.50	5.00	30.00	26.82	9.13	64.05	29.46	10.89	19.22	4.16
8	450.00	1.00	5.00	30.00	26.17	9.37	64.46	30.94	13.54	16.12	3.87
9	390.00	0.50	1.00	60.00	8.08	9.64	82.28	30.03	18.92	20.98	12.34
10	390.00	1.00	5.00	30.00	8.46	8.96	82.58	6.61	9.91	30.55	35.51
11	450.00	0.50	1.00	60.00	28.04	8.67	63.29	32.91	12.66	14.87	2.85
12	450.00	1.00	1.00	60.00	27.51	8.43	64.06	34.59	11.21	14.74	3.84
13	390.00	0.50	5.00	30.00	8.12	8.42	83.46	5.42	10.43	31.3	36.31
14	450.00	0.50	5.00	60.00	28.94	8.96	62.1	35.71	11.49	12.42	2.48
15	390.00	1.00	1.00	30.00	6.42	7.96	85.62	6.85	13.27	28.99	36.39
16	450.00	1.00	5.00	60.00	28.68	8.29	63.03	36.56	11.35	12.29	2.84
17	390.00	0.50	1.00	30.00	5.92	7.55	86.53	5.19	14.28	29.86	37.21

Table C-2 The 2^k experimental design of catalytic pyrolysis of rapeseed oil over MgO in micro-reactor

Experiment no.	Parameter				Product yield (%wt)			Product distribution (%wt)			
	Temperature (°C)	Catalyst (%wt)	Pressure (bar)	Time (Min)	Gas (%wt)	Solid (%wt)	Liquid (%wt)	Naphtha (%wt)	Kerosene (%wt)	Diesel (%wt)	Long residue (%wt)
1	420.00	0.75	3.00	45.00	21.02	5.57	73.41	32.3	16.15	18.35	6.61
2	390.00	1.00	5.00	60.00	7.75	8.76	83.49	31.31	20.87	21.29	10.02
3	450.00	0.50	1.00	30.00	23.51	7.83	68.66	32.27	13.39	16.14	6.87

Experiment no.	Parameter				Product yield (%wt)			Product distribution (%wt)			
	Temperature (°C)	Catalyst (%wt)	Pressure (bar)	Time (Min)	Gas (%wt)	Solid (%wt)	Liquid (%wt)	Naphtha (%wt)	Kerosene (%wt)	Diesel (%wt)	Long residue (%wt)
1	450.00	1.00	5.00	60.00	35.63	6.96	57.41	32.72	11.19	10.97	2.41
2	450.00	0.50	1.00	30.00	19.57	11.08	69.35	32.11	15.19	19.83	2.22
3	450.00	1.00	1.00	30.00	21.61	12.58	65.81	29.88	13.49	19.81	2.63
4	450.00	1.00	1.00	60.00	31.67	12.00	56.33	32.67	10.65	9.91	3.1
5	390.00	0.50	5.00	30.00	15.76	8.00	76.24	4.73	9.23	21.27	41.02
6	390.00	1.00	1.00	30.00	18.41	6.53	75.06	4.13	8.03	24.47	38.43
7	390.00	1.00	1.00	60.00	17.44	9.68	72.88	25.95	17.64	23.39	5.9
8	390.00	1.00	5.00	30.00	18.56	8.48	72.96	4.38	7.59	23.2	37.79
9	450.00	0.50	5.00	60.00	34.17	7.04	58.79	34.74	9.58	10.88	3.59
10	390.00	0.50	1.00	60.00	15.55	10.22	74.23	26.28	16.03	24.87	7.05
11	390.00	0.50	1.00	30.00	16.26	4.86	78.88	4.5	9.62	24.61	40.15
12	390.00	0.50	5.00	60.00	16.45	9.70	73.85	25.63	19.05	23.85	5.32
13	450.00	1.00	5.00	30.00	25.05	10.44	64.51	29.29	10.52	22.9	1.81
14	450.00	0.50	5.00	30.00	23.77	7.81	68.42	31.54	12.04	21	3.83
15	450.00	0.50	1.00	60.00	31.45	10.60	57.95	34.71	9.1	11.18	2.96
16	390.00	1.00	5.00	60.00	17.82	9.59	72.59	26.64	20.69	19.96	5.3
17	420.00	0.75	3.00	45.00	21.67	11.19	67.14	26.86	13.43	20.81	6.04

Table C-4 The 2^k experimental design of catalytic pyrolysis of rapeseed oil over 1%wt Fe/AC in micro-reactor

Experiment no.	Parameter				Product yield (%wt)			Product distribution (%wt)			
	Temperature (°C)	Catalyst (%wt)	Pressure (bar)	Time (Min)	Gas (%wt)	Solid (%wt)	Liquid (%wt)	Naphtha (%wt)	Kerosene (%wt)	Diesel (%wt)	Long residue (%wt)
1	390.00	1.00	5.00	30.00	12.75	7.28	79.97	4.4	4.4	44.78	26.39
2	390.00	0.50	5.00	60.00	12.74	7.73	79.53	12.33	5.96	42.55	18.29
3	450.00	0.50	1.00	30.00	21.73	7.99	70.28	34.79	11.95	18.98	4.57
4	450.00	0.50	5.00	60.00	23.5	7.59	68.91	39.62	12.75	12.92	3.84
5	450.00	1.00	1.00	30.00	22.25	7.33	70.42	36.27	13.38	16.20	4.23
6	450.00	0.50	1.00	60.00	24.27	5.89	69.84	40.86	12.57	12.57	4.19
7	390.00	0.50	5.00	30.00	11.78	5.99	82.23	3.29	5.76	43.99	29.6
8	450.00	1.00	1.00	60.00	25.52	6.64	67.84	42.06	12.89	10.85	2.04
9	450.00	1.00	5.00	30.00	24.4	6.31	69.29	34.99	14.55	16.98	2.77
10	420.00	0.75	3.00	45.00	22.1	13.90	64	30.08	12.8	16.64	4.48
11	390.00	0.50	1.00	60.00	12.67	7.00	80.33	11.25	5.62	43.38	20.08
12	390.00	1.00	1.00	60.00	13.15	6.32	80.53	12.48	6.85	43.89	16.91
13	450.00	0.50	5.00	30.00	23.77	7.01	69.22	33.57	12.81	18.69	4.15
14	450.00	1.00	5.00	60.00	24.68	8.37	66.95	40.84	13.39	10.04	2.68
15	390.00	1.00	5.00	60.00	13.18	7.19	79.63	13.54	5.97	41.41	18.31
16	390.00	0.50	1.00	30.00	10.2	6.80	83	2.08	6.23	43.16	31.54
17	390.00	1.00	1.00	30.00	11.1	8.14	80.76	3.63	6.46	42.40	28.27

Table C-5 The 2^k experimental design of catalytic pyrolysis of rapeseed oil over 5%wt Fe/AC in micro-reactor

Experiment no.	Parameter				Product yield (%wt)			Product distribution (%wt)			
	Temperature (°C)	Catalyst (%wt)	Pressure (bar)	Time (Min)	Gas (%wt)	Solid (%wt)	Liquid (%wt)	Naphtha (%wt)	Kerosene (%wt)	Diesel (%wt)	Long residue (%wt)
1	450.00	0.50	5.00	30.00	20.32	10.15	69.53	34.7	13.21	16.62	5.01
2	450.00	0.50	5.00	60.00	25.58	8.11	66.31	38.46	12.4	9.95	5.5
3	420.00	0.75	3.00	45.00	25.79	8.78	65.43	30.1	14.39	14.39	6.54
4	390.00	0.50	5.00	30.00	8.29	10.34	81.37	3.66	5.78	26.45	45.49
5	450.00	1.00	5.00	60.00	25.64	8.38	65.98	39.06	18.47	8.31	3.76
6	390.00	1.00	1.00	60.00	10.45	11.50	78.05	8.74	8.43	34.19	26.22
7	450.00	0.50	1.00	60.00	24.97	7.57	67.46	39.73	11.54	12.41	3.78
8	390.00	0.50	1.00	60.00	10.28	10.69	79.03	8.85	7.74	36.91	25.53
9	450.00	1.00	5.00	30.00	20.48	11.27	68.25	34.74	14.33	14.81	5.19
10	390.00	1.00	1.00	30.00	8.64	10.80	80.56	2.98	2.66	29.08	47.61
11	390.00	1.00	5.00	60.00	10.12	10.90	78.98	7.98	11.61	31.59	29.06
12	450.00	1.00	1.00	60.00	25.12	7.76	67.12	40.2	14.16	10.47	2.28
13	390.00	1.00	5.00	30.00	8.2	10.85	80.95	3.89	4.94	27.12	45.01
14	450.00	0.50	5.00	30.00	10.08	9.70	80.22	7.62	6.9	35.62	30.08
15	450.00	0.50	1.00	60.00	31.45	10.60	57.95	34.71	9.1	11.18	2.96
16	390.00	1.00	5.00	60.00	17.82	9.59	72.59	26.64	20.69	19.96	5.3
17	420.00	0.75	3.00	45.00	21.67	11.19	67.14	26.86	13.43	20.81	6.04

APPENDIX D

THE KINETICS STUDY

Table D-1. The kinetic study of HZSM-5

Temperature (°C)	Time (min)	Gas (%wt)	Liquid (%wt)	Solid (%wt)	Product Distribution				Total
					Naphtha (%wt)	Kerosene (%wt)	Diesel (%wt)	Long Residue (%wt)	
390	0	3.58	90.33	6.09	0.00	1.06	40.75	58.19	100.00
	15	4.30	88.62	7.08	5.28	2.65	39.83	52.24	100.00
	25	5.74	86.59	7.67	8.49	5.53	38.44	47.54	100.00
	35	6.63	85.23	8.14	11.89	8.16	36.74	43.21	100.00
	45	7.87	83.17	8.96	14.11	13.97	36.64	35.28	100.00
	60	8.49	81.39	10.12	15.86	20.13	35.99	28.02	100.00
410	0	5.45	89.35	5.20	1.21	2.43	38.67	57.69	100.00
	15	5.93	87.85	6.22	7.97	6.19	37.57	48.27	100.00
	25	6.57	85.14	8.29	12.36	9.86	36.57	41.21	100.00
	35	7.27	83.76	8.97	16.68	13.81	35.49	34.02	100.00
	45	8.11	81.98	9.91	20.40	16.91	33.33	29.36	100.00
	60	9.69	79.45	10.86	23.35	18.79	31.62	26.24	100.00
430	0	7.99	88.37	3.64	3.93	3.73	35.12	57.22	100.00
	15	9.64	85.49	4.87	9.70	7.09	34.97	48.24	100.00
	25	10.63	84.62	4.75	17.55	10.56	33.46	38.43	100.00
	35	11.73	81.37	6.90	19.72	14.81	33.50	31.97	100.00
	45	13.08	78.98	7.94	22.95	18.32	32.87	25.86	100.00
	60	15.62	75.94	8.44	27.37	21.27	31.34	20.02	100.00
450	0	10.23	87.48	2.29	5.65	4.07	33.79	56.49	100.00
	15	12.27	84.99	2.74	12.58	10.91	32.71	43.80	100.00
	25	13.66	82.37	3.97	18.82	14.80	31.12	35.26	100.00
	35	15.26	79.41	5.33	24.50	17.39	29.93	28.18	100.00
	45	17.14	77.05	5.81	27.56	19.74	29.77	22.93	100.00
	60	20.76	73.57	5.67	33.36	21.01	28.56	17.07	100.00

Table D-2. The kinetic study of MgO

Temperature (°C)	Time (min)	Gas (%wt)	Liquid (%wt)	Solid (%wt)	Product Distribution				Total
					Naphtha (%wt)	Kerosene (%wt)	Diesel (%wt)	Long Residue (%wt)	
390	0	6.62	92.56	0.82	0.00	2.14	37.25	60.61	100.00
	15	7.63	90.72	1.65	5.87	2.17	33.30	58.66	100.00
	25	8.28	88.21	3.51	8.11	2.83	32.74	56.32	100.00
	35	9.07	86.70	4.23	9.42	6.96	28.76	54.86	100.00
	45	9.92	84.49	5.59	14.75	8.70	23.66	52.89	100.00
	60	11.48	81.88	6.64	17.69	10.81	20.05	51.45	100.00
410	0	7.83	91.83	0.34	3.44	1.51	35.68	59.37	100.00
	15	9.98	87.46	2.56	7.07	2.49	35.06	55.38	100.00
	25	10.81	85.18	4.01	10.47	3.74	33.68	52.11	100.00
	35	11.79	83.69	4.52	13.29	5.86	32.16	48.69	100.00
	45	12.81	81.75	5.44	17.23	6.39	31.73	44.65	100.00
	60	14.97	79.63	5.40	20.09	8.79	30.25	40.87	100.00
430	0	6.62	92.56	0.82	4.59	1.62	34.85	58.94	100.00
	15	7.63	90.72	1.65	8.65	3.87	33.65	53.83	100.00
	25	8.28	88.21	3.51	12.63	7.12	32.46	47.79	100.00
	35	9.07	86.70	4.23	16.07	9.47	31.55	42.91	100.00
	45	9.92	84.49	5.59	19.36	10.85	30.14	39.65	100.00
	60	11.48	81.88	6.64	23.61	11.18	28.33	36.88	100.00
450	0	7.83	91.83	0.34	6.24	2.10	34.03	57.63	100.00
	15	9.98	87.46	2.56	10.75	4.82	32.57	51.86	100.00
	25	10.81	85.18	4.01	17.33	7.16	29.86	45.65	100.00
	35	11.79	83.69	4.52	23.63	10.52	27.59	38.26	100.00
	45	12.81	81.75	5.44	31.73	11.54	25.14	31.59	100.00
	60	14.97	79.63	5.40	39.15	12.73	22.24	25.88	100.00

Table D-3. The kinetic study of 1%wt Fe/AC

Temperature (°C)	Time (min)	Gas (%wt)	Liquid (%wt)	Solid (%wt)	Product Distribution				Total
					Naphtha (%wt)	Kerosene (%wt)	Diesel (%wt)	Long Residue (%wt)	
390	0	2.54	93.34	4.12	0.00	2.26	37.26	60.48	100.00
	15	2.90	91.33	5.77	6.32	4.57	36.71	56.25	100.00
	25	3.16	88.90	7.94	9.49	7.14	36.55	52.43	100.00
	35	3.43	86.11	10.46	12.89	9.56	35.73	48.05	100.00
	45	3.75	84.64	11.61	14.29	11.57	34.65	45.37	100.00
	60	4.31	82.91	12.78	16.39	13.39	33.29	42.54	100.00
410	0	4.75	92.17	3.08	2.47	3.41	34.56	59.56	100.00
	15	5.44	89.83	4.73	9.71	5.62	33.13	53.54	100.00
	25	5.93	87.55	6.52	13.22	8.12	32.91	47.76	100.00
	35	6.46	85.04	8.50	16.15	11.47	32.26	42.85	100.00
	45	7.11	83.38	9.51	20.45	11.67	30.22	37.66	100.00
	60	8.12	81.19	10.69	25.59	13.48	28.52	32.41	100.00
430	0	7.29	91.38	1.33	5.29	3.46	33.14	57.81	100.00
	15	8.40	88.08	3.52	13.81	6.11	30.87	50.68	100.00
	25	9.11	85.68	5.21	17.57	6.61	32.70	44.53	100.00
	35	9.90	82.76	7.34	20.14	12.39	30.23	37.24	100.00
	45	10.85	80.89	8.26	23.67	13.11	28.35	31.87	100.00
	60	12.60	78.16	9.24	29.83	14.57	28.19	26.41	100.00
450	0	9.31	90.54	0.15	8.44	3.93	30.4	56.29	100.00
	15	10.79	87.11	2.10	15.22	8.50	28.47	48.31	100.00
	25	11.81	84.29	3.90	20.56	11.21	26.79	40.44	100.00
	35	12.96	81.88	5.16	26.70	13.38	24.28	33.64	100.00
	45	14.33	79.42	6.25	31.56	14.66	23.44	26.89	100.00
	60	14.42	77.36	8.22	38.25	16.17	20.44	19.36	100.00

APPENDIX E

THE CONTINUOUS EXPERIMENTAL RESULT

Table E-1 The 2^k experimental design of catalytic pyrolysis of rapeseed oil over MgO in continuous reactor

Experiment No.	Parameter								
	Temperature (°C)	Catalyst content (%wt)	N_2 flow rate (bar)	Feeding rate (Min)	Liquid (%wt)	Naphtha (%wt)	Kerosene (%wt)	Diesel (%wt)	Long residue (%wt)
1	390.00	60.00	150.00	3.00	33.42	49.8	11.5	33.9	4.8
2	390.00	30.00	150.00	3.00	41.97	30.7	22.9	28.9	17.5
3	450.00	60.00	50.00	9.00	80.14	52.4	7.9	37.2	2.5
4	450.00	30.00	50.00	3.00	69.01	41.6	29.7	22.5	6.2
5	450.00	30.00	50.00	9.00	84.21	52	9	22.8	16.2
6	390.00	60.00	50.00	3.00	25.14	46.5	18	26.7	8.8
7	450.00	60.00	150.00	3.00	69.04	50	10.5	34.1	5.4
8	450.00	60.00	150.00	9.00	71.5	49.8	8.5	38.2	3.5
9	390.00	30.00	150.00	9.00	25.73	39.5	22	33.7	4.8
10	450.00	30.00	150.00	3.00	78.11	45.3	22	28	4.7
11	390.00	30.00	50.00	9.00	34.43	43.3	21	26.2	9.5
12	390.00	60.00	150.00	9.00	21.84	42.5	15.4	38	4.1
13	450.00	60.00	50.00	3.00	69	46.8	15.1	27.6	10.5
14	450.00	30.00	150.00	9.00	79.45	50.2	8	33.8	8
15	390.00	60.00	50.00	9.00	31.01	44.3	12.5	36.7	6.5
16	390.00	30.00	50.00	3.00	33.45	45.3	21	22	11.7
17	420.00	45.00	100.00	6.00	80.24	53.9	10.5	27	8.6

APPENDIX F

The use of Design Expert program.

Two-level factorial experimental design is commonly used in experiments involving many factors which aimed to study the interaction that affect the effects of such factors. The most important factorial experimental design was in case of k factors which each factor consists of 2 levels. Each level was due to quantitative data such as temperature, pressure or time, for example or due to qualitative data such as machines or workers, for example. In these 2 levels represent “high” or “low” values of factor or represent “present” or “absent” of factors. In one complete replicate of this design consists of in total of $2\times2\times2\times...\times2 = 2k$ data. This design is called 2k factorial experimental design which is very useful for the experiment in the first period when there are many factors that need to be studied. This design can reduce the number of trials in order to study the effect of k factors completely by using 2-level factorial design. It is therefore not surprising that this design has been used widely to filter and to reduce the number of factors. This is each factor of factorial design consists of 2 levels. The responses are linear over the range of factor level studied which the hypothesis is acceptable for the experiment aimed to use factors in studying the system. The study of interaction revealed the effects of factors in Latin capital letters. A represented the effect of factor A, B represents the effect of factor B and AB represented the interaction of factor AB. In 22 factorial design low and high levels of factors were represented by + and – on A and X axis, respectively. For the experimental design with 4 factors they were represented by lowercase letters. High level of any factor was represented by lowercase letter of that factor. For low level, there was no letters presented in the study of interaction effect. Therefore, for this 2k design a represented the interaction effect of high A and low B, b represented interaction effect of low A and high B, ab represented both high A and high B and (1) represented both low A and low B.

Equation for calculation : Contrast was the sum of experimental values of each treatment multiplied by coeffecient (-1 or +1) of factors of the interaction between factors.

From ANOVA analysis using Design Expert the mathematical equation was obtained as shown in equation (D.1). This equation showed the relationship between %yield of liquid and factors and equation (D.2) showed the relationship between diesel fraction in liquid product and factors.

Design Expert: Design Expert version 7.0.0 was used in this study with the procedures from designing the experimental to calculation as followed:

1. Choosing model and defining variables for designing the experimental.

a. Enter the program, click File --> New Design, the display will show as figure b.1. Select the model according to the variables to be studied. In this study 4 variables were studied so 2^K level model was chosen.

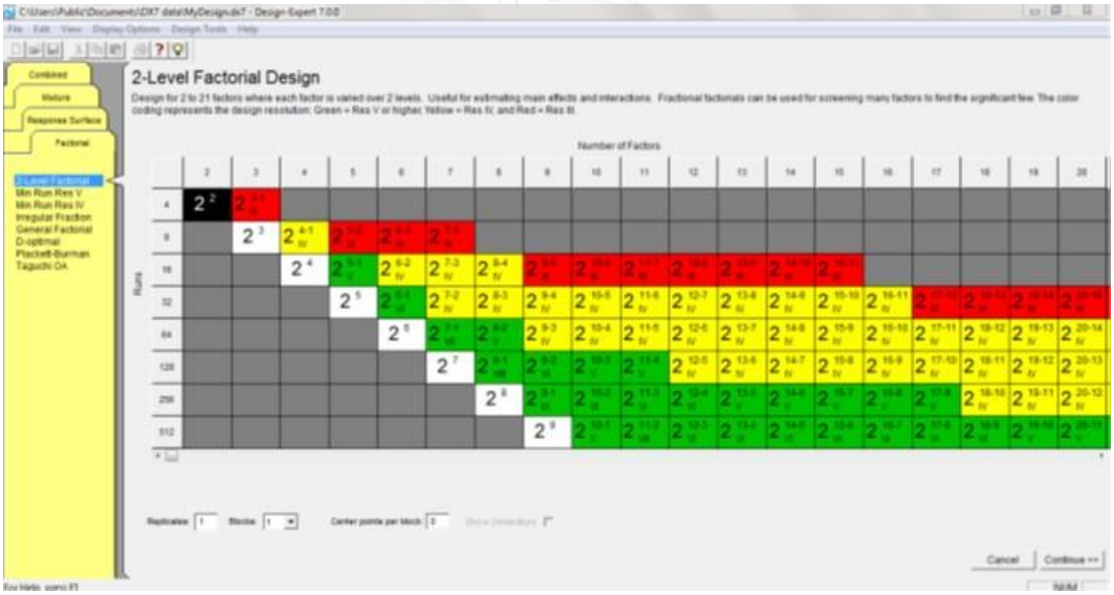

Fig. F-1 The table of 2 level factorial design.

b. Choose the option as 1.a the display will show as Fig. F-2. fill the following data.

Fill the name of variable in Name

Fill unit of variable in Units

Fill lower value of variable in Low

Fill higher value of variable in High.

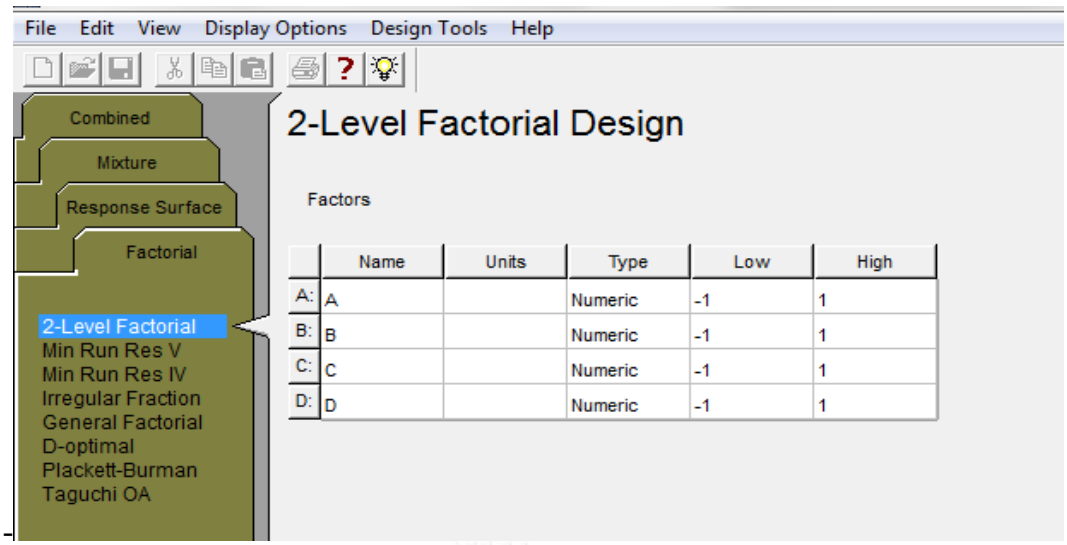

Fig. F-2 The variables determining

Click Continue, the display will show as Fig F-3. Choose the number of responses and fill the name as well as unit of response and click Continue.

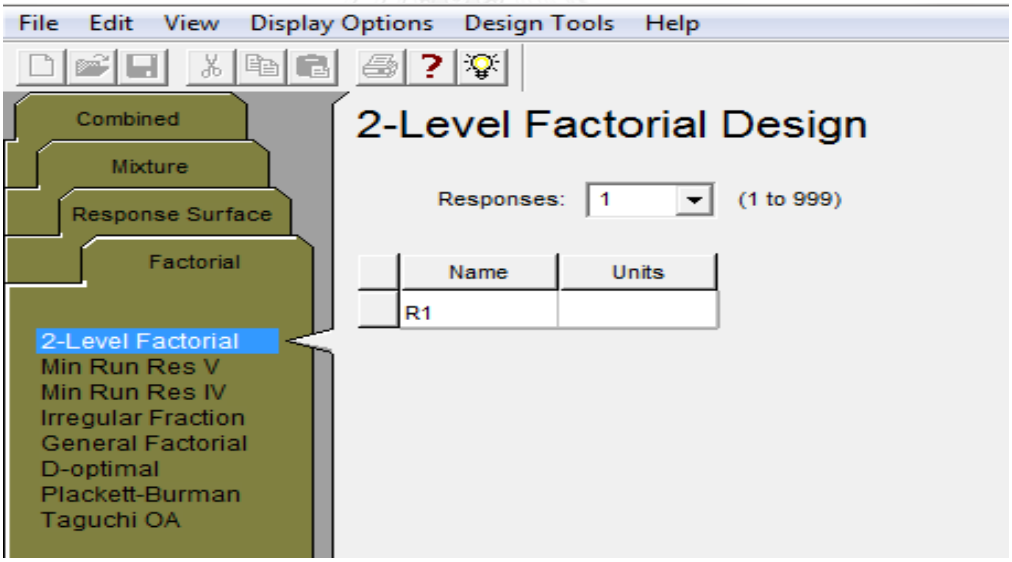

Fig. F-3 The responses determining

c. After setting the value as 1.b, the software will display a table as shown in figure b.4. This table consists of the sequence of trial, variable value in each trial and blank for defining responses from the experiment. After all trials are performed and response values are defined, the next step is analyzing the experimental results.

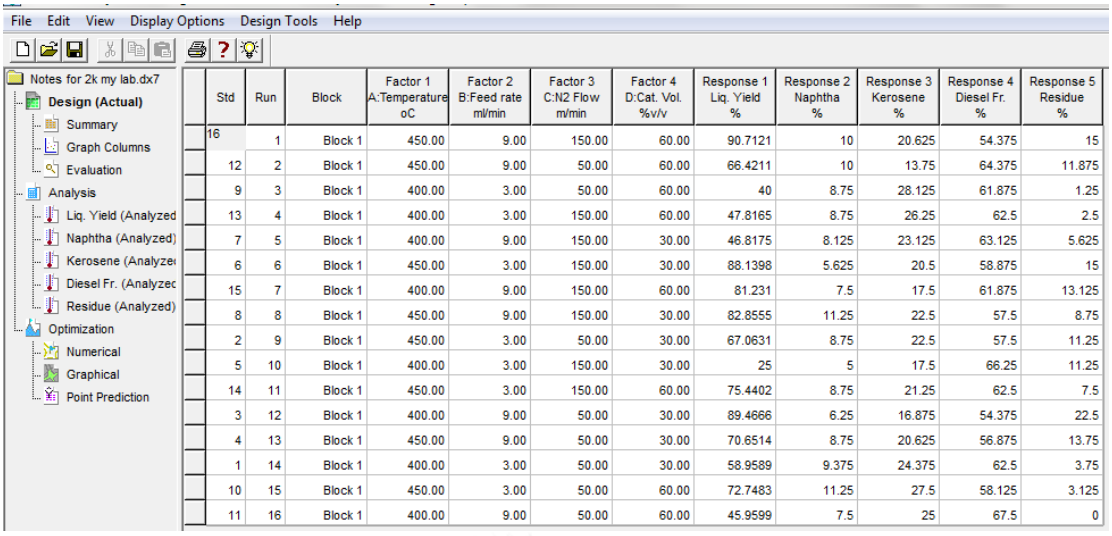

Std	Run	Block	Factor 1 A:Temperature oC	Factor 2 B:Feed rate ml/min	Factor 3 C:N2 Flow m/min	Factor 4 D:Cat. Vol. %v/v	Response 1 Liq. Yield %	Response 2 Naphtha %	Response 3 Kerosene %	Response 4 Diesel Fr. %	Response 5 Residue %
16	1	Block 1	450.00	9.00	150.00	60.00	90.7121	10	20.625	54.375	15
12	2	Block 1	450.00	9.00	50.00	60.00	66.4211	10	13.75	64.375	11.875
9	3	Block 1	400.00	3.00	50.00	60.00	40	8.75	28.125	61.875	1.25
13	4	Block 1	400.00	3.00	150.00	60.00	47.8165	8.75	26.25	62.5	2.5
7	5	Block 1	400.00	9.00	150.00	30.00	46.8175	8.125	23.125	63.125	5.625
6	6	Block 1	450.00	3.00	150.00	30.00	88.1398	5.625	20.5	58.875	15
15	7	Block 1	400.00	9.00	150.00	60.00	81.231	7.5	17.5	61.875	13.125
8	8	Block 1	450.00	9.00	150.00	30.00	82.8555	11.25	22.5	57.5	8.75
2	9	Block 1	450.00	3.00	50.00	30.00	67.0631	8.75	22.5	57.5	11.25
5	10	Block 1	400.00	3.00	150.00	30.00	25	5	17.5	66.25	11.25
14	11	Block 1	450.00	3.00	150.00	60.00	75.4402	8.75	21.25	62.5	7.5
3	12	Block 1	400.00	9.00	50.00	30.00	89.4666	6.25	16.875	54.375	22.5
4	13	Block 1	450.00	9.00	50.00	30.00	70.6514	8.75	20.625	56.875	13.75
1	14	Block 1	400.00	3.00	50.00	30.00	58.9589	9.375	24.375	62.5	3.75
10	15	Block 1	450.00	3.00	50.00	60.00	72.7483	11.25	27.5	58.125	3.125
11	16	Block 1	400.00	9.00	50.00	60.00	45.9599	7.5	25	67.5	0

Fig. F-4 The number of trials and variables of each experiment.

d. Result analysis begin from choosing responses to be analyzed in left panel and click Effects as shown in Fig. F-5. Choose the point that deviate from linear relationship.

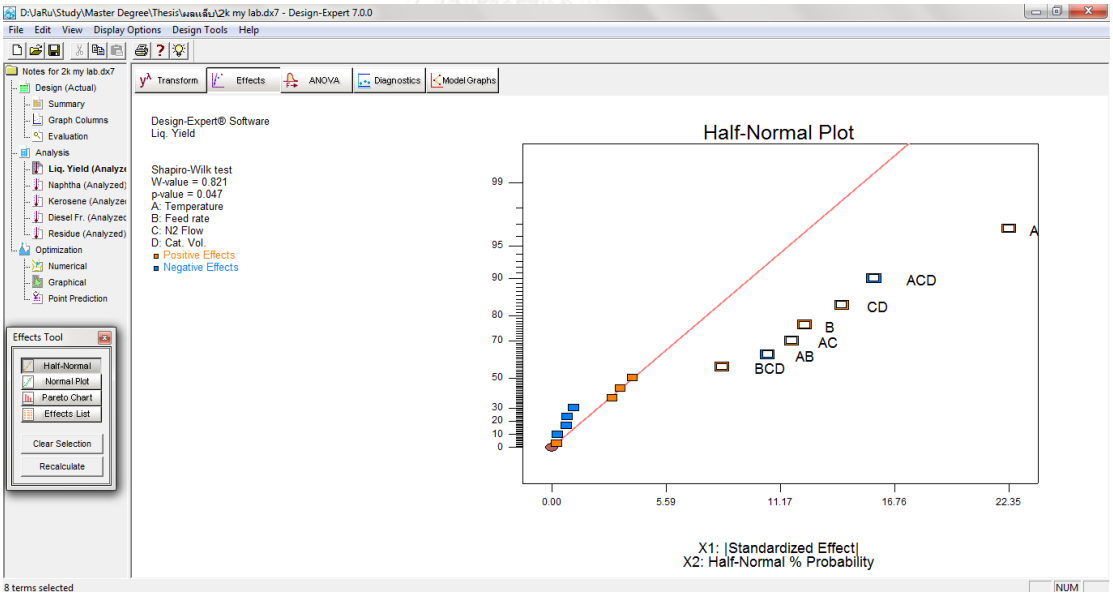

Fig. F-5 Half normal plot

e. Click ANOVA, the table will show as in Fig. F-6 which showed ANOVA table from the analysis then read and analyze the value according to step 1.d and 1.e for all repsonses.

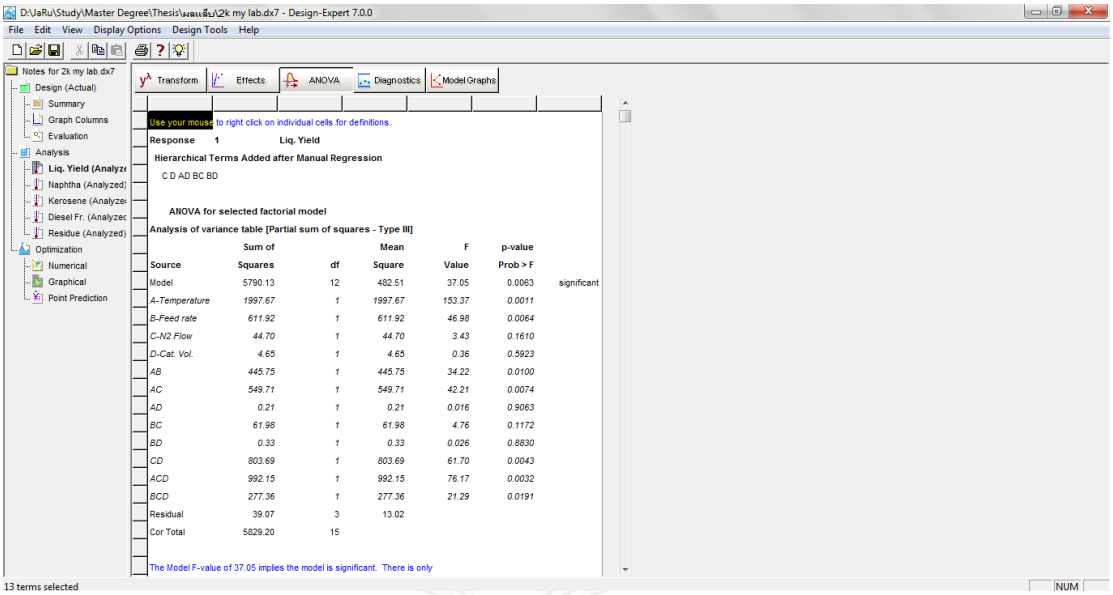

Fig. F-6 ANOVA analysis of variables.

f. After all responses are analyzed, the next step is to fine the optimum condition. Select Numerical at the bottom of Optimization in left panel as shown in Fig. F-7. Define the values of responses such as maximum. Then click Solution it will show the table from the calculation for optimum condition as shown in Fig. F-8.

Fig. F-7 The responses determining for optimum condition.

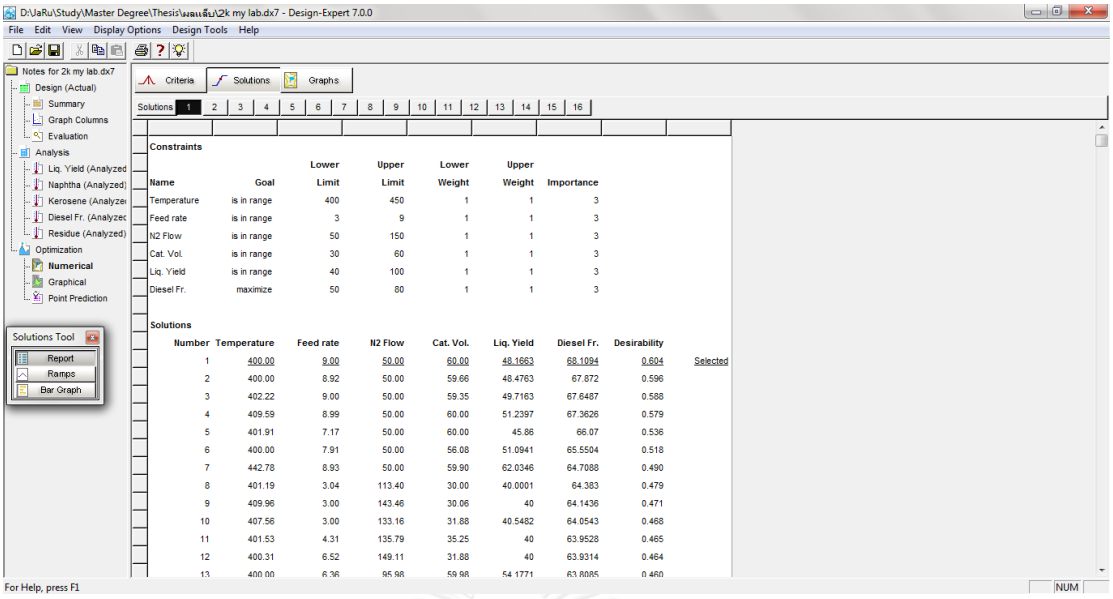

Fig. F-8 Calculation results for optimum condition.

g. For changing the rendering into 3D chart it can be performed by selecting Graphs then select the rendering format by clicking View at menu bar and select 3D plot.

The software will change the rendering into desired format. Moreover, the value of each axis can be change by selecting at Factor Tools to provide various rendering format as shown in Fig. F-9.

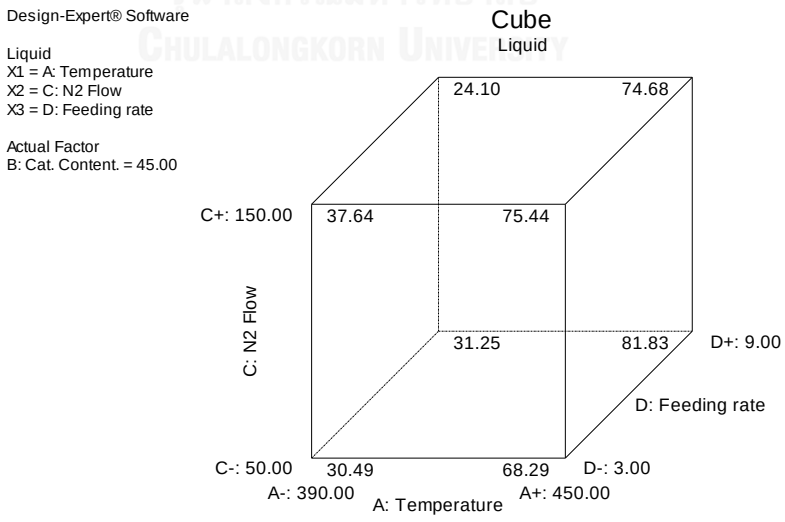

Fig. D.9 Cube surface of interaction between reaction temperature and feeding rate affect on percentage of liquid product

VITA

Ms. Walairat Uttamaprakrom graduated Bachelor's Degree, Department of environmental health Science,Faculty of Public Health, Mahidol University, 2004. In early 2005, I worked as an environmental impact analysis, Energy policy and Planning Office, Ministry of Natural Resources and Environmental. In 2008, I graduated Master's Degree, Department of environmental science, Graduate school, Chulalongkorn University, In 2009 - present, I worked as a researcher, Energy Research Institute, Chulalongkorn University, Bangkok, Thailand. The research mainly focuses on the Waste to Energy such as changing the waste plastic into energy fuel, the waste water and foodwaste into biogas etc. It also works in Pyrolysis Technology to transform vegetable oil, used cooking oil and used lubricants oil as biofuel for diesel engine.